Dynamic Time History and Pushover Analysis of Special Truss Moment Frames by Using Eurocodes

Ali Setvatishayesteh

Submitted to the
Institute of Graduate Studies and Research
in partial fulfilment of the requirements for the degree of

Master of Science
in
Civil Engineering

Eastern Mediterranean University
February 2016
Gazimağusa, North Cyprus

Approval of the Institute of Graduate Studies and Research

Prof. Dr. Cem Tanova
Acting Director

I certify that this thesis satisfies the requirements as a thesis for the degree of Master of Science in Civil Engineering.

Prof. Dr. Özgür Eren
Chair, Department of Civil Engineering

We certify that we have read this thesis and that in our opinion it is fully adequate in scope and quality as a thesis for the degree of Master of Science in Civil Engineering.

Asst. Prof. Dr. Mürüde Çelikağ
Supervisor

Examining Committee

1. Asst. Prof. Dr. Mürüde Çelikağ

2. Asst. Prof. Dr. Giray Özay

3. Asst. Prof. Dr. Umut Yıldırım

ABSTRACT

Special Truss Moment Frames (STMFs)were introduced in USA (1994) as a new system alternative to ordinary Truss Moment Frames (TMF). STMFs are resistant to both gravity and lateral loads over long spans and AISC 341-10 has all the necessary design procedures. STMF design procedures are not available in Eurocodes. Therefore, the main objective of this research was to investigate STMF by using Eurocodes and European steel sections. A numerical study was undertaken to study the seismic behaviour of (STMFs) using dynamic time history and pushover analysis. Performance-based Plastic Design (PBPD) methodology was used to design the STMF based on Eurocode 8 and in some parts AISC 341-10 code was used. Seismostruct software was used to design frames with 4, 7 and 10 stories and to investigate parameters, such as, maximum base shear, drift story, capacity curve and also performance criteria (chord rotation) according to Eurocodes through extensive nonlinear dynamic analysis for an appropriate number of ground motion records. In second phase, a set of nonlinear static (pushover) analysis carried out to find the capacity curve, base shear and story drifts. In the third phase, SAP2000 was used to find performance limit state of STMF and TMF and the results were compared together. In fourth phase, the behaviour factor of STMFs was calculated and compared with the behaviour factor of other structural framing systems. The results obtained were compared with the results of similar frames from past literature. Overall, the results confirmed the validity of the proposed framing system by meeting all the performance design objectives, such as, target drifts and intended yield mechanism. Generally, nonlinear analysis do not required the structural performance check after PBPD and this can be considered as an advantage.

Keywords: STMF, PBPD, Dynamic time history, pushover, performance criteria

ÖZ

Özel Kafes Moment Çerçeveler (ÖKMÇ) 1994 yılında ABD'de sıradan Kafes Moment Çerçeveler'e (KMÇ) alternatik yeni bir sistem olarak sunulmuştur.ÖKMÇ uzun açıklıklı düşey ve yatay yüklere dirençli bir sistemdir ve AISC-10'da tüm gerekli tasarım prosedürleri vardır.Fakat ÖKMÇ tasarım prosedürleri Avrupa Standardlarında yoktur.Bu nedenle, bu araştırmanın ana hedefi Avrupa Standardları ve Avrupa çelik kesitlerini kullanarak ÖKMÇ'yi incelemektir.ÖKMÇ'ninsismik davranışını dinamikzamantarihveitme analizikullanarak incelemek için bir nümerik çalışma yapıldı.Performansa Dayalı Plastik Tasarım(PDPT) yöntemi kullanılarak ÖKMÇ'nin Avrupa Standardı 8'e göre tasarımı yapılmış ve bazı kısımlarda ise AISC 341-10 standardı kullanılmıştır.Seismostruct yazılımı 4, 7 ve 10 katlı çerçeveleri tasarlamak ve en yüksek taban kesme kuvveti, kat sürüklenmesi, kapasite eğrisi ve performans kriteri (acor rotasyonu) için kullanılmıştır. Bu tasarım Avrupa Standardına göre yapılmış ve de yeterli derecede ve/sayıda yer hareketi kayıtları kullanılarak yapılmıştır. İkinci kısımda kapasite eğrisini, taban kesme kuvvetini ve sürüklenme oranını elde etmek için bir dizi doğrusal olmayan statik (itme) analiz yapıldı.Üçüncü kısımda SAP2000 kullanılarak ÖKMÇ ve sırada KMÇperformans sınır durumu incelenmiş ve sonuçlar karşılaştırılmıştır.Dördüncü kısımda ÖKMÇ davranış katsayısı hesaplanmış ve diğer yapısal çerçeve sistemlerinin davranış katsayıları ile karşılaştırılmıştır.Elde edilen sonuçlar ayrıca literatürden benzer çerçeve sonuçları ile karşılaştırılmıştır. Tümünde elde edilen sonuçlar önerilen sistemin performans tasarım hedeflerini, örneğin, hedef sürüklenme ve amaçlanan verim mekanizmasını sağladığını onaylamaktatır. Genelde, doğrusal olmayan

analizlerde, performansa dayalı plastik tasarım yöntemi kullanıldıktan sonra, yapısal performans çekinin yapılmasına gerek yoktur.Bu da bir avantaj olarak düşünülebilir.

Anahtar kelimeler: ÖKMÇ, KMÇ, PDPT, Dinamikzamantarih, itme, performans kriteri

DEDICATION

To My Family

ACKNOWLEDGMENT

I would like to express my deepest appreciation to my supervisor Asst. Prof. Dr. Mürüde Çelikağ for her great efforts in guiding and acquainting me throughout this work.

I would like to show my sincere gratitude to my family for their support and encouragement.

My special thanks go to all the members of the Civil Engineering Department at Eastern Mediterranean University and all my friends in North Cyprus, for their friendship and hospitality.

TABLE OF CONTENTS

LIST OF TABLES

LIST OF FIGURES

LIST OF SYMBOLS

g	Acceleration
F	Force
D	Displacement
P	Axial force
T_1	Fundamental period of vibration
C_t	Structural coefficient
H	Height of structure in meters
F_b	Base shear
*S*d (*T*1)	Ordinate of the design spectrum at the T_1
M	Total mass of the building
λ	Correction factor
S	Soil factor
ag	design ground acceleration
Tb Tc Td	Corner periods in spectrum
DCM	Ductility class medium
DCL	Ductility class low
DCH	Ductility class high
q	Bihavior factor
S_i	Relative displacement in rigid point
V_i	Shear force of stories
F_i	Horizontal force acting on story i
F_b	Seismic base shear
H_i,h_j	Heights of the masses w_i,w_j above the level of application of the

Seismic action (Foundation or top of a rigid basement).

W_i,w_j	Story masses
d	Height of special segment of truss
L_s	Length of segment
L	Spans length
F_y	Yield stress
M_{nc}	Symbolic flexural strength of a specific segment, chord component
EI	Symbolic flexural elastic stiffness of a specific segment
P_{nt}	Specific segment, diagonal component's symbolic tensile strength
P_{nc}	Specific segment, diagonal component's symbolic compressive
α	Angle of diagonal component with the horizontal
$R\mu$	Decreasing behaviour factor
Ω	Increasing strength factor
Y	Tension factor
U_y	Displacement of yielding point
Ω_0	According to NEHRP 1997 code is equal to 3 for STMFs
F_1	Ratio of real tension and yielding tension
F_2	Loading acceleration effect

LIST OF ABBREVIATIONS

STMFs	Special Truss Moment Frames
OTMFs	Ordinary Truss Moment Frames
TMFs	Truss Moment Frames
UBC	Uniform Building Code
AISC	American institute of steel construction
FEMA	Federal Emergency Management Agency
DTHA	Dynamic Time History Analysis
LRFD	Load Resistance Factor Design
PBPD	Performance-based Plastic Design
BRB	Buckling Restrained Bracing
IO	Immediate Occupancy
LS	Life Safety
CP	Collapse Prevention

Chapter

INTRODUCTION

1.1 General Introduction

Because of architectural limitations or structural characteristics, sometimes engineers forced to use moment frames for long spans. This leads to the use of large beam and column sections and therefore uneconomic design. Recently, a new system of design approach is introduced in AISC 341-10code [1]. This new approach improved performance leads to use of smaller sections sizes, reduced storey drifts and hence achieved design that is more economical. Using truss beams in commercial and industrial multi storey buildings with long spans is one of the best and suitable alternatives for structural designers. When a structure is subject to lateral loads, such as earthquake loads, depending on the shape and stiffness of the beams, the plastic hinges may appear in the columns, beams or connections. From an engineering point of view, location of plastic hinges is an important problem that requires appropriate solution. Special Truss Moment Frames (STMF)(Figure 1.1) have improvised fuse in the middle of the beams and hence they are able to control plastic hinges and possible damages to frame. Therefore, STMFs could be an ideal solution to this kind of problem.

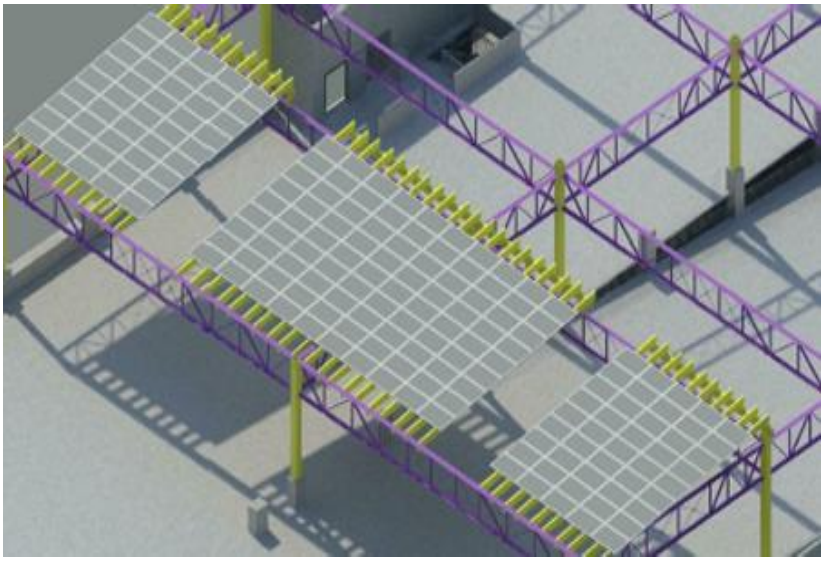

Figure 1.1: Special truss frames [2]

1.2 Types of Beams Usable in Long Span Structures

1.2.1 Plate Girders (Solid Web Beams)

One of the suitable beams for long span is solid web beams or plate girders, they have some advantages, for example, non-limitation in geometrical dimensions and simply build-up and fabricated on site. Goel and Itani investigated the dynamic behaviour of moment frames with plate girders. In his research, to investigate the performance and behaviour of this type of frames, he considered the mechanism of surrender and failure under dynamic loads. The results revealed that the mechanism of collapse and plastic hinges appeared in connections and because of high stiffness of beams versus columns the rotation of connection cause large displacements in beams Figure 1.2 [3].

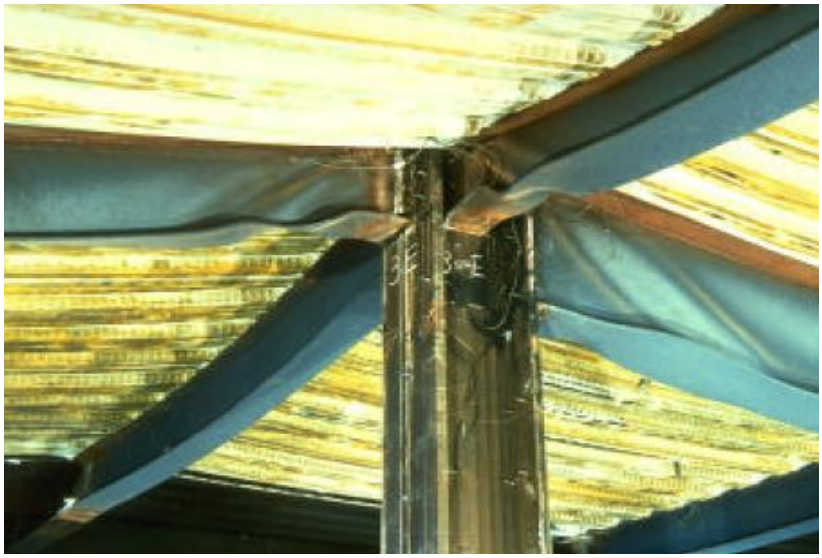

Figure 1.2: One of the problem of plate beams, plastic hinges in connections [3]

1.2.2 Ordinary Truss Moment Beams (TMF)

Simple truss beam is one of the systems used in long span structures. It can be defined as a moment frame with openings in the beam to allow space for piping and ducting (Figure 1.2). This system is more economical due to having smaller and lighter steel sections when compared to moment frame with plate girders. Hence opening in beam and simple connection details are the advantages (Figures 1.3, 1.4 and 1.5).

Figure 1.3: Ordinary truss moment frames (TMF) [3]

Figure 1.4: STMF with piping and ductwork [4]

Figure 1.5: STMF with piping and ductwork [4]

In Uniform Building Code (UBC) [5] the behaviour factor of this system is suggested as R=6, the experimental research showed that the high strength and stiffness of beams in comparison with columns is the main problem. In some cases and some special conditions, UBC allowed to use R=12 for this systems to keep the truss components in elastic region [5].

1.2.3 Special Truss Moment Frames (STMF)

In STMFs the inelastic deformation and dissipation of energy can appear in the middle of the truss beams. Vertical shear force is very small and by removing or un-bracing the segments or Vierendeel middle panel, the inelastic region for inelastic deformation and dissipation can be obtained (Figure 1.6).

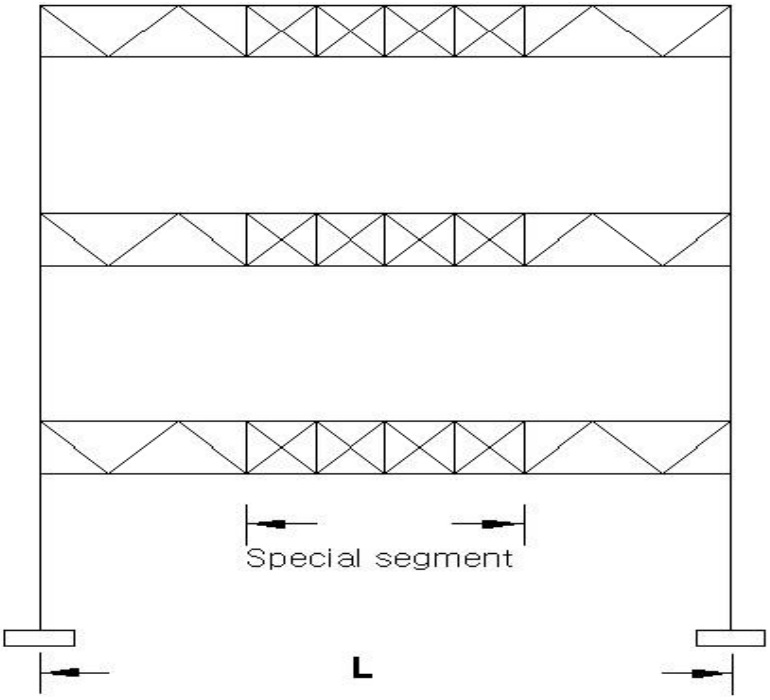

Figure 1.6: X pattern segment [1]

Some researchers do believe that STMFs, in addition to having appropriate collapse mechanism and appropriate energy dissipation, are more economical and lighter than other systems. The truss of STMFs was designed in X style, diagonal pattern or even without any member (Vierendeel middle panel).Figure 1.7 shows the expected hysteretic cyclic force displacement curve for special truss moment frames. The plastic members in the middle of the truss indicate that the truss have smooth behaviour. Segment or special Vierendeel can prevent the buckling of the diagonal

members, prevent the sharp drop of lateral stiffness and the hysteretic shape can remain stable.

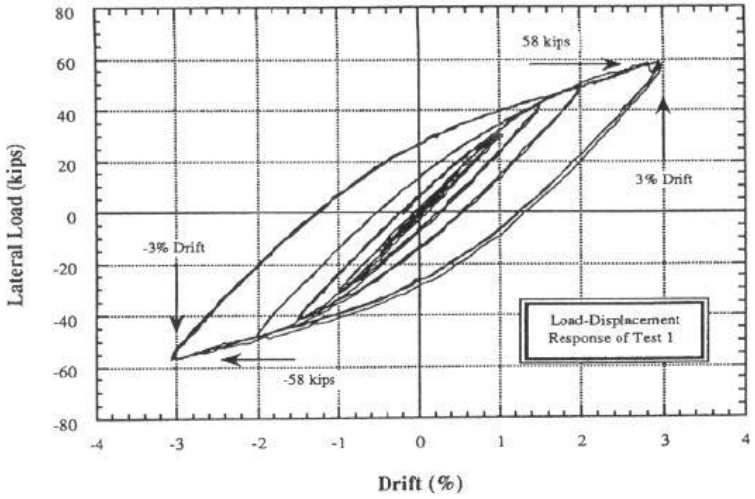

Figure 1.7: Hysteretic loops of STMFs [4]

Gaul and Itani suggested changing the diagonal members of the warren truss with X style so that they can carry the lateral force. In this way, the problems of eccentric braced frames associated with the unbalanced force on the horizontal members, sharp drop of stiffness and strength can be resolved. Researchers tried to limit the inelastic deformation in the special region of the truss called segment[4].According to Figure 1.4horizontal and vertical members were arranged in X pattern and two special segments are designed to carry the large inelastic deformation. On the other hand, the rest of the structure remains in elastic region when subjected to seismic loads. STMF was tested by using full-scaled specimen. As can be seen in Figures 1.7 and 1.8the STMF have more stable hysteretic cyclic behaviour with 3% drift [2].

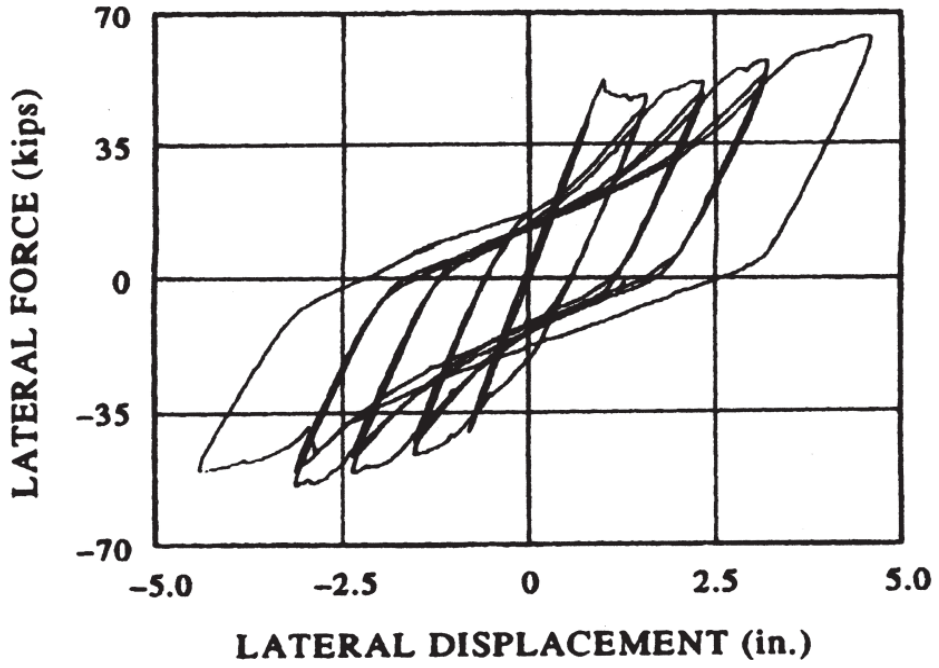

Figure 1.8: A typical load-displacement response for an STMF with X-type diagonals [2]

1.3 Scope of the Study

Nowadays, there are numerous constraints regarding availability of land for construction. When steady increase in population, especially in commercial and industrial areas, is also considered then multi-storey building construction becomes essential. Furthermore, the modern approach and requirements to residential and commercial buildings(parking, shopping etc.) warrants the use of long span construction. Few options are available for this kind of construction; simple truss frames can be one of the best to carry the vertical and lateral forces. When compared to moment frames the truss frames have simple connections, lighter and smaller sections, enough space for piping and ducting systems, which are more appropriate for this kind of construction (Figure1.1).However, according to research carried out so far truss beams found to have less ductility and more stiffness when compared with columns in this type of system [4].

Goel and Itani had studied both the experimental and the theoretical behaviour of simple truss frames[6]. They found that the simple truss frames have less ductility due to buckling and early failure in the truss sections subjected to cyclic loads. More than 70% of the primary stiffness was disappeared in the primary loading cycles causing significant damages when subjected to seismic loads. The hysteretic–displacement cyclic behaviour showed that the sharp drop in load caused the sharp drop in stiffness. The vertical component carries the shear forces in trusses and for this reason, the diagonal members buckle due to the cyclic loads. Reduction of stiffness in diagonal members and existence of post buckling force caused a sharp drop in the lateral stiffness capacity and shear capacity of the other members of truss. After buckling in compression members and the adjacent tension members, respectively, the horizontal members receive the unbalanced force and the absence of vertical members lead to the loss of performance in truss. Researchers were proven that the moment frames with truss girder have less ductility, less hysteretic cyclic behaviour coupled with sharp reduction in strength and stiffness because of the buckling of members before managing to absorb energy.Figure1.9 shows the drift versus ground motions with 0.5g and 0.4g acceleration [6].

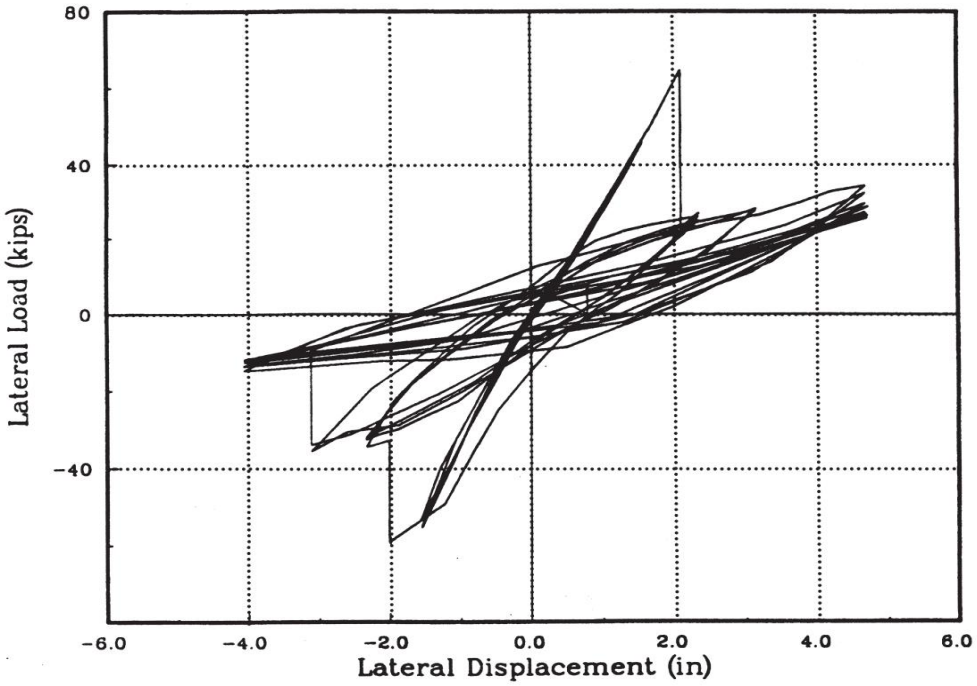

Figure 1.9: A typical load-displacement response for an STMF, single diagonals [2]

1.4 Objective of Study

The following are the main objectives of this research:

1- To determine the seismic behaviour of special truss moment frames (STMFs) by using nonlinear static (pushover) and dynamic time history analyses. STMFs are not used in Europe. Therefore, design was carried out by using Eurocodes to find out the adequacy of Eurocodes and how the results compare with those of AISC

2- To compare the results of the analysis obtained from the two methods mentioned above.

3- To compare the results with those from literature which were designed by using AISC code.

4- To compare the performance limit state of STMF and TMF.

5- To calculate the ductility of STMF system.

1.5 Outline of Thesis

This thesis includes6 chapters and the brief content of these chapters are as given below. Chapter 1providesthe general introduction to the subject matter together with scope and objective of this study. Background to STMFs is given in chapter 2 whereas chapter 3 details the methodology and modelling assumptions used in this study to achieve the analysis results. Chapter 4 gives the results and discussions obtained from the pushover, dynamic time-history analysis of STMFs and TMF. The ductility calculations of the STMFs are also given in this chapter. The conclusions drawn from this study and the recommendations for future work are given in chapter 6.

Chapter

LITERATURE REVIEW

2.1 Literature Review

2.1.1 Introduction

In commercial land industrial structures, normal and special truss moment frames are common. Because of some limitation the structural designer, have to use long span to allow space for shops parking machines and etc. Generally, the truss beams can be dividing in two groups.

2.1.2 Ordinary Truss Moment Frames (TMFs)

This type of frames mostly use in public structures like parking, shops e.t.c. Some of advantages of this system motivate the engineers to use it. Simple connections lighter structure and space for piping system and ductwork are the advantages of TMF. When subject to lateral loads the elements of this system may fracture and buckling, which leads to large and sudden diminution in stiffness and strength of the whole system, therefore TMFs were not found adequate to sustain and endure against lateral load such as ground motion and wind [7]. Beams have higher stiffness than columns. In normal truss moment frames the stiffness of beam is higher than column so according to experimental and numerical study in this system the plastic hinges appear in connection or in column and from engineering point of view is the mean problem [7].

2.1.3 Special Truss Moment Frames (STMFs)

STMFs were developed form the ordinary truss moment frames which are recently used in steel buildings due to their excellent capability to sustain gravity live and dead load over long spans, however this type of frames provide a lateral load resist system[8].

Special truss moment frames and ordinary truss moment frames compared to solid web beams (plate girders)frames are more economical, details required for moment connections are simple because of their shapes, have higher strength versus weight ratios [7] [8].

As it was mentioned in section 2.1.2 the problem with TMF was the position of plastic hinges. Therefore, in 1994, Goel and Itani, at university of Michigan, have introduced Special Truss Moment Frames (STMFs).

In special truss, moment frames the position of plastic hinges and collapse mechanism can be control by fuses, which the designers consider them in the middle of the beam. When the lateral loads or earthquake load are applied to the frames the fuses start to work by dissipating energy coming from the loads. They reach inelastic region before other members of the structure. The practically repairable plastic hinges, according to their position (middle of beam) is one of the most important advantages of this system.

After the applied load (wind or earthquake), the members with plastic hinges can be repaired easily by replacing them with new ones.

2.1.4 Background

In 1994,Goel and Itani carried out the first research on STMFs, to investigate the moment truss frames with opening in the web. For this purpose a prototype structure based on Uniform Buildings Code 1998 (UBC 1998) was designed. three full-scale half-span truss columns were verified under cyclical load. Truss beams, where each panel has one single diagonal member, were also tested. The diagonal member was buckled under cyclic loading. The capacity of the diagonal member significantly was reduced after buckling. Typical load displacement diagrams are given in Figures 1.8 and 1.9.

In addition, the authors had several numerical analysis on this type of system they investigated the performance of the system under earthquake load. The researchers reached to the conclusion that because of the early failure and fracture in truss members the hysteretic behaviour of beams with openings in web is very poor[8].Furthermore, 1the dynamic nonlinear analysis has shown that such systems have very large drift at each story level with accompanying large inelastic deformations in columns and truss members[8]. The second study on STMFs was in 1994 at Michigan University. Goel and Itani tried to investigate the potential of using X pattern in STMFs. whilst the poor behaviour in the first research with single diagonal members was unsatisfactory the use of X pattern led to better result. Therefore, when one of the diagonal members was subjected to compression and buckled under load, the other diagonal member was subjected to tension and was capable of carrying the shear forces [9]. For this propose they have tested one story sub-assemblage consisting of full span truss and two columns in full scale and the results have shown that the structure had stable behaviour. In addition, the

researchers have conducted the dynamic time history analysis on the model to investigate the cyclic performance of the truss. The researchers have found that the system had excellent and efficient seismic resistance and suitable performance [9].

In 1994, Basha and Goel investigated the potential of energy dissipation of the Vierendeel segment. In their previous study, Goel and Itani [8] [9] placed the diagonal members at mid span of the truss. However, in this study, vierendeel segment was suggested; the work was based on an experimental test and numerical analysis. In experimental test a four story structure was selected and designed based on UBC 1991 code, then the STMF with and without gravity loads were tested [8] [9].

1-bay sub-assemblage of typical floor was examined. For this purpose, they tested the sub-assemblage without gravity force, two kinds of displacement histories were applied after the sub-assemblage was tested with gravity load. All tests have shown the hysteretic behaviour of the models is stable. The researchers terminated that the behaviour of the sub-assemblages under earthquake force, entirely as well as under combination of both gravity and earthquake force were without any pinched and degraded and stable. Patterns of modelling testimonial were nominated for this type of systems with a vierendeel special segment. The kinetic innate reflex from numerical studies on this system was excellent[7].Goel,and his colleagues Rai and Basha in introduced guidelines for the design of STMFs in 1998. Philosophy of limit states in design procedure was applied to special STMFs. The specific segment of the system awaited to yield for depreciate energy, whereas the other part of system shall behave elastically. Yielding was permitted only for the column bases. In this procedure, several laws based on performance criteria design were suggested to

division the truss components that placed outside of specific segment. STMFs, Design procedure with X pattern bracing and Vierendeel segment was informed by use of tested specimens both numerical analysis by computer and hand. After offering some rules for STMFs design procedure, researchers introduced several analytic responses on those representative designs. Nonlinear static analysis and dynamic time history analysis were organized to find out the limit state and performance the systems. The report terminated with a set of design, which was adopted by UBC 1997 requirements [5].In 2006,Parra-Montesinos,and his teammates Goel, and Kim worked on the performance and efficiency of built-up double-channel chords of STMF. Instead, of testing the complete truss, the authors focused on the chord components. the sections that used for this propose were Back-to-back channel sections , to maximize shear capability for STMFs which designed with a vierendeel segment. for this propose, 6 cantilever beams with double-channel components were under taken to modify cyclic earthquake load to find out the performance of them. The principal constant were to investigate lateral bracing and stitch spacing for the channel components. They reached to the conclusion that the AISC2010demands for lateral bracing and stitch spacing are not proportionate to make large rotation capability in built-up double-channel components. A new was suggested according to results of test [10]. The principal aim of the Chao and Goel with their research in 2008 was to recommend an equation for the awaited strength of shear the specific segment. The external components of the specific segment were adequate using capability design roots and the practical loads were derived according to strength of shear of specific segment. After the years, Goel et al investigated equation for the awaited shear strength and their improvements conduct to the code requirements. Chao and Goel investigated shear strength equations in the AISC2010

may lead to uneconomic and over design of the components where the moment of inertia is large. In order to develop a investigate equations, the researchers carried out pushover and nonlinear time- history analyses. The researchers terminated that the AISC2010 mathematical statements significantly overrate the awaited shear strength [11].

In 2008, Chao and Goel investigated plastic based design of STMFs. Before this study, elastic analysis method was used for design purposes. Elastic analysis purpose lead to have non-uniform distribution of yielding mechanism and story drifts in specific segments on the structure height, because of this reason to achieve a uniform distribution of drift story and yielding mechanism, the researchers tried to develop the plastic base design whereas this method based on energy theorem therefore the drift target shall be calculate [7]. According to the energy theorem, three definitions of design were changed. Base shear capacity was changed to target drift, yielding mechanism was changed and also elastic linear design spectrum was calculated for limit states in new proposal. The changed or developed base shear capacity in reality was equal to ultimate base shear of structure in collapse state; therefore, the base shear capacity can be calculated directly from plastic design. The result shown that the special base shear capacity calculated from codes is less than changed or developed base shear capacity by Goel and Chao in 2007 [12]. Finally the authors were tested a nine story building with STMFs subjected to the SAC earthquake load. The results were shown uniform story drift distribution along the height of building and maximum drift story was smaller than the target displacement [12].

Chapter

METHODOLOGY

3.1 Analysis Methods Used For This Study

3.1.1 Pushover Analysis

Nowadays nonlinear static (pushover) analysis became a well-known method of predicting seismic loads for the purpose of performance and limit states evaluation of existing and new structures. Nonlinear static (pushover) analysis is a relatively simple solution to the complex problem of predicting loads and deformation demands imposed on building and their components by severe earthquake loads. Nonlinear static (pushover) analysis is one of the analysis methods recommended by FEMA 273and Eurocode.

3.1.2 Advantages of Pushover Analysis

Nonlinear static analysis supply valuable in tuition on many response characteristics, such as, demand of load son potentially brittle components. It is a technique by that a building is subjected to a incremental lateral force. The following are data that can be obtained by using nonlinear static analysis [13].

- Strength degeneration effects of individual components on the whole structural behavior.
- Indicate unsafe area with high deformation demands.
- The process of cracks, yielding, plastic hinge formation and failure of various structural elements.

- The repeating analysis goes on, until to satisfies a pre-established criteria.
- Nonlinear static analysis is a very useful tool for the evaluation of new and existing structures. The following are the comparison of pushover analysis with other analysis methods.
- Offer useful data that cannot be obtained from other methods.
- It is approximate in nature and is according to static loading and it cannot represent the dynamic phenomena with a large degree of accuracy.
- It does not create good solutions, it only evaluates solution.
- Load pattern choice makes a huge difference to the analysis results.

3.2 Dynamic Time-History Analysis

Dynamic Time History Analysis (DTHA)is generally used to predict the nonlinear-inelastic response of a building subjected to ground motion loading. In addition, dynamic time history analysis may also be used for modelling of pulse loading cases. (e.g. blast, impact, etc.). In many cases instead of acceleration time-histories at the foundations, load pulse functions of any given shape (rectangular, triangular, parabolic, etc), can be used to find out the transient loading applied to the appropriate buildings. Based on Eurocode 8 [24] if time-history analyses are required, at least three pair of ground motion records should be used [14].

In order to investigate the behavior of the STMFs under major earthquakes pushover and time history dynamic analysis were performed using Seismostruct program. The design loading described in chapter 4 section 4.2and load combination of 1.1×(DL+LL), 0.9×(DL+LL) and (DL+LL) were applied to the frames for pushover and (DL+LL)+E (earthquake) also was applied for time history analysis.

3.3 Limit States Definition

3.3.1 Material Nonlinearity Limit States

Material nonlinearity is associated with the inelastic behavior of a component or system. Inelastic behavior may be characterized by a force-deformation (F-D) relationship, also known as a backbone curve, which measures strength against translational or rotational deformation. The general F-D relationship shown to the right indicates that once a structure achieves its yield strength, additional loading will cause response to deviate from the initial tangent stiffness (elastic behavior). Nonlinear response may then increase (hardening) to an ultimate point before degrading (softening) to a residual strength value[29].

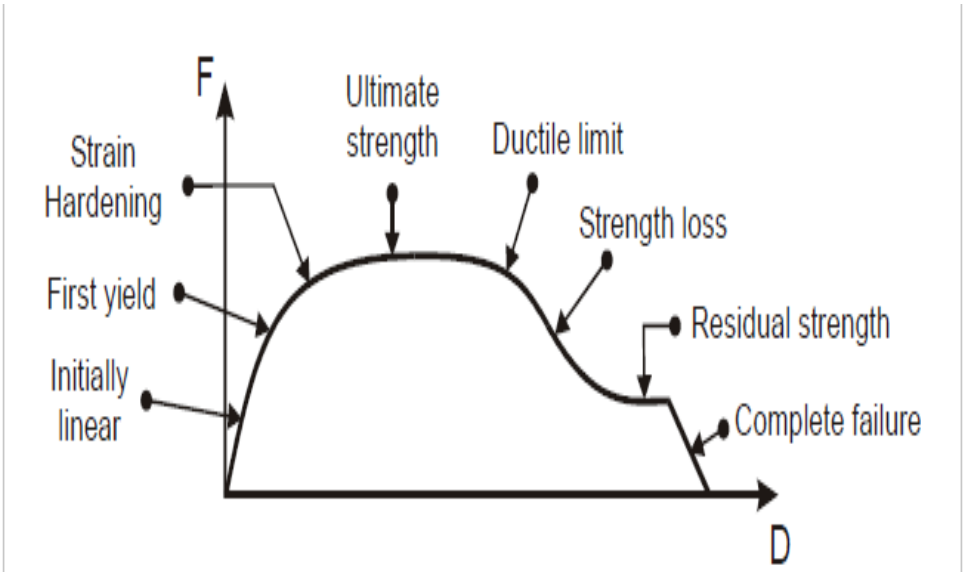

Figure 3.1: Material nonlinearity limit state [29]

A diversity of F-D relevance can delineate material nonlinearity, containing the following:

- Monotonic curve
- Hysteretic cycle

- Interaction surface

3.3.2 Monotonic Curve Limit States

- A monotonic graph is created when a load template is progressively applied to a member or system like that the deformation amount continuously increases from zero to an ultimate condition. The corresponding force-based type is then plotted according to this range, assigning the type of material nonlinearity.
- Nonlinear static analysis is a way which produce a monotonic graph response. The moment (P-M2-M3) hinge is one of the best suited for modeling a situation of nonlinear static analysis. Some in stances of monotonic F-D relevance covering stress-strain moment-curvature (axial), (flexure), and rotation of plastic-hinging.
- To make the expression simple, and to provide F-D relationship for numerically-efficient equation, the nonlinear graph may be simplified as a series of linear segments. Figure 3.2 presents one such model.

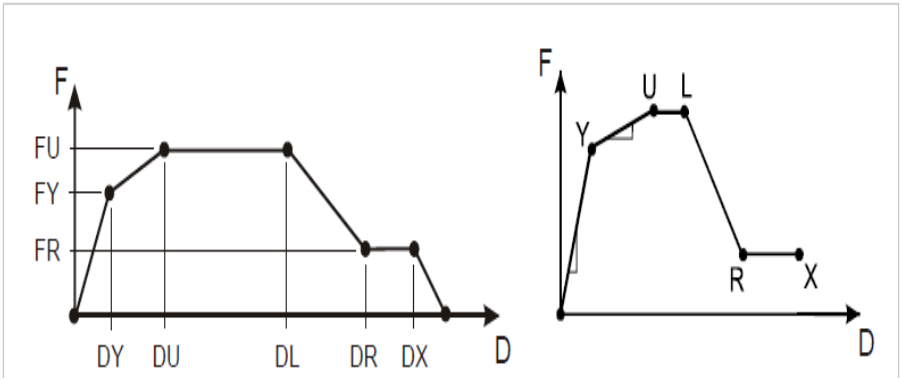

Figure 3.2: Monotonic curve limit states [29]

3.3.3 Serviceability Limit States

Parameters of Serviceability may then be surplus on to the nonlinear F-D relevance to purvey indicate in to building limit states performance. in this case for better understanding for general public and the limit states of performance indicate like the list below

- Immediate-Occupancy (IO)
- Life-Safety (LS),
- Collapse-Prevention (CP)

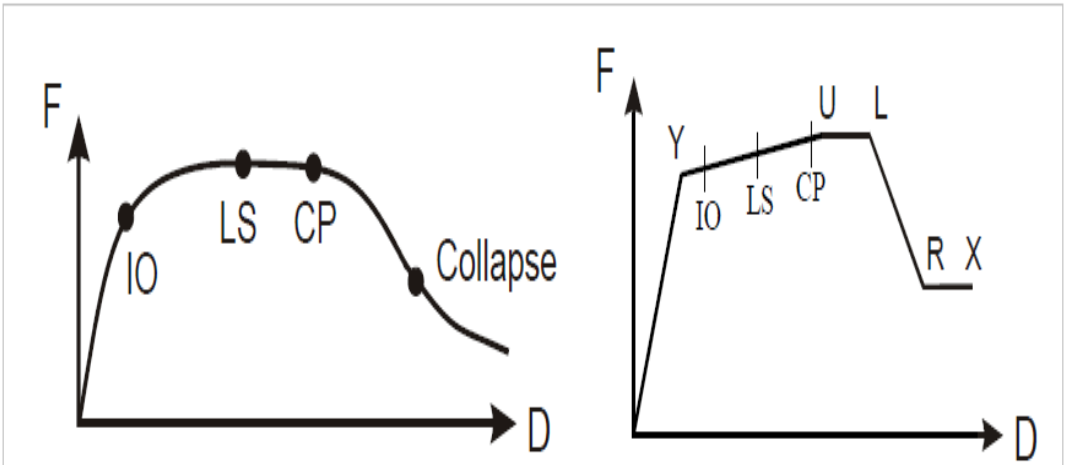

Figure 3.3: Serviceability curve limit states [29]

Limit states may also be specific to inelastic behavioral thresholds. For example, under static pushover, a confined reinforced-concrete column may experience 1) yielding of longitudinal steel, 2) spaling of concrete cover, 3) crushing of core concrete, 4) Fracture of transverse reinforcement, and 5) fracture of longitudinal steel [29]

Limit states may also be specific to inelastic behavior thresholds. For example under static pushover a confined reinforced-concrete column may experience : 1) yielding of longitudinal steel, 2) sapling of concrete cover, 3) crushing of core concrete, 4) Fracture of transverse reinforcement, and 5) fracture of longitudinal steel [29].

3.3.4 Hysteretic Cycle Limit States

Hysteretic cycle is also an indication for material nonlinearity. When cyclic loading is applied on a system or component then this may led to the development of the F-D relationship and hence the production of hysteretic loops. The fibre hinge is best applied when modeling hysteretic dynamics. Hysteretic behavior is illustrated in Figure3.4. Rotational deformation is an independent variable. As a result of the continuous reversal of the load orientation a plot showing the physical oscillation versus strength-based parameter is plotted. Hysteresis is useful for characterizing dynamic response under application of a time-history record.

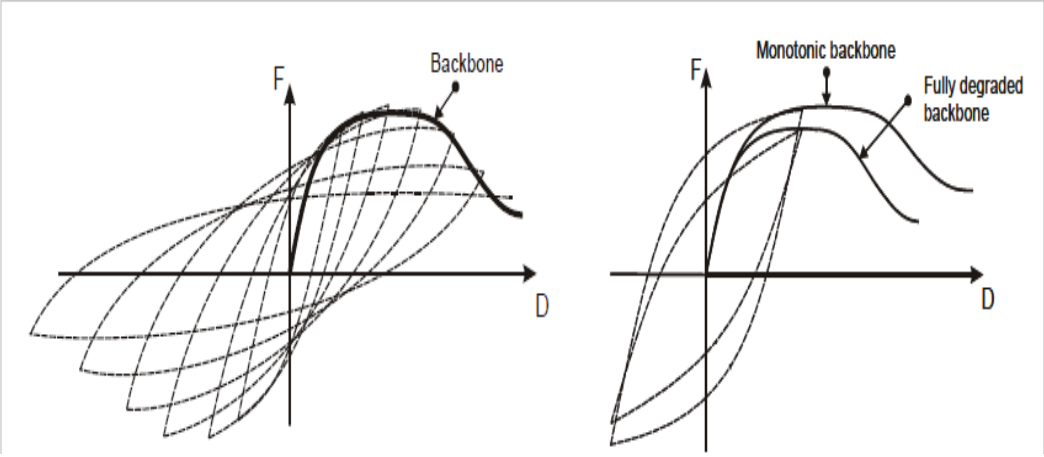

Figure 3.4: Hysteresis loop [29]

Figure 4 shows, both stiffness and strength deviate from their initial relationship once yielding occurs. This behavior advances with additional hysteretic cycles, and becomes more pronounced with greater inelastic deformations. Initially, strength

may increase through hardening behavior, though ultimately, stiffness and strength will both degrade through softening behavior. Whereas strength gain or loss are indicated by the strength level achieved, the decrease in slope upon load reversal indicates degradation of stiffness. During hysteretic behavior, while there is increase in the levels of deformation, a ductile system is the one that can maintain the strength levels after reaching the peak strength. The cyclic envelope is formed from the peak values of the profile obtained from the hysteresis loops. The backbone curve produced by the cyclic envelope will be less than the monotonic curve which would result from the same structure being subjected to monotonic loading. This may be attributed to strength and stiffness degradation. An important provision of nonlinear modeling is the accurate characterization of strength and stiffness relationships as a structure progresses through hysteretic behavior. There is a wide variety of hysteretic cycle patterns, which are influenced by structural geometry and materials.. Four possible hysteretic-behavior types are illustrated in Figure 3.5 [29].

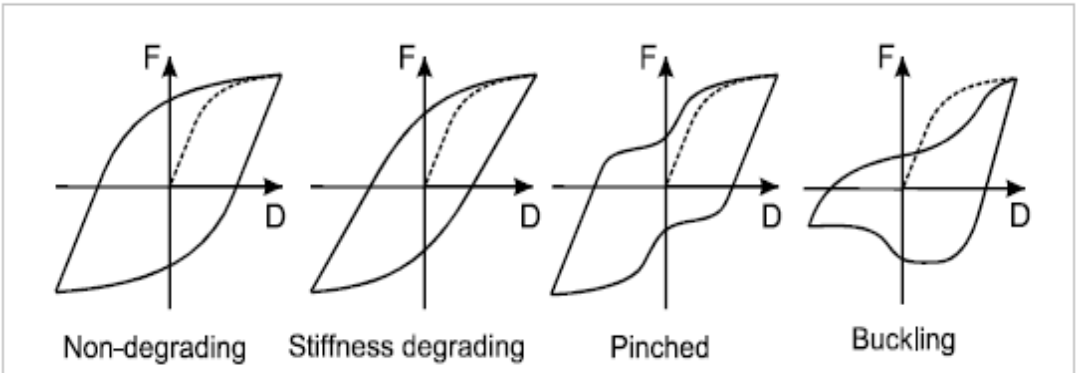

Figure 3.5: Hysteresis loop types [29]

Information on plotting hysteresis loops is available in the Plotting link hysteresis article.

3.3.5 Interaction Surface

Development of a inter action surface for a structural element is via the plot of a combined relationship between various strength parameters. For a given limit state a performance envelope via 2D or 3D surface development can be formed by using Von Mises, Mroz or plasticity. An outside envelope performance measure means that the behavior exceeds the limit state. An example; yielding of a column under combined axial, strong-axis and weak-axis bending described by 3D P-M2-M3 interaction surface. Interaction of the P-M2-M3 performance measures can be plotted to create a 3D ellipse. Column is considered to be yield when the response is measured outside of the P-M-M envelope.

3.4 Geometric Assumptions

4, 7 and 10 story frames were designed. Each frame has 5 bays in x-direction, each with 9.14 m of span length (Figure 3.1). All frames were modelled and designed in two-dimensions. Each frame model has one basement level with 4.3 m high. First floor has 5.5 m and the rest of the floors have 4.3 m floor height. ETABS v 9.7.4 was used for the main design and Eurocodes 1, 3 and 8 were used as references. Since there is no consideration of special truss moment frames in the Eurocodes, AISC2010 and FEMA 356 were also used in some cases. Since the reliability class was considered in class 1 therefore the collapse performance level expected.

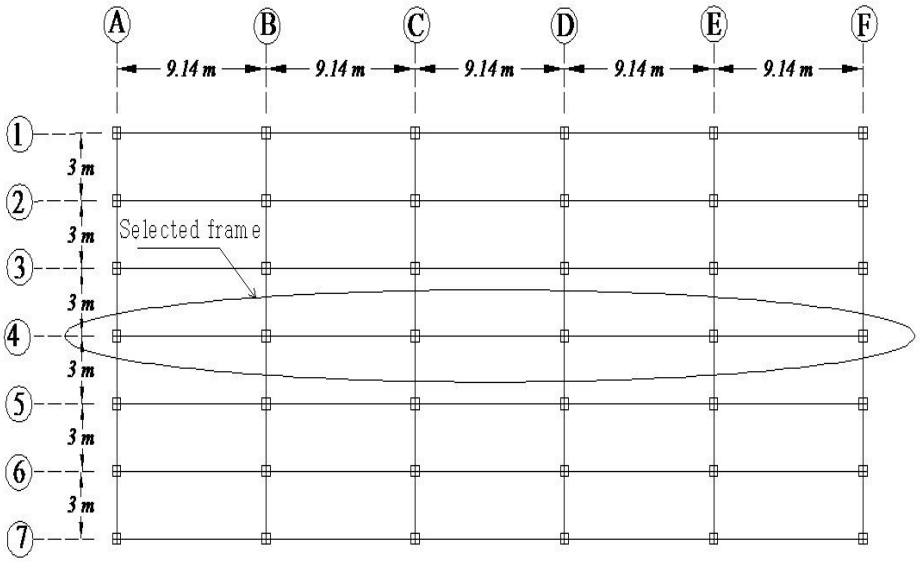

Figure 3.6: Plan layout of models

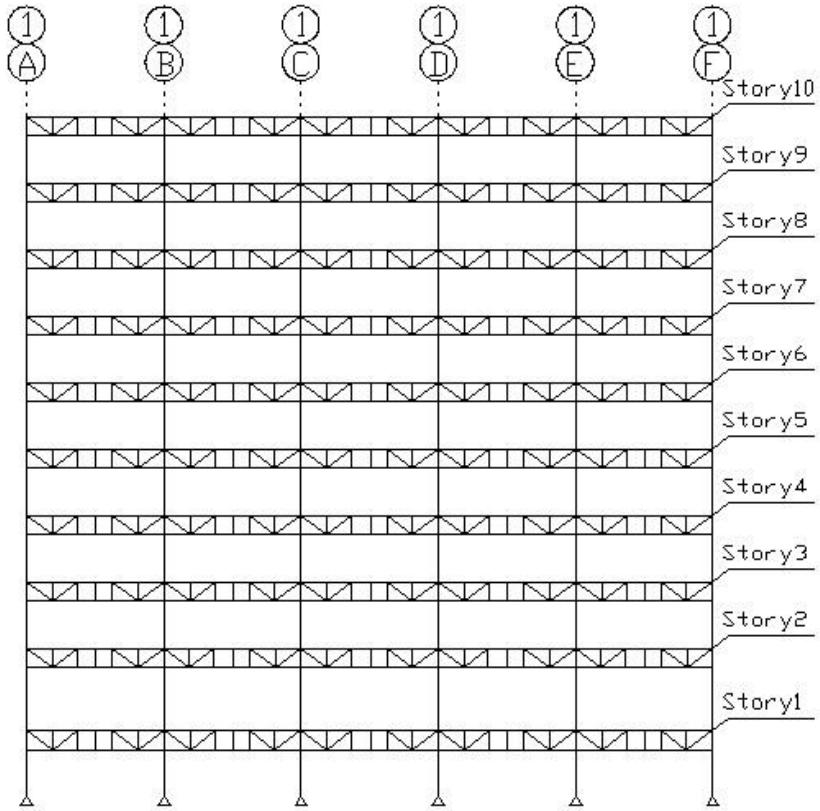

Figure 3.7: Elevation of Frame1

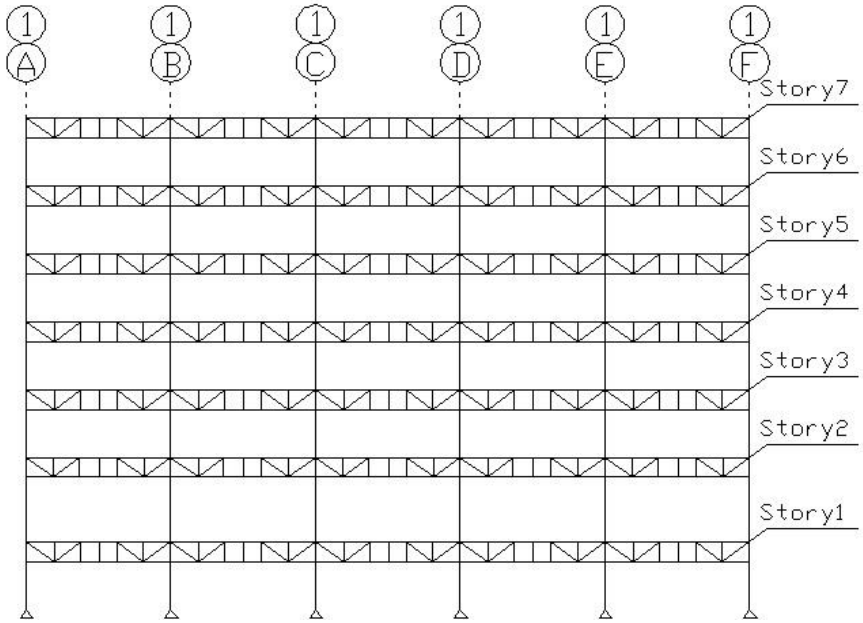

Figure 3.8: Elevation of Frame 2

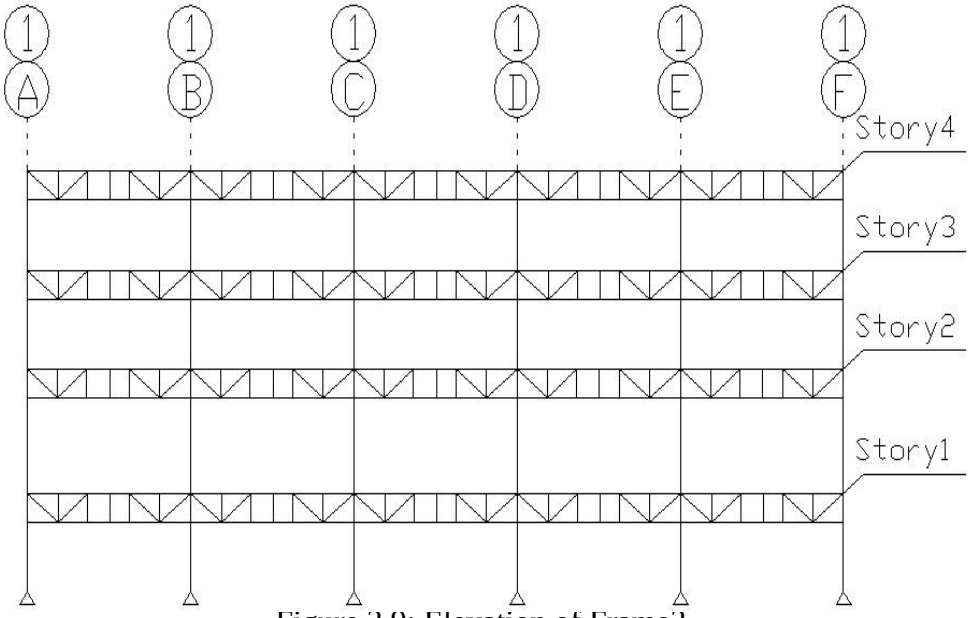

Figure 3.9: Elevation of Frame3

3.4.1 Calculation of Dead and Live According to Eurocode 1

Dead and live loads were calculated by using Eurocode 1[15], and it has listed in Table 3.1[15].

Table 3.1: Loading parameters according to Eurocode 1 [15]

	Load	unit
Roof dead load	600	kg/m^2
Typical floors dead load	600	kg/m^2
Typical floors live load	500	kg/m^2
Roof live load	150	kg/m^2
Design live load participations	40%	%

3. 4.2 Earthquake Load Calculations

3.4.3 Calculations of Period T_1

$T_1$is the fundamental period of vibration of the building for lateral motion in the direction considered [14].According to the Eurocode 8 for structures with up to 40m height the period $T_1$is

$$T_1 = C_t.H^{3/4} \quad (3.1)$$

C_t is 0.05For all other structures including STMFs

H is the height of structure in meters

T_1= 0.793

3.4.4 Calculation of Base Shear According to Eurocode 8 [14]

3.4.5 Identificationof Ground Type According to Eurocode 8

Table 3.2: Soil type parametersaccording to Eurocode 8 [14]

Ground type	S	Tb(s)	Tc(s)	Td(s)
B	1.2	0.15	0.5	2

$$`F_b = S\ (T_1) \times m \times \lambda \quad (3.2)$$

$S_d(T_1)$ is the ordinate of the design spectrum at the T_1

T_1 is the fundamental period of vibration

M is the total mass of the building

λ is the correction factor the value of which is equal to $\lambda=0.85$

and the building has more than two story or $\lambda=0$ otherwise

3.4.6 Mass Calculation of Frame 1

According to the Figures 3.1 and 3.2dimensions and Table 3.1:

The total live load for Frame 1 is 2,550,060 N

The total dead load for Frame 1 is 8,226,000 N

Table 3.3: Recommended values of parameters describing the vertical elastic response spectra according to Eurocode 8 [14]

Ground type	Avg/ag	Tb(s)	Tc(s)	Td(s)
B	0.90	0.05	0.15	1

$$0.9 * 1.2 * \frac{2.5}{4} * \frac{0.15}{0.793} = 0.128 \qquad 2 < q < 4$$

$$3.9 \begin{cases} 3 * {a_u}/{a_1} \\ \frac{a_u}{a_1} \end{cases} \text{DCM}$$

$F_b=0.128\times1105\times1=1414.4kN$

3.4.7 Stability Index of Frame 1

Table 3.4: Stability index of frame 1

Story	Ps	Pi	Si	Hi	θ
W10	107783	107783	0.0102	39.9	0.0025
W9	264757	156974	0.0128	35.6	0.0026
W8	422331	157574	0.0138	31.3	0.0022
W7	581009	158678	0.0134	27.0	0.0020
W6	740398	159938	0.0134	22.7	0.0020
W5	900286	159887	0.0130	18.4	0.0021
W4	1060770	160484	0.0120	14.1	0.0024
W3	1222309	161539	0.0090	9.80	0.0024
W2	1393616	171307	0.0060	5.50	0.0030
W1	1563167	169552	0.0000	0.00	0.0000

S_i is relative displacement in rigid point of story

V_i is shear force of stories

H_i is height of story

$$F_{i=}F_{b}\frac{W_i h_i}{\sum W_i h_i}(3.3) \qquad (3.3)$$

F_i is the horizontal force acting on story i.

F_b is the seismic base shear

H_i,h_j are the heights of the masses w_i,w_j above the level of application of the Seismicaction (Foundation or top of a rigid basement).

W_i,w_j are the story masses

$$\sum_{j=1}^{m} W_i h_i = 109.680(4.3 + 9.8 + 14.1 + 18.4 + 22.7 + 27 + 31.3 + 35.6 + 39.9)$$

$$+ 90.484 * 44.2) = 25{,}803.78 \ \text{ton} - \text{m}$$

$$F_1 = 141.44 \times \frac{109.680 \times 4.3}{25803.777} = 2.585 \text{ tonnes}$$

According to equation (3.3) the horizontal force for each story is calculated (Figure 3.5)

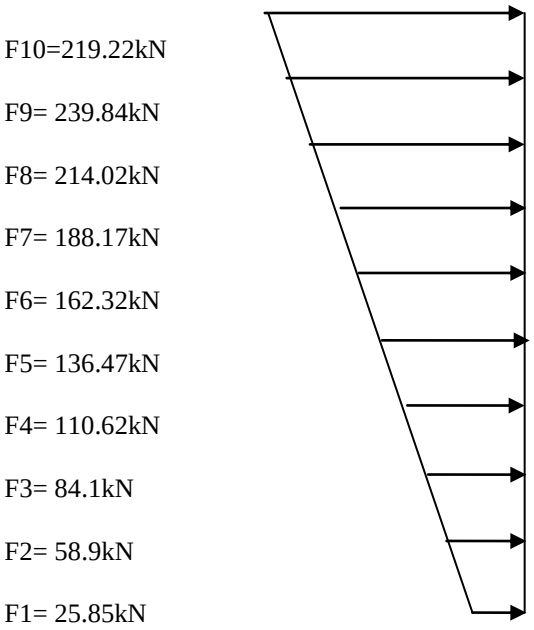

Figure 3.10: Base shear diagram Frame 1

3.4.8 Base Shear Calculation of Frame 2

According to equations and procedure in section 3.1.3 the Figure 3.11 shows the base shear and horizontal force distributions for Frame 2.

Table 3.5: Horizontal force of Frame 1

Story	h_s (m)	h_i (m)	w_i	$\sum W_i h_i$	f_i kN
w10	4.3	39.9	90.48	25803.8	219.220
w9	4.3	35.6	109.68	25803.8	239.384
w8	4.3	31.3	109.68	25803.8	214.020
w7	4.3	27.0	109.68	25803.8	188.170
w6	4.3	22.7	109.68	25803.8	162.320
w5	4.3	18.4	109.68	25803.8	136.470
w4	4.3	14.1	109.68	25803.8	110.620
w3	4.3	9.8	109.68	25803.8	84.100
w2	5.5	5.5	109.68	25803.8	58.900
w1	4.3	0.0	109.68	25803.8	25.850

F7 =270.6kN 258.3kN

F6= 283.0kN 496.0kN

F5=237.9 kN 695.8kN

F4=192.8 kN 857.8kN

F3=147.8 kN 981.9kN

F2=102.7 kN 1068.1kN

F1=44.0 kN 1106.1kN

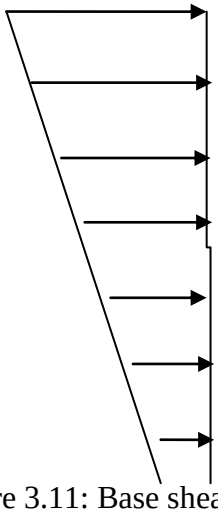

Figure 3.11: Base shear diagram Frame 2

3.4.9 Base Shear of Frame 3

According to equations and procedure in section 3.1.3 the horizontal force distributions for Frame 3 is listed below.

F1=115.6 kN

F2=263.5 kN

F3=379.1 kN

F4=408.1 kN

3. 4.10 Steel Sections Used for Model Frames

In this study, the European steel sections were used to design the structures (Fig. 3.12, Table 3.6 to 3.8).

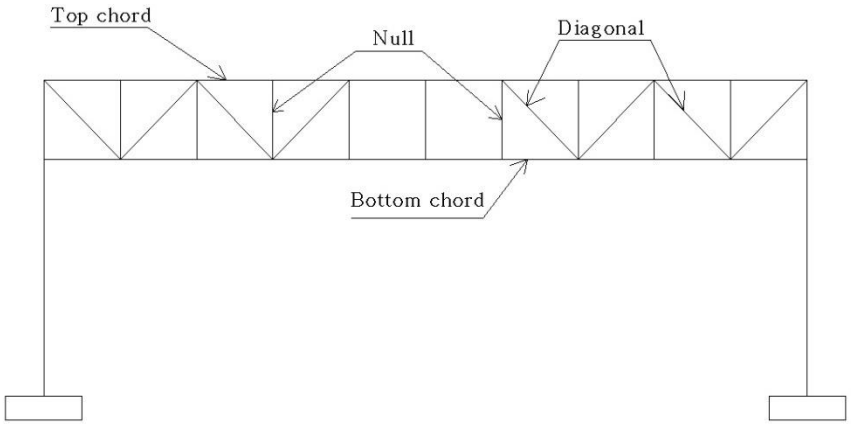

Figure 3.12: Positions of elements.

Table 3.6: Section properties of Frame 1

Storey	Column	Top chord	Bottom chord	Diagonal	Null
10	180x180x12.5	HEA100	HEB100	60x60x4.00	60x60x4.00
9	180x180x20	HEA100	HEB140	60x60x8.00	60x60x8.00
8	200x200x25	HEA100	HEB140	70x70x5.00	70x70x12.5
7	240x240x25	HEA100	160HEB	70x70x8.00	80x80x14.2
6	240x240x28	HEB100	160HEB	70x70x10.0	90x90x17.5
5	240x240x35	HEB100	160HEB	70x70x12.5	90x90x17.5
4	280x280x30	HEB120	HEB160	70x70x12.5	100x100x16
3	280x280x30	HEB120	HEB160	80x80x12.5	120x120x2.5
2	320x320x35	HEB120	HEB180	80x80x14.2	120x120x17.5
1	320x320x35	HEA100	HEB120	70x70x8.00	80x80x14.20

Table 3.7: Section properties of Frame 2

Storey	Column	Top chord	Bottom chord	Diagonal	Null
7	180x180x20	HEA100	HEB100	60x60x4.00	60x60x4.00
6	200x200x25	HEA100	HEB140	60x60x8.00	70x70x10.0
5	200x200x30	HEA100	HEB140	70x70x10.0	80x80x14.2
4	240x240x25	HEA100	HEB160	70x70x12.5	90x90x12.5
3	260x260x25	HEB100	HEB160	80x80x12.5	90x90x17.5
2	280x280x30	HEB120	HEB180	80x80x14.2	100x100x16
1	280x280x30	HEA100	HEB120	70x70x8	80x80x14.2

3.4.11 Properties of Ground Motions

Three pairs of ground motions were used in this thesis (Table 3.9). Based on the assumption that the ground motions were in short period range (less than 50km) and the soil type was type 2 near fault, therefore 6-ground motion was selected from Peer ground motion database [16].

Table 3.9: Properties ofground motions obtainedfrom Peer ground motion Database

	Name	Date	Duration	PGA	Effectiveduration
1	KoBe1	1/16/1995	48"	0.599g	9.5"s
2	KoBe2	1/16/1995	48"	0.821g	10.7"s
3	North ridge E1	1/17/1994	38"	0.514g	8.54"s
4	North ridge E2	1/17/1994	38"	0.568g	9.08"s
5	superstitio 1	11/24/1987	36"	0.682g	12.28"s
6	superstitio 2	11/24/1987	36"	0.894g	12.24"s

3.4.12 Ground Motion Matching (Scaling Procedure)

Based on Eurocode 8 and AISC 341-10code,each paired ground motion with 5 per cent damping were scaled with maximum gravity acceleration and response spectrum. Then each pair of ground motions were combined together to build one individual response spectrum. The period of each model was separately calculated. Eventually the average response spectrum of each three pair of ground motions and the responses between the period of 2.0T and 0.2Twere calculated. The chosen factor was greater than 1.4 times of the standard response [1].

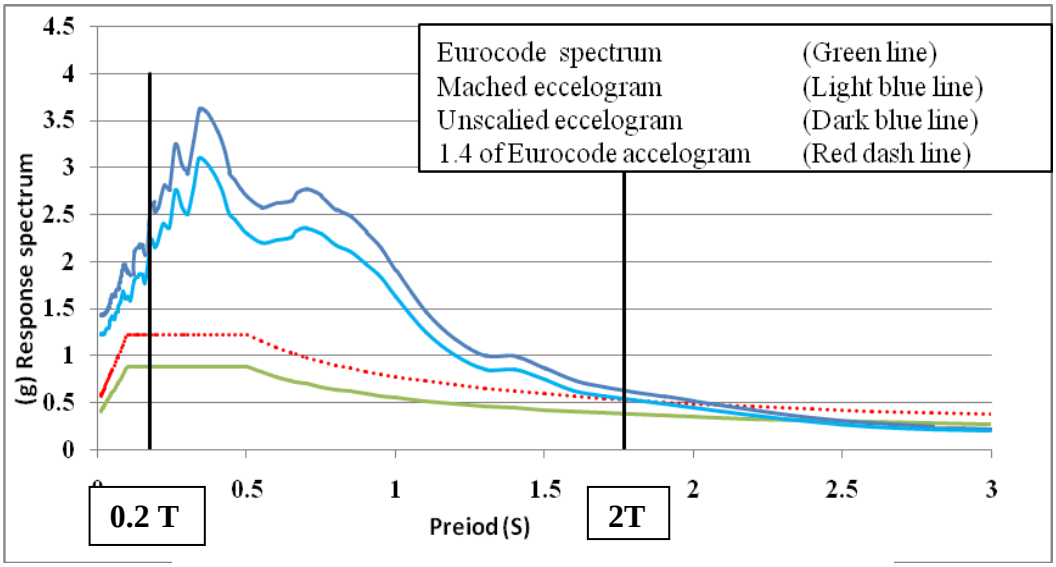

Figure 3.16: Scaled ground motion spectrum of Frame 1

3.5 Design Procedure of STMF According to AISC2010

3.5.1 Collapse Mechanism

In STMFs some of the openings were designed for inelastic deformation or they were in inelastic region subjected to lateral loads. These segments shall with stand gravity loads. Therefore, the best place to arrange the segments is the middle of the truss beam where the shear force due to the gravity loads is very small .By increasing the lateral loads after the buckling of diagonals members (segments), the plastic hinges may appear in the connections of horizontal, vertical and diagonal members. Plastic hinges can clearly be seen in Figure 3.15.

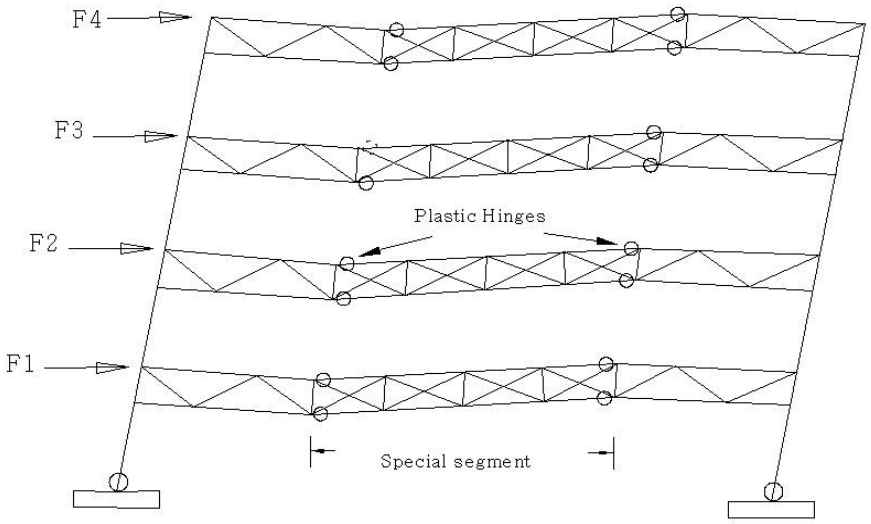

Figure 3.17: Yielding mechanisms for STMFs [3]

3.5.2 Requirements, Limitations and Rules of STMFs in AISC Code [1]

STMFs are expected to behave elastically with specially designed members (segments) when subjected to lateral loads like earthquake or wind (Fig. 3.16). According to AISC 341-10 code[1] the maximum span length is limited to20m(65ft).The overall maximum depth of the truss is also limited to 1.8m (6ft).All column and truss segments except special segment will be able to withstand elastic region [1].

$$1.8\ \text{m} \leq \text{L} \leq 20\ \text{m} \tag{3.4}$$

$$0.1 \leq \frac{LS}{L} \leq 0.5 \tag{3.5}$$

$$\frac{2}{3} \leq \frac{LP}{D} \leq \frac{B}{2} \tag{3.6}$$

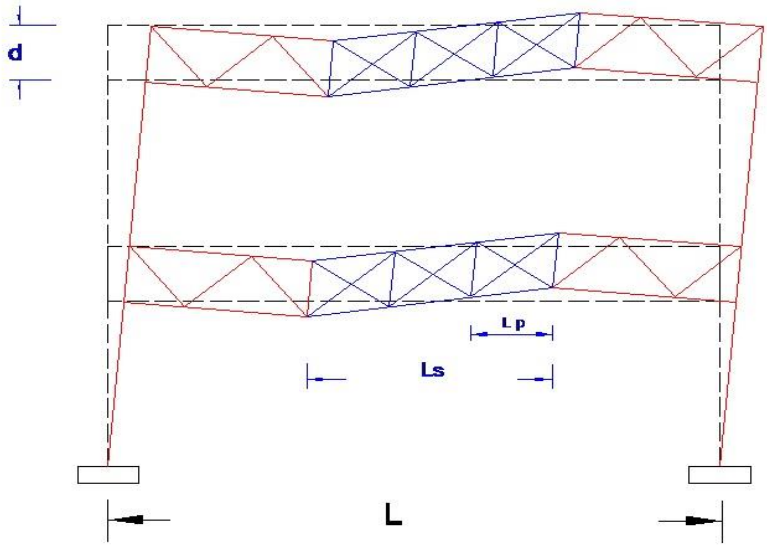

Figure 3.18: Limitation of STMFs [1]

3.5.3 Special Segment [1]

Each horizontal truss shall have a specific segment in quarter of the span length. The length of the special segment can be between 0.1 to 0.5 times the truss lengths. Length to depth ratio recommended being between0.67 and1.5. Special part of the truss segment should be either all Vierendeel or all X braced panel (Fig. 3.17).The combinations of these patterns are not allowed in design. Each member of the X pattern used by special segment members is separated by vertical component. Each diagonal component interconnects at points where they cross each other. The interconnection should satisfy the 0.25 times the nominal tensile strength of diagonal component. Bolted connections cannot be used in web components of special segment. Flat bars and identical sections should be used for each diagonal web components. The chord components are not allowed to splice within the special segment, nor within one-half of the segment length from the ends of the specific segment. The required axial strength of the diagonal web components in the specific segment due to dead and live loads within the specific segment shall not exceed $0.03F_yA_g$ (LRFD) or$(0.03/1.5)$ F_yA_g(ASD), as appropriate.

F_y is yield strength.

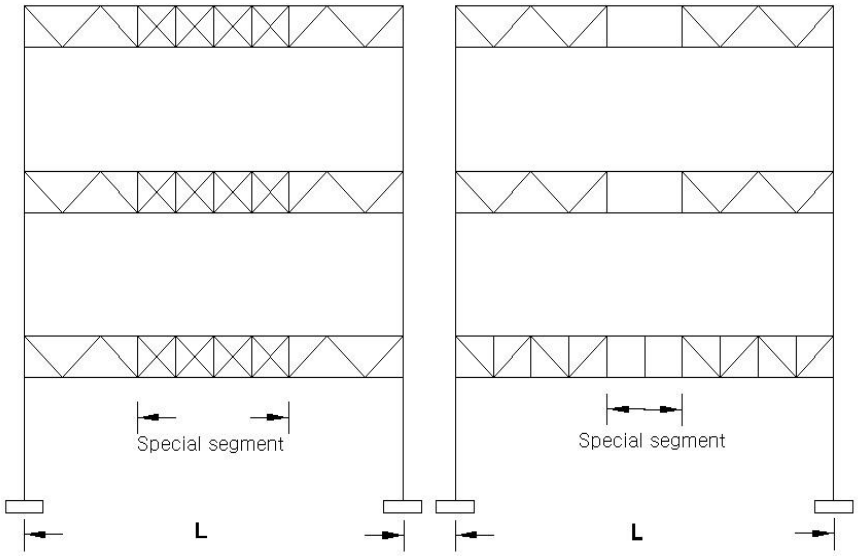

Figure 3.19: STMFs with two different type of segment

3.5.4 Strength of STMF According to AISC 341-10 Code [1]

The required shear strength of specific components shall be designed for summation of the require shear strength of the chord components through the flexure and in addition the shear strength corresponding to the require tensile strength and 0.3 times of require compressive strength of the diagonal components. The identical sections were used for top and bottom of the chord components and are prepared with a minimum value of 25 percent of the needed vertical shear strength. The axial strength needed in the chord components, measured based on the performance state of tensile yielding, cannot be greater than 0.45 times φP_n (LRFD) or P_n / Ω (ASD), as appropriate.

$$\varphi = 0.90 \text{ (LRFD)} \quad \Omega = 1.67 \text{ (ASD)} \tag{3.9}$$

Where

$$P_n = F_y A_g \tag{3.7}$$

The connections at the end of diagonal web components in the specific panel shall satisfied strength which is at least equal to the expected yield strength, in tension of the web member, $R_y F_y A_g$ (LRFD) or $R_y F_y A_g$ / 1.5 (ASD), as appropriate.

3.5.5 Strength of Non-Special Segment Members [1]

STMF components and connections should satisfy the strength as per the building code, except for the special segment detailed in AISC 341-10section 12-2..Replacementofthe lateral load, term E, with the earthquake load is essential to improve the vertical shear strength expected from the specific panel.

V_{ne} (LRFD) or V_{ne} /1.5 (ASD), as appropriate, at mid-length, given as:

$$v_{ne} = \frac{3.75R_y M_{nc}}{L_s} + 0.075EI\frac{(L - L_s)}{L_s^3} + R_y(P_{nt} + 0.3P_{nc})sin\alpha \qquad (3.8)$$

Where

M_{nc} symbolic flexural strength of a specific segment, chord component,

EI symbolic flexural elastic stiffness of a specific segment chord component

L distance between columns, in (mm)

L_s specific segment length, in (mm)

P_{nt} specific segment, diagonal component's symbolic tensile strength

P_{nc} specific segment, diagonal component's symbolic compressive strength

α angle of diagonal component with the horizontal.

3.5.6 Width-thickness limitations [1]

Diagonal web and chord components within the specific panel can be satisfy the essentialities of Section 8.2bof the AISC 341-10 code.

3.5.7 Lateral Bracing

At the ends of the specific segment lateral bracing can be provided to the top and bottom chords of the trusses at a spacing not greater than L_p (Specification Chapter F), along the whole length of the system. The strength needed for each transverse brace at the ends of and within the specific segment can be:

$$v_{ne} = \frac{3.75 R_y M_{nc}}{L_s} + 0.075 EI \frac{(L - L_s)}{L_s^3} + R_y (P_{nt} + 0.3 P_{nc}) sin\alpha \qquad (3.9)$$

$P_u = 0.06\ R_y\ P_{nc}$ (LRFD) or

$P_a = (0.06/1.5)\ R_y\ P_{nc}$ (ASD), as suitable,

Where

P_{nc} is the nominal compressive strength of the special segment chord members.

Lateral braces outside of the special segment shall have a required strength of

$P_u\ 0.02\ R_y\ P_{nc}$ (LRFD) or

$P_a\ (0.02/1.5)\ R_y\ P_{nc}$ (ASD), as appropriate

The needed brace stiffness can meet.

$P_r = P_u = R_y\ P_{nc}$ (LRFD) or

$P_r = P_a = R_y\ P_{nc}\ /1.5$ (ASD), as appropriate.

3.6 Determination of Performance Limit States

In SAP2000 program, the performance of limit states can be defined manually or by program defaults. Pushover analysis was used to create the hinge properties.FEMA-356 criteria was used to provide default hinge properties. According to codes each element has specific factor based on material, load type and reaction of element when subjected to load. Therefore, according to FEMA 356 2 types of plastic hinges

were defined in the program for3-performance levels. The plastic hinge properties are shown in Table 3.10.

Table 3.10: Plastic hinge properties

Element type	Hinge property name	Hinge type	IO	LS	CP
Beam	Beam M3	Deformation controlled	1	6	8
Beam	Beam M2	Deformation controlled	1	6	8
Beam	Beam P	Deformation controlled	1	6	8
Brace	Brace M3	Deformation controlled	1	6	8
Brace	Brace P	Force controlled	1	6	8
Column	Column P	Force controlled	1	6	8
Column	Column M3+M2	Deformation controlled	1	6	8

Chapter

SEISMOSTRUCT ANALYSIS RESULTS AND DISCUSSIONS

4.1 Introduction

In primary work, ETABS software was used to design different storey frames. The models designed which are 4, 7 and 10 floor frames were designed based on Eurocode 8 and 3 [14] [28] requirements. In Eurocode 3 and 8 there is no consideration and limitation for special moment truss frames, this deficiency was amended by supplementing ASCI2010code into the model design for this study. Applying limit state in Seismostruct software is not available and the software has default performance criteria based on Eurocode 8 [14].

Nonlinear static (pushover) analysis and dynamic time history analysis carried out to find the parameters, which listed below.

1) Performance criteria -section curvature
2) Performance criteria –chord rotation
3) Performance criteria- steel strain
4) Maximum base shear and drift from pushover analysis
5) Maximum base shear and drift carried out from dynamic time history analysis
6) Performance criteria –shear force
7) Hysteretic graph of element in plastic region
8) Interstory drift of frames

9) Maximum shear of story

10) Ductility(behaviour factor) of each model by using pushover analysis

4.2 Load Combination of Each Analysis and Calculation of Period, s

According to the Eurocode 8 [14] and FEMA 356 [24] the load, combination are given in Table 4.1.

Table 4.1: Loading parameters

No	Load Type	Load Case Name
1	Gravity-Pushover	Gravity 1.1 × (DL+LL)
2	Gravity-Pushover	Gravity 0.9 × (DL+LL)
3	Gravity-Pushover	Gravity (DL+LL)
4	Earthquake	Kobe
5	Earthquake	Kocaeli
6	Earthquake	Imprial-Valley
7	Earthquake	Chichi
8	Earthquake	Lemo-perieta
9	Earthquake	Northridge

4.3 Results of Pushover Analysis

Based on effective mass factors, which are less than 75%, the linear distribution load factor was selected. For this reason, 90% of the mass was participated in the mode that it was used. Tables 4.2 to 4.4 give the period and effective mass factors for Frames 1 to 3respectively. Capacity curves for Frame 3 with various load combinations are given in Figure 4.1.

Table 4.2: Period and effective mass factor for Frame 3

Mode	Mode period (s)	Effective mass factor	Accumulated mass factor
1	1.0100	0.6849	0.6849
2	0.3657	0.0532	0.7382
3	0.7508	0.0125	0.8139
4	1.0000	0.2492	0.0606

Table 4.3: Period and effective mass factor for Frame 1

Mode	Mode period (s)	Effective mass factor	Accumulated mass factor
1	1.7690	0.6501	0.6501
2	0.7054	0.1168	0.7669
3	0.4335	0.0470	0.8139
4	0.3135	0.0287	0.8427
5	0.2389	0.0191	0.8618
6	0.1878	0.0154	0.8773
7	0.1464	0.0130	0.8903
8	0.1098	0.0125	0.9028
9	0.0714	0.0191	0.9219
10	0.0402	0.0779	0.9999

Table 4.4: Period and effective mass factor forFrame 2

Mode	Mode period (s)	Effective mass factor	Accumulated mass factor
1	1.4620	0.6499	0.6499
2	0.5963	0.1195	0.7694
3	0.3740	0.0433	0.8127
4	0.2622	0.0255	0.8383
5	0.1894	0.0175	0.8558
6	0.1270	0.0187	0.8745
7	0.0545	0.1255	1.0000

Table 4.5: Total drift and base shear according to target displacement

		Frame 1		Frame 2		Frame 3	
No	Pushover load	Total drift (cm)	Base shear (kN)	Total drift (cm)	Base shear (kN)	Total drift (cm)	Base shear (kN)
1	1.1x(DL+L)	0.0071	1900	0.0087	1700	0.0094	1450
2	(DL+LL)	0.0071	2000	0.0087	1800	0.0104	1500
3	0.9x(DL+L)	0.0066	2200	0.0082	2000	0.0101	1600

4.3.1 Investigation of Base Shear Obtained From Frame 3 Pushover Analysis

Considering the capacity curves of Frame 3 for three different loading combinations the average displacement is 0.906 m and the average base shear is 1500 kN.

However, the static base shear calculated according to the Eurocode 8 is 1238kN. Therefore, the estimated base shear is nearly 80 percent of the one obtained from pushover analysis. Figure 4.1 give base shear versus displacement graphs where the first plastic hinge occurs at a displacement of 0.25 m and 1400 kN was the force responsible for pushing force. So from the results in Tables 4.2 to 4.5 and graphs of inter story drift that belong to Frame 3, it is clear that the first plastic hinge will appear in Floor 1.

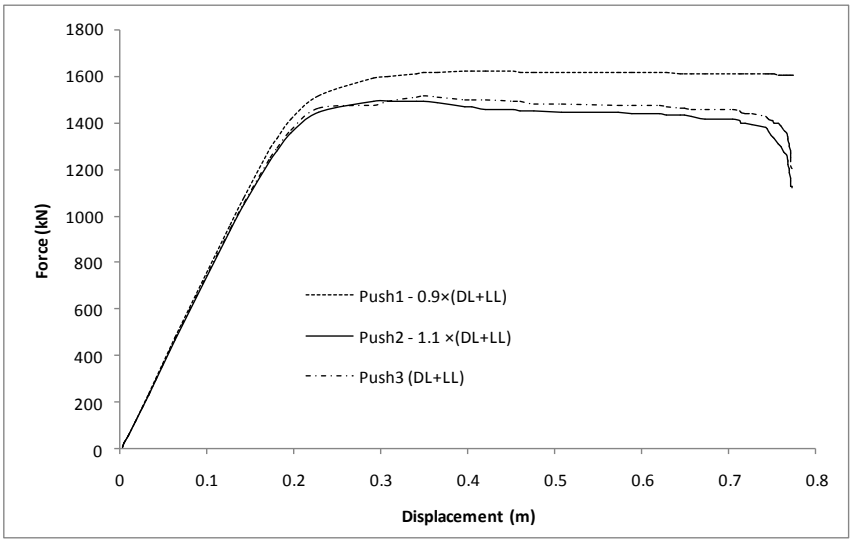

Figure 4.1: Capacity curves of Frame 3 with three load combinations

4.3.2 Investigation of Base Shear for Pushover Analysis of Frame 2

For Frame 2, the base shear versus displacement graphs shows that the average base shear is 1780 kN and the first plastic hinge happened at 0.35 m of target point displacement. However, according to Eurocode 8, the base shear calculated for Frame 2 is 1280 kN. Hence, the estimated static base shear is nearly 80 percent of the one from pushover results. According to Seismostruct pushover analysis result the first failure and first plastic hinges appear at floor 6, therefore, the first plastic hinges occurred in mode 2 or at higher modes (Figure 4.2).

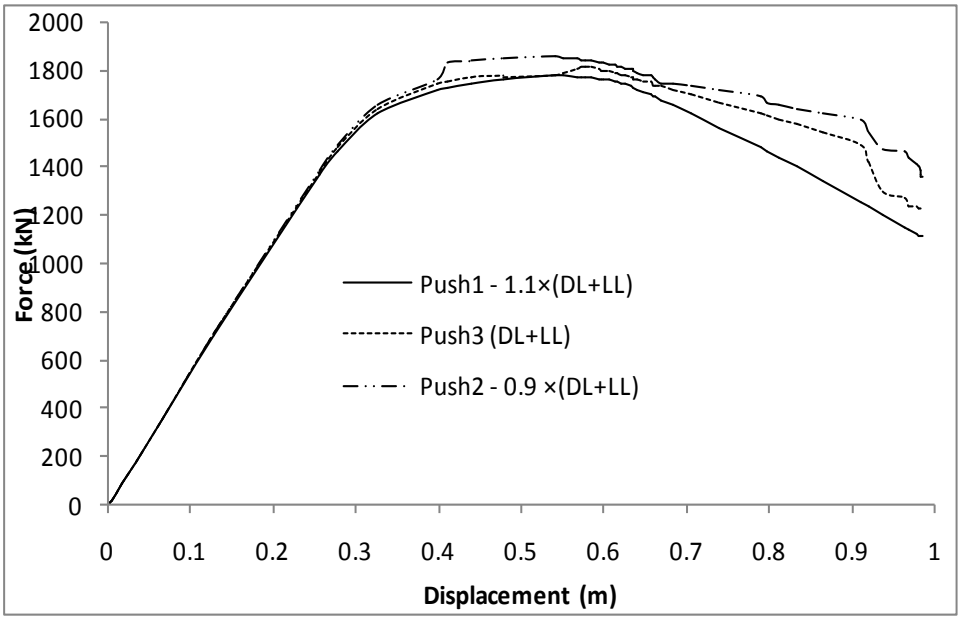

Figure 4.2: Capacity curves of Frame 2 with three load combinations

4.3.3 Investigation of Base Shear of Pushover Analysis of Frame 2

The base shear and displacement of Frame 1 shows that the average displacement of these three loading system analysis is about 0.45 m and of the base shear is 1835 kN. However, the estimated base shear force according to Eurocode 8 is about 1400 kN. Once again, the static base shear is nearly 80 percent of the base shear came from pushover analysis (Figure 4.3).

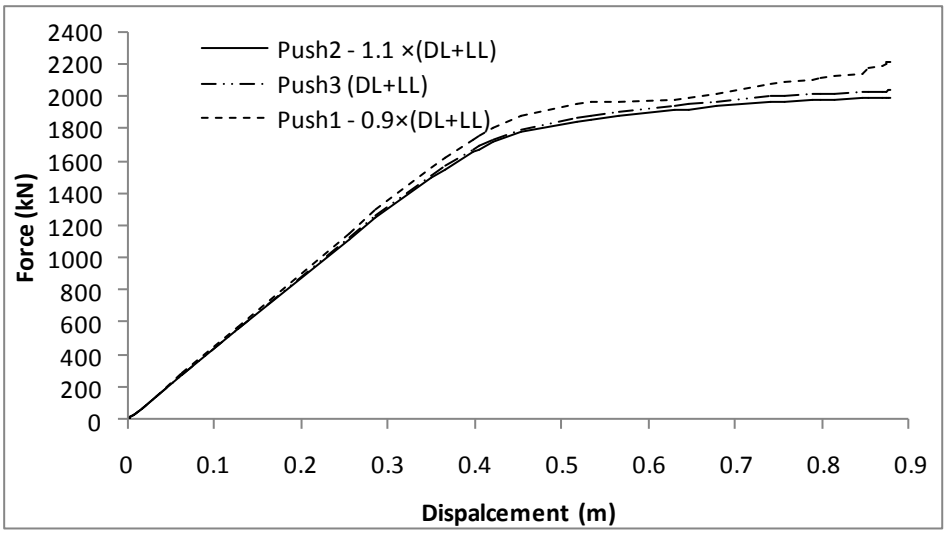

Figure 4.3: Capacity curves of Frame 1with three load combinations

4.4 Dynamic Time History Analysis Results

The response of a structure can be calculated by using its dissipated energy during an earthquake. The damping viscous energy of inelastic analysis can be estimated through the inelastic behaviour of members.

4.4.1 Investigation of Energy Dissipation of Frame 1

In STMFs engineers place fuses, preferably in the middle of beam, so that when subjected to earthquake loads these fuses dissipates the earthquake energy by turning to plastic region. However, the other members of structure remain elastic and damages can be controlled. One of the advantages of Seismostruct is that it provides the percentage of energy dissipated by the structural members.

Inelastic energy dissipated by Frame 1 range from 11 % to 15 %, and BETA-K viscous energy ranges from 32 % to 41% for used ground motions. However, the ALPHA-M viscous varies from 10 % to 11 % and the highest energy dissipation was in modal damping,32 % to 36 %.The lowest energy dissipation was by strain energy, range between-9 % to 1%respectively according to Table 4.6.

Table 4.6: Energy dissipation percentage of Frame 1

Earthquake load	Dissipated inelastic energy	BETA-K viscous energy	ALPHA-M viscous energy	Modal damping energy	Strain energy	Maximum Energy kgf-cm(10^{7})
Kobe	13.75	38.14	9.68	32.93	5.5	1.57
Kocaeli	12.03	40.72	10.31	35.74	1.2	1.49
Imperial-Valley	12.2	36.77	10.14	34.53	6.36	1.49
Chichi	11.51	39.01	10.82	36.25	2.41	1.44
Lemo-perieta	15.12	32.3	10.31	33.16	9.11	1.58
Northridge	13.57	34.2	11.16	35.23	5.84	1.50

4.4.2 Investigation of Energy Dissipation of Frame 2

Energy dissipation of Frame 2 subjected to six ground motions is between 16% and 22% for BETA-K viscous energy, and 30% and 39% for ALPHA-M viscous energy. However modal damping energy dissipated minimum 11%and maximum 33% and the energy dissipated by strain was between 1.5% and 9% (Table 4.7).

Table 4.7: Energy dissipation percentage of Frame 2

Earthquake load	Dissipated inelastic energy	BETA-K viscous energy	ALPHA-M viscous energy	Modal damping energy	Strain energy	Maximum energy kgf-cm(10^{6})
Kobe	19.07	33.51	9.79	31.96	5.67	9.43
Kocaeli	16.15	36.26	10.82	35.4	1.37	8.60
Imperial-Valley	24.05	38.98	9.97	29.04	8.76	1.09
Chichi	20.00	30.52	10.30	33.17	6.01	1.05
Lemo-perieta	21.31	29.55	11.00	33.74	4.4	1.24
Northridge	17.53	31.61	12.37	37.29	1.2	1.22

4.4.3 Investigation of Energy Dissipation of Frame 3

Dissipated inelastic energy for each of the 6 earthquakes used for this study is between 24 % and 30 %.(Tables 4.8 to 4.10).However BETA-K viscous energy for

Kobe, Kocaeli, Imperial Valley and Chichi is between 25% and 27%, but for Lemo-Perieta it is 35% and for Northridge it is about 36%. ALPHA-M viscous energy dissipation is between10% and 13%, modal damping energy(dissipated energy) are between 28% and 25%, and lowest energy dissipation was the strain energy dissipation, between0.5% and 2.5%.

Table 4.8: Energy dissipation percentage of Frame 3

Earthquake load	Dissipated inelastic energy	viscous energy	ALPHA-M viscous energy	Modal damping energy	Strain energy	Maximum energy kgf-cm(10^7)
Kobe	25.8	26.1	12.2	34.2	1.7	1.16
Kocaeli	24.9	27	12.5	35.1	0.5	1.17
Imperial-Valley	29.4	24.9	11.4	31.9	2.4	8.04
Chichi	28.4	25.9	12	33	0.7	8.00
Lemo-perieta	25.6	34.9	9.8	27.5	2.2	9.00
Northridge	24.1	36	10.8	28.2	0.9	3.47

4.4.4 Investigation of Energy Dissipation in Members of Frame 1

Table 4.9 shows the percentage of energy dissipated in each group of members. The horizontal and vertical truss members as expected by the designer did the highest dissipation of energy. In this frame the Imprial –Valley, Chichi and Northridge ground motion have the highest percentage of dissipated energy for horizontal truss members and Kocaeli, Chich iNorthridge have the highest percentage of energy dissipated by the vertical truss members.

Table 4.9: Energy dissipation percentage of members in Frame 1

Earthquake load	Horizontal truss members	Columns	Vertical truss members	Diagonal truss members	Summation of energydissipated in plastic phase (10^6)
Kobe	13.4	50.5	30.9	5.2	2.12
Kocaeli	16.3	46.7	35.9	1.1	1.81
Imperial-Valley	35.2	21.1	34.7	8.2	1.82
Chichi	42.5	13.9	39.3	4.3	1.67
Lemo-perieta	29.6	32.3	30.8	7.3	2.37
Northridge	37.7	23.3	35.9	3.1	2.04

4.4.5 Investigation of Energy Dissipation of Members Frame 2

In Frame 2 the highest percentage of energy dissipation belongs to columns with 65%.For horizontal truss members when subjected to Northridge and Imperial-valley loads this percentage is about 12.4 % and for other ground motions the average dissipation is about 3%. However, for vertical truss members this percentage is average 1.5% except Chichi ground motion, which is about 21% (Table 4.10).

Table 4.10: Energy dissipation percentage of members in Frame 2

Earthquake load	Horizontal truss members	Columns	Vertical truss members	Diagonal truss members	Summation of energy dissipated in plastic phase (10^6)
Kobe	1.6	84.5	13.1	0.8	1.79
Kocaeli	1.0	82.2	16.8	0	1.39
Imperial-Valley	12.4	69.5	14.6	3.4	2.63
Chichi	2.2	21.5	55	21.3	2.08
Lemo-perieta	5.7	77.8	13.7	2.8	2.66
Northridge	12.4	66.3	20.4	0.1	2.65

4.4.6 Investigation of Energy Dissipation of Members Frame 3

In Frame 3 the highest percentage of energy dissipation belongs to horizontal truss members with 50% in average. For columns members when subjected to ground

motions loads is 25 %, in this frame columns and vertical truss members had almost similar amount of energy dissipating (Table 4.11).

Table 4.11: Energy dissipation percentage of members in Frame3

Earthquake load	Horizontal truss members	Columns	Vertical truss members	Diagonal truss members	Summation of energy dissipated in plastic phase (10^6)
Kobe	44.4	27.9	20.1	7.6	2.98
Kocaeli	52.1	22.5	21.7	3.7	2.92
Imperial-Valley	43.2	30.4	18.6	7.8	2.36
Chichi	50.4	26.4	20.1	3.1	2.27
Lemo-perieta	39.6	31.7	22.5	6.2	2.31
Northridge	45.9	26.7	24.9	2.5	2.16

4.4.7 Investigation of Base Shear Result From Dynamic Analysis

Table 4.12 shows the base shear of steel frames subjected to 6 ground motions selected for this study. The highest and the lowest base shears among the 3 frames were 2376 kN for Frame 1 and 225.3 kN for Frame 3 and both were due to Kobe earthquake. Chichi earthquake caused the highest base shears 1294 kN and 268.2 kN for Frames 2 and 3 respectively. Lemo-perieta and Kocaeli earthquakes cased the lowest base shears of 2131 kN and 762.1 kN for Frames 1 and 2 respectively.

Table 4.12: Maximum base shear for Frames 1, 2 and 3

Earthquake load	Base shear Frame 1 kN	Base shear Frame 2 kN	Base shear Frame 3 kN
Kobe	2376	767.6	225.3
Kocaeli	2330	762.1	265.2
Imperial-Valley	2165	1251	263.1
Chichi	2208	1294	268.2
Lemo-perieta	2131	971.4	258.2
Northridge	2191	978.2	263.3

4.4.8 Investigation of Story Drift of Frame 1

The inter story drift graph of Frame 1, which was subjected to 6 ground motions selected for this study, shows that the frame behaves in similar manner when subjected to all6 ground motions. For example, drift ratio caused by all ground motions is about 0.003 at story 2 and from story 2 up to story 7 the direction of frame movement and the rate of increase in drift ratio are similar. Floor 6 has the highest number of different drift ratios as shown in Figure 4.4.

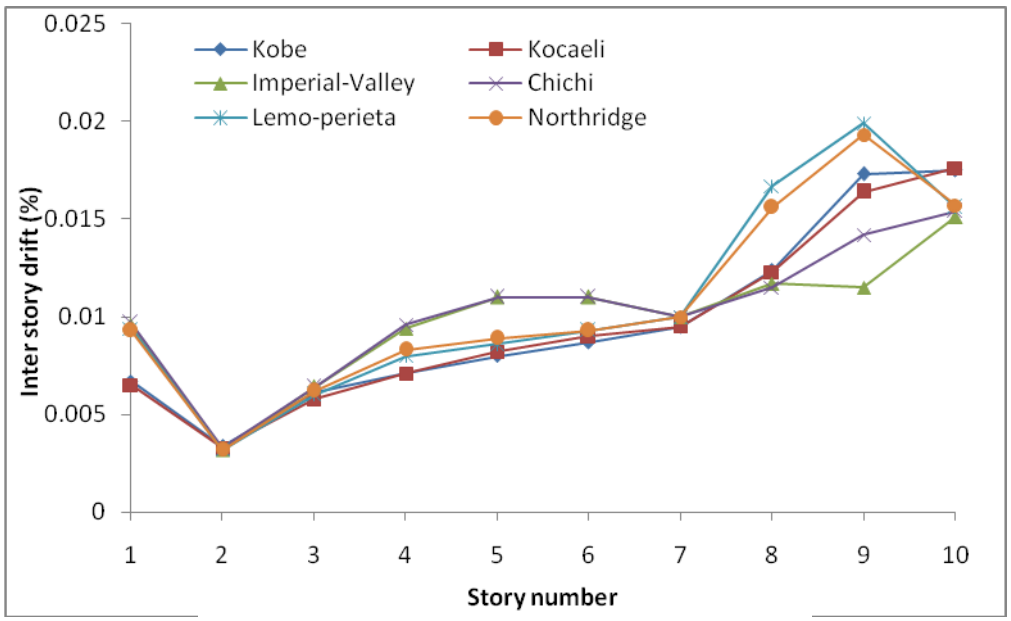

Figure 4.4: Maximum intestory drift of Frame 1

4.4.9 Investigation of Story Drift for Frame 2

All ground motions caused similar behaviour and story drift ratios for Frame 2, except Imperial-Valley and Chichi at story 3, Northridge and Lemo-perieta at stories 6 and 7. The story drift ration at story 3 caused by Imperial-Valley is almost compared to other ground motions. On the other hand, the story drifts ratios caused by Northridge and Lemo-perieta is nearly 200% and 25 % more than the other ground motions at stories 6 and 7 respectively (Figure 4.5).

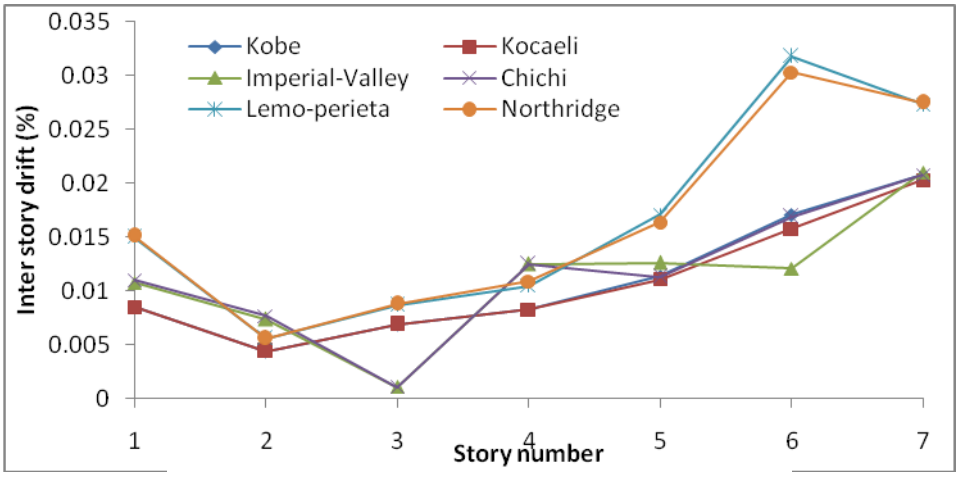

Figure 4.5: Maximum interstory drift of Frame 2

4.4.10 Investigation of Story Drift for Frame 3

Considering the 4 stories high building, story 2 had the highest inter story drift when subjected to Lemo-perieta and Northridge earthquake loads. On the other hand, the lowest percentage of drift was obtained when the structure was subjected to Kobe and Kocaeli earthquake loads. Behaviour of the frame is the same in all earthquakes but the value of drift is different (Figure 4.6).

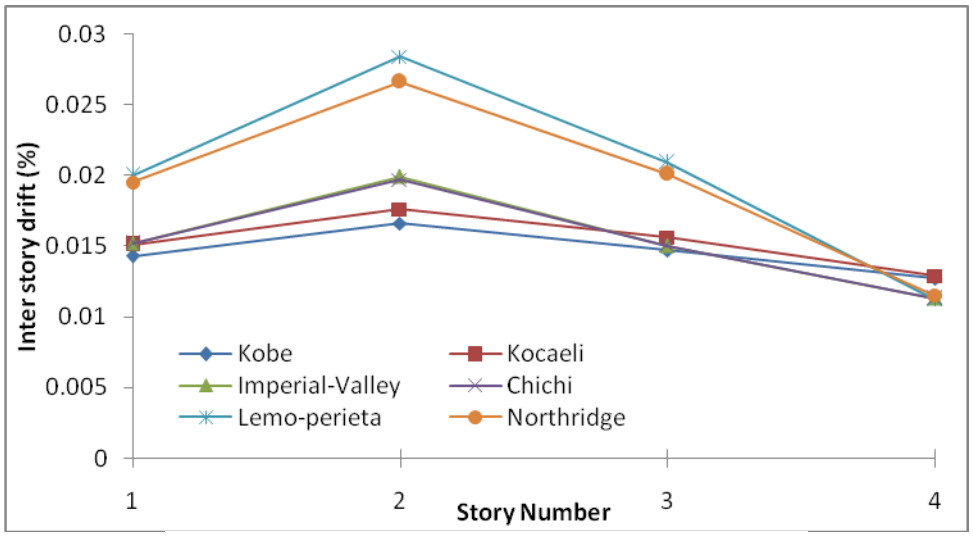

Figure 4.6: Maximum inter story drift for Frame 3

4.4.11 Investigation of Base Shear Result From Dynamic Analysis for Frame 1

Base shear diagram of Frame 1 under Kobe earthquake load shows that the maximum base shear achieved between 5 to 9 seconds where the extreme damage also happened in this period. All base nodes have the same manner in earthquake, however, the distance of first node to end node is about 45.7m.No expansion joint was provided in this structure (Figure 4.7).

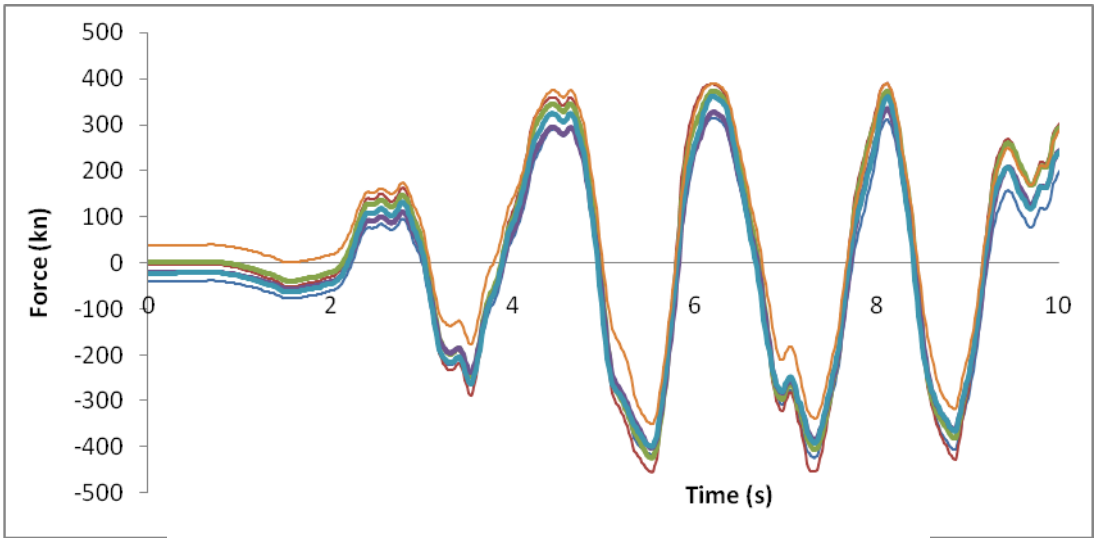

Figure 4.7: Kobe earthquake base shear of Frame 1

4.4.12 Investigation of Base Shear Result From Dynamic Analysis of Frame 2

Figure 4.4 shows that when Fame 2 was subjected to Kobe earthquake the peak base shear (250 kN) was achieved after 4.5 seconds. After 5 seconds the structure reached to its elastic limit hence the stiffness matrix did not converge leading the structure to failure with large displacements (Figure 4.8).

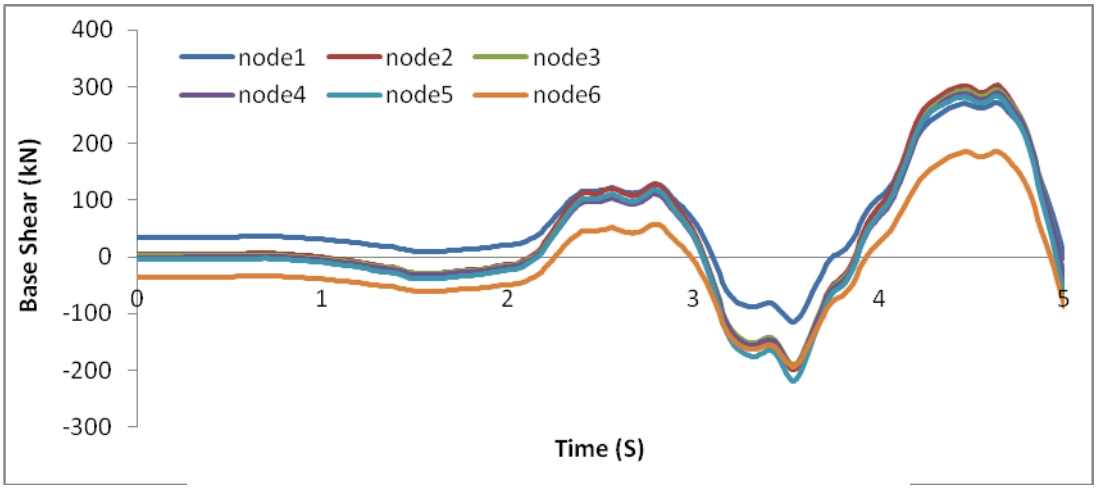

Figure 4.8:Base shear of Frame 2 from Kobe earthquake

4.4.13 Investigation of Frame 3 Base Shear Results From Dynamic Analysis

The Frame 3 base shear under Kobe ground motion shows the greatest number of force between second 5 and second 15 and this graph shows that the frame 3 remain about 20 second in elastic region and after second 20 turn to inelastic region (Figure 4.9).

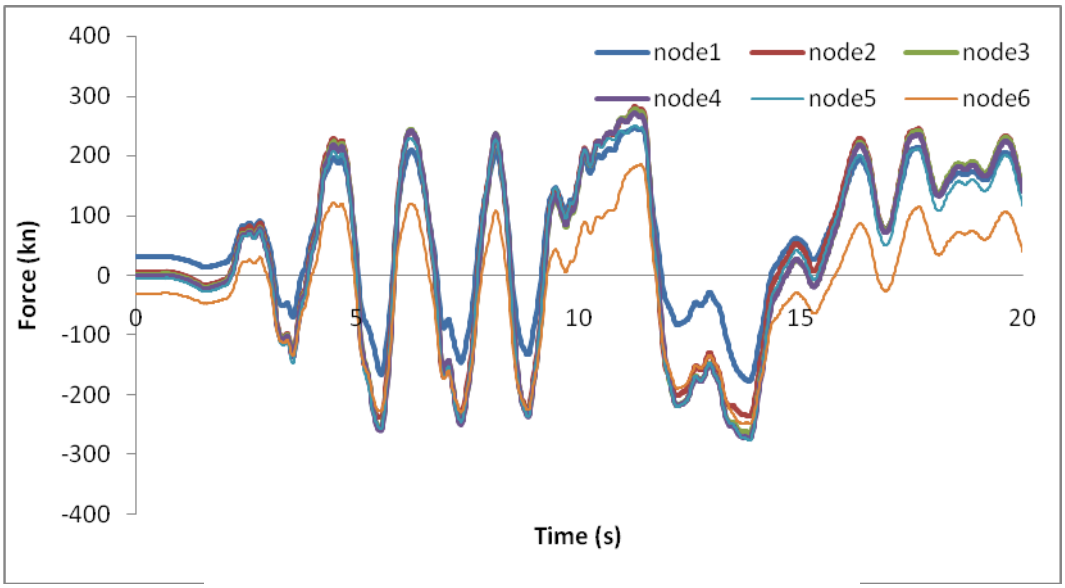

Figure 4.9: Kobe earthquake base shear of Frame 3

4.4.14 Investigation of Frame 1 Total Inertia and Damping Force From Chichi Earthquake

Total inertia and damping force of Frame 1 from 0 to 3 seconds is zero (force and total inertia force are equal with opposite sign when damping force is equal to zero).According to Figure 4.10 it can be calculated that from 0 second up to 6 seconds stiffness force and total inertia are equal with opposite sign. However, when it has low value of damping in this situation this is not theoretically correct.

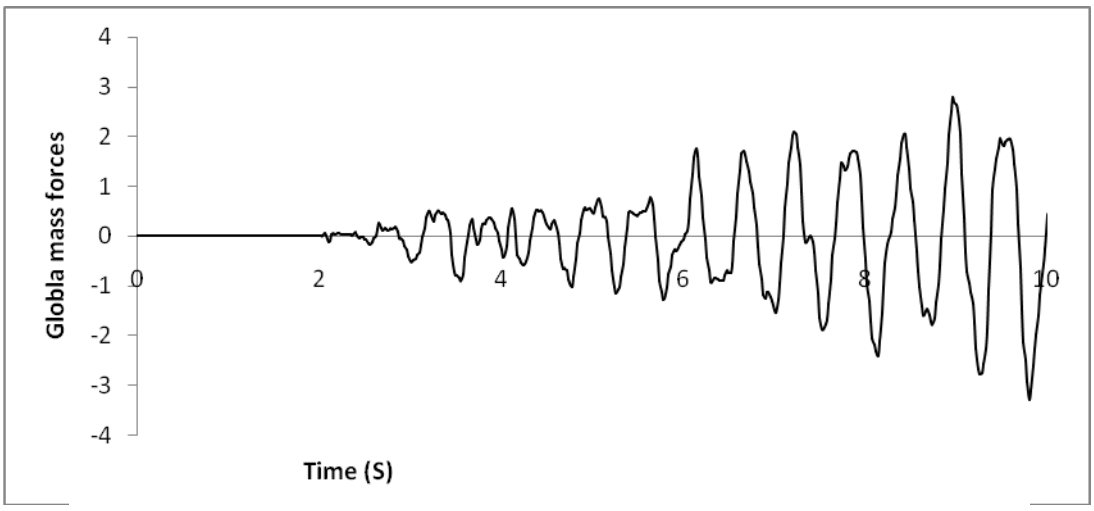

Figure 4.10: Chichi earthquake total inertia and damping force for Frame 1

4.4.15 Investigation of Base Shear Result From Dynamic Analysis of Frame 1

Base shear of Frame 1 subjected to Northridge earthquake loads that gradually increase from 0 to 400 kN between 0 up to 5.5 periodic time, and starting from 5.5 seconds the sign of base shear changed to negative and went to opposite region up to -500 kN. Finally, from 6.5 seconds it has changed again in positive sign and increase up to +400 kN (Figure. 4.11).

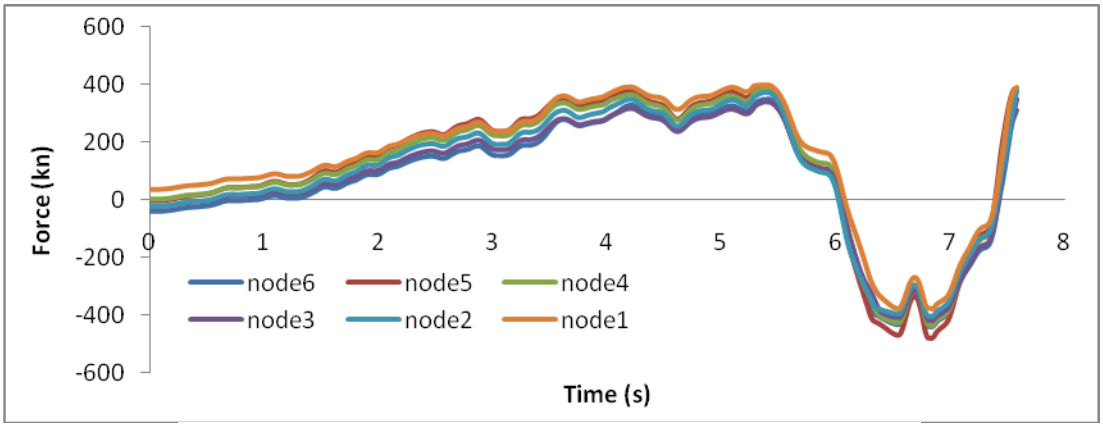

Figure 4.11: Northridge earthquake base shear of Frame 1

4.4.16 Investigation Northridge Earthquake Total Inertia and Damping Force of Frame 1

Figure 4.12 shows the total inertia and damping force of Frame 1 subjected to Northridge, where the damping force equal to zero from 0 up to 3 seconds and after this time it increased gradually to -200 and +100 tonnes in 7.5 seconds. At the end, global mass forces of -200 tonnes in the negative region and +100 tonnes in positive region were achieved.

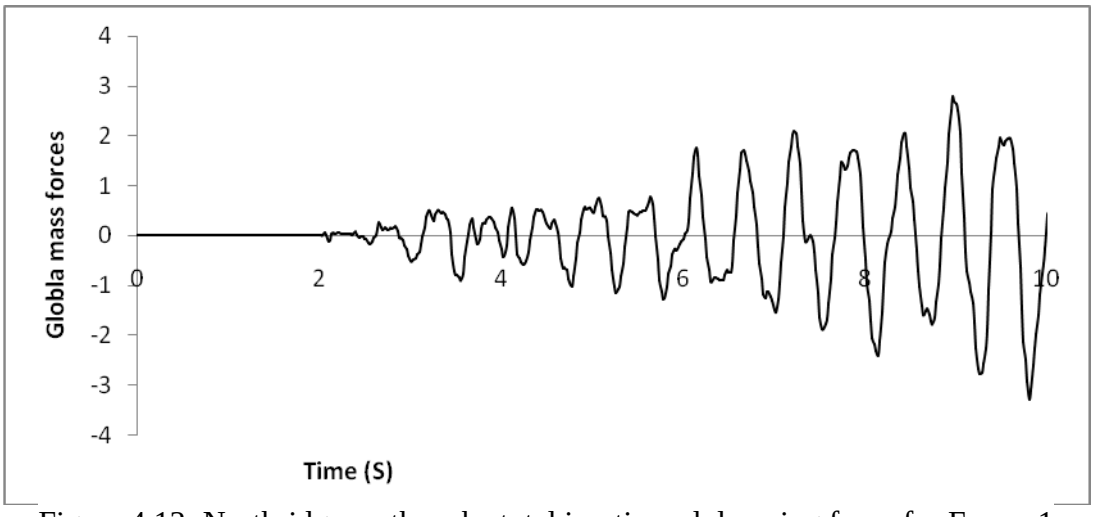

Figure 4.12: Northridge earthquake total inertia and damping force for Frame 1

4.4.17 Investigation of Base Shear Result From Dynamic Analysis of Frame 2

Northridge earthquake caused effects similar to those of Kobe on the frame models. Frames collapsed before 8 seconds and according to Figures 4.11and4.12the effective duration of Northridge earthquake was between 3 to 8 seconds.

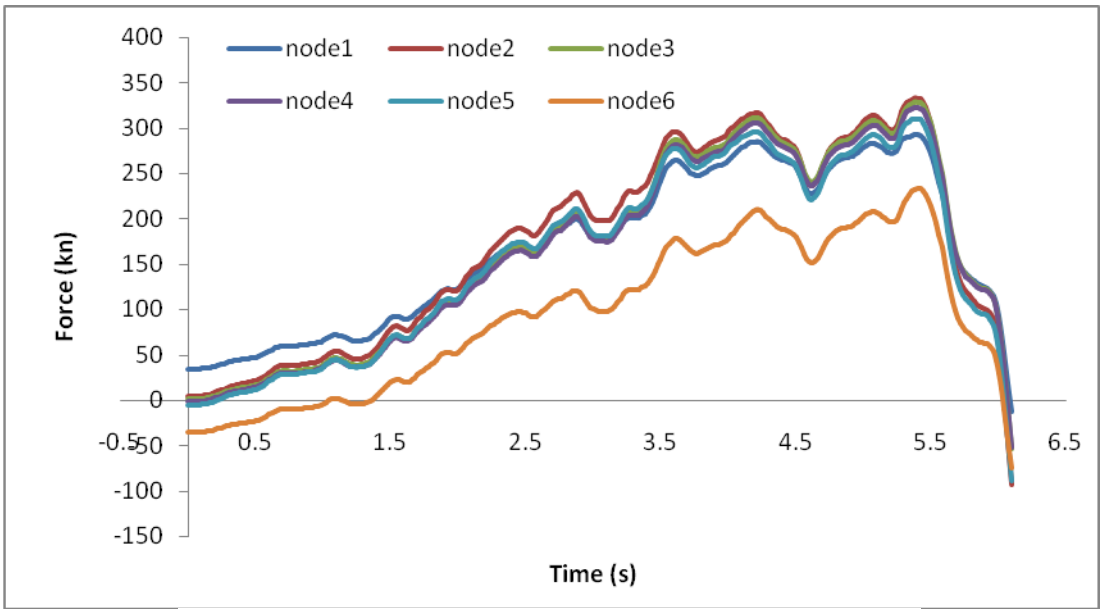

Figure 4.13: Northridge earthquake base shear of Frame 2

4.4.18 Investigation of Northridge Earthquake, Total inertia and Damping Force of Frame 2

Total inertia of Frame 2 subjected to Northridge ground motion shows the most global mass force accrued in seconds 5.5 and 6, which according to base shear of these frames under same ground motion clearly can be seen the highest value of the base shears also belongs to this period (Figure 4.14).

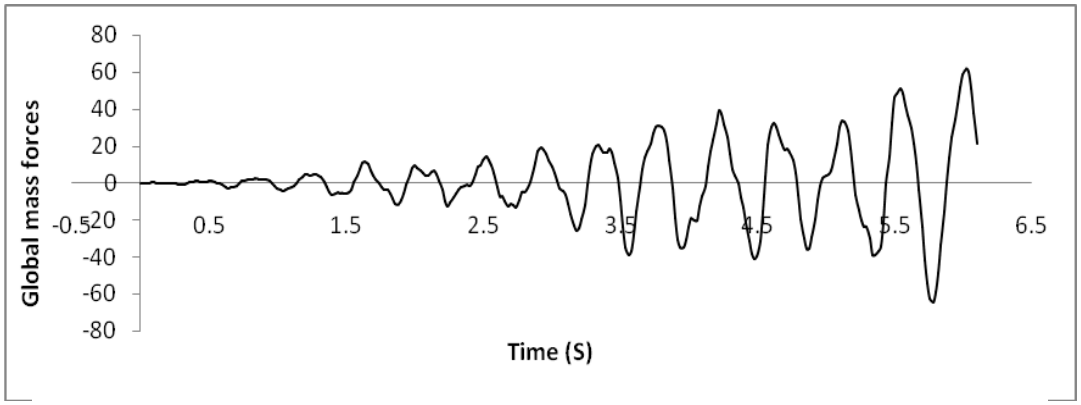

Figure 4.14: Northridge earthquake total inertia and damping force for Frame 2

4.4.19 Investigation of Base Shear Result From Dynamic Analysis of Frame 3

Frame 3 base shear graph shows the behaviour of this frame subjected to Northridge earthquake is similar to the two other frames as regards frame 3 resist under earthquake load up to second 20 but tow others collapse before 8 second. Figure 4.15 shows Frame 3 behaviours under Northridge ground motion is different tocompare with two other frames, it started from zero and increase gradually up to ±80 in second 8 and decrease gradually to ±40 in second 12 and remain flat up to end of period.

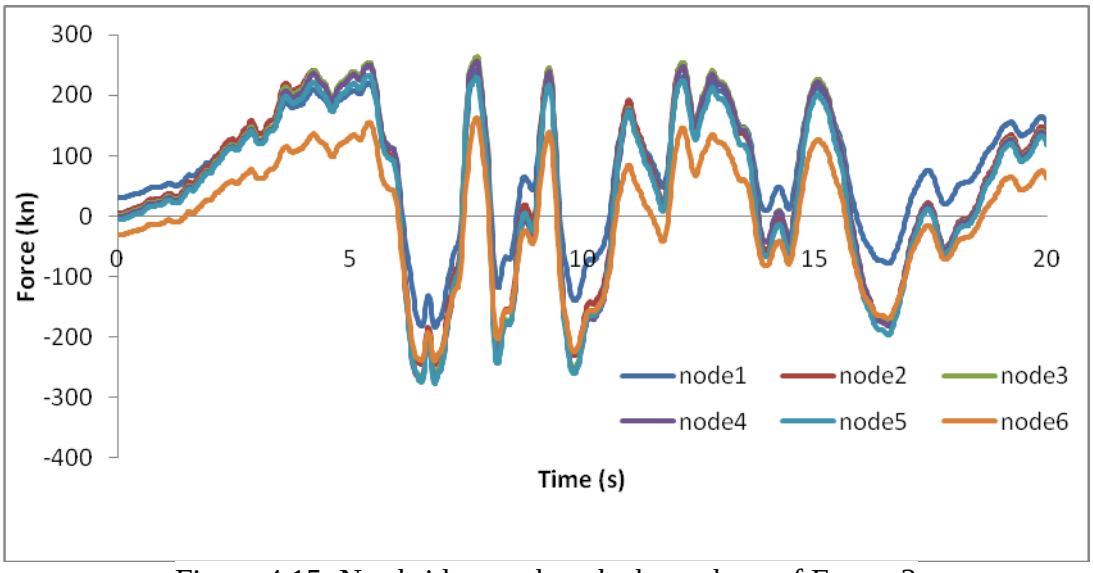

Figure 4.15: Northridge earthquake base shear of Frame 3

4.4.20 Investigation of Displacement of Frame 1

According to Figure 4.16, the displacement of Frame 1 gradually increased from 0 cm at the basement up to 25 cm at the story 6 and from story 6 to 7 the displacement decreased to 15 cm. From story 7 to 10 the displacement increase from 15 to 40 cm. As it can be seen from Figure 4.16 all ground motions have similar effect on Frame 1.

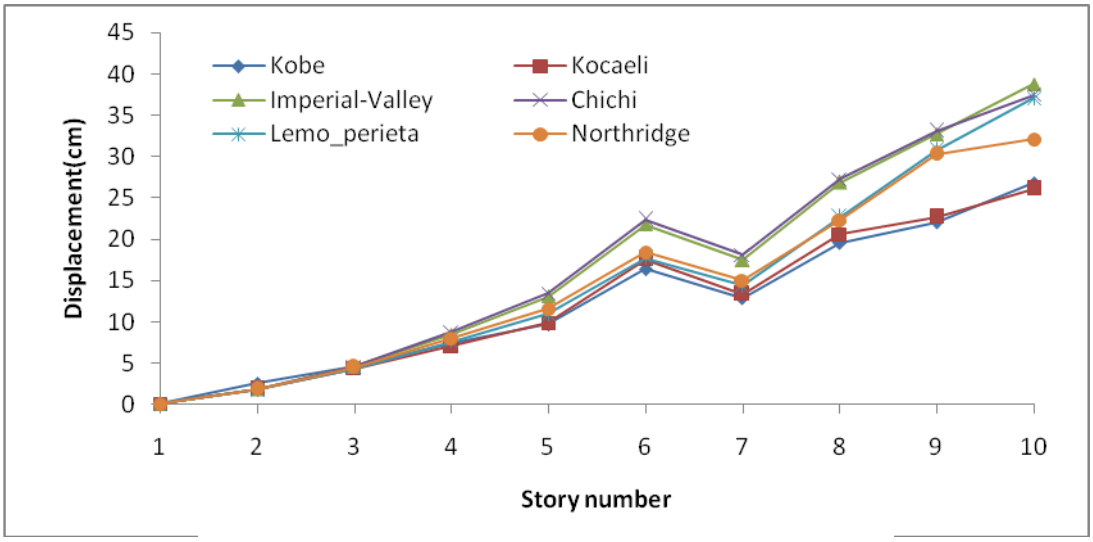

Figure 4.16: Maximum story displacement of Frame 1

4.4.21 Investigation of Story Accelerations of Frame 1

Acceleration at each story level due to six ground motions can be seen in Figure 4.17. Kobe and Kocaeli and Lemo-perieta and Northridge earthquakes cause almost the same acceleration for each story level, except for stories 9 and 10 where all ground motions caused similar accelerations to these stories.

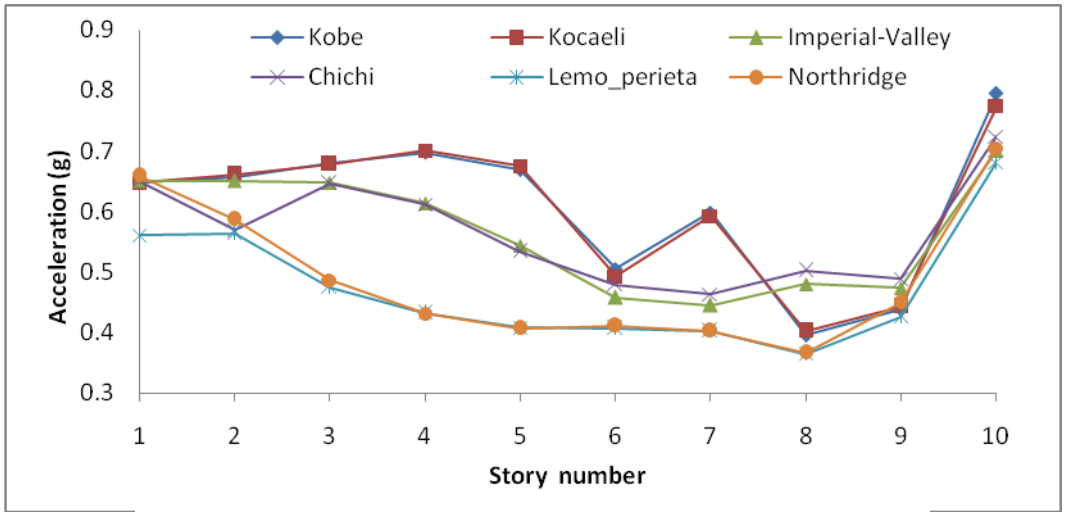

Figure 4.17: Maximum accelerations of each story of Frame 1

4.4.22 Investigation of Displacement of Frame 2

Displacements of frame 2 for all ground motions are same , it start from 0 in the base of frame and gradually increase to 30 cm in floor 6 and decrease from 30 cm to 20 cm in the floor 7 , as it can be seen in figure Northridge and Kobe have more than 40 cm in floor 6. This graph shows the critical floor is floor 6 where there is a sharp drop and sharp growth before and after of this floor in displacement (Figure 4.18).

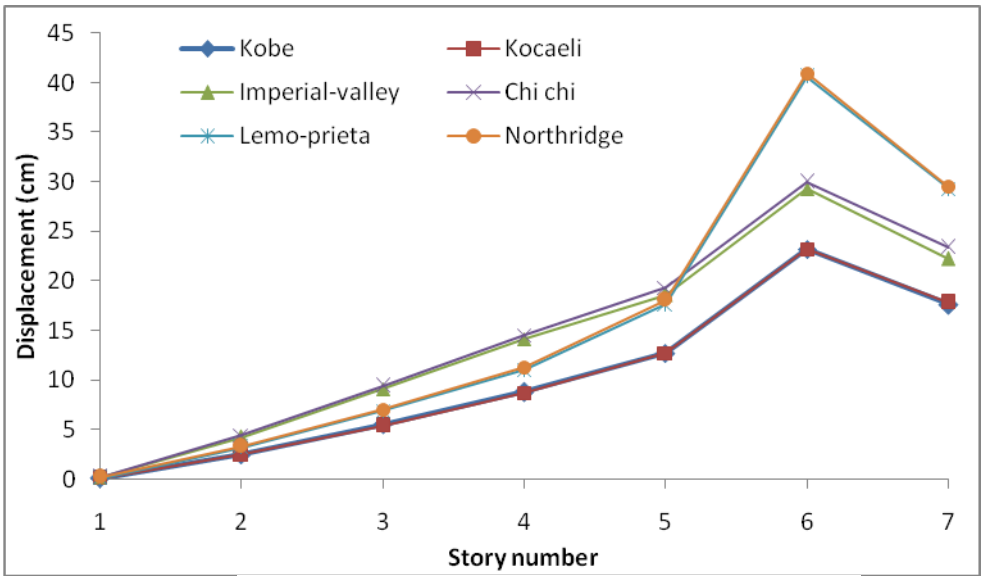

Figure 4.18: Maximum displacement of Frame 2

4.4.23 Investigation of Acceleration of Frame 2

The acceleration graph of frame 2 clearly shows each two pair ground motion effected similar on structure, for example Kobe and kocaeli have similar effect on model, Chichi and imperial – valley have also similar effect on structure and also Northridge and Lemo-perieta have similar effect. From base up to floor 5 there are different in the value of acceleration but from story number 5 to story number 7 all the ground motion behave in same pattern. The critical story is 6 in this model, where the sign of acceleration changed and there is a sharp drop and sharp growth before and after of this floor (Figure 4.19).

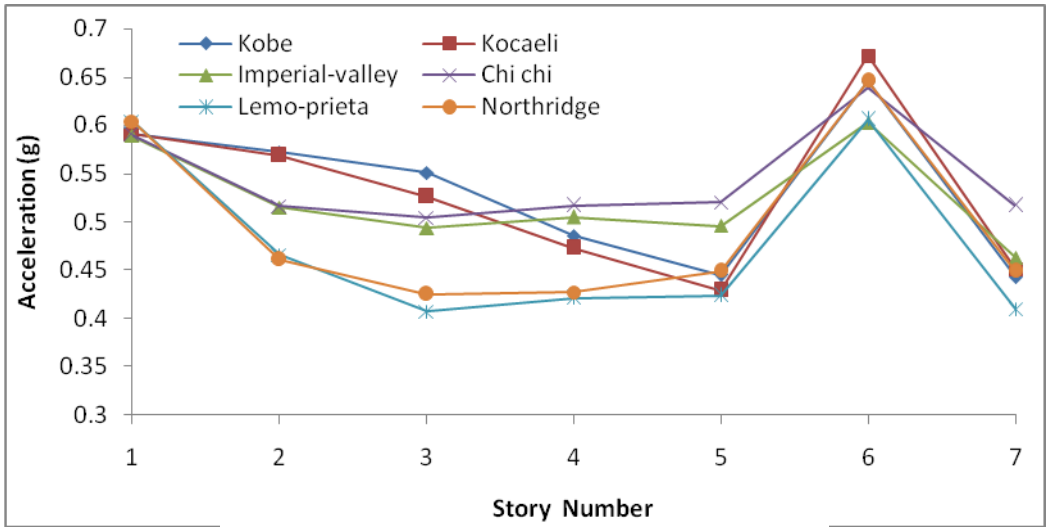

Figure 4.19: Maximum acceleration of Frame 2

4.4.24 Investigation of Displacement of Frame 3

Frame 3 displacement diagrams show steady increase in all ground motions from 0 to 30 cm. Lemo-perita and Northridge achieved higher values when compared to other ground motions (Figure 4.20).

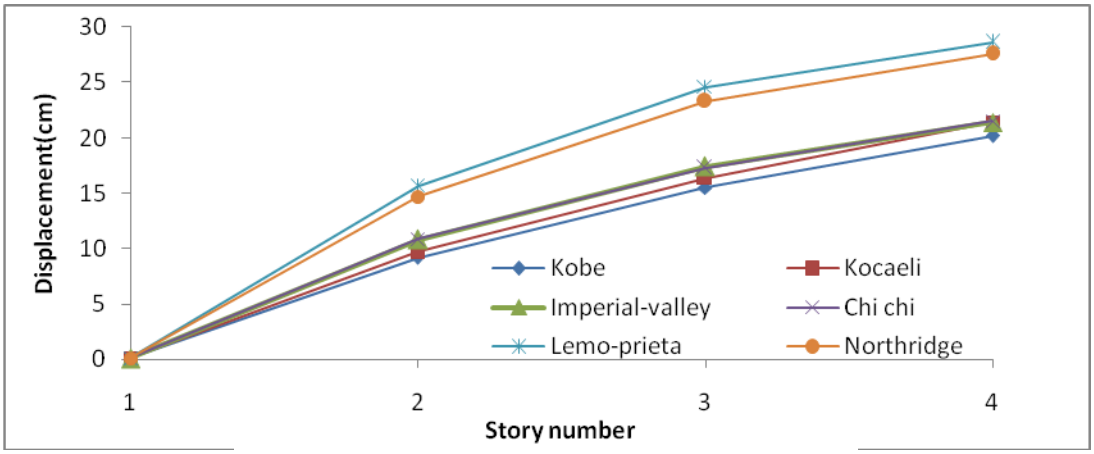

Figure 4.20: Maximum displacement of Frame 3

4.4.25 Investigation of Acceleration of Frame 3

Northridge and Lemo-prieta are slightly different from other ground motions in effect on structure the minimum acceleration can be seen on floor 2 belongs to these two earthquake loads (Northridge,Lemo-prieta) and at story 4 all ground motions have same value of maximum acceleration (Fig. 4.21).

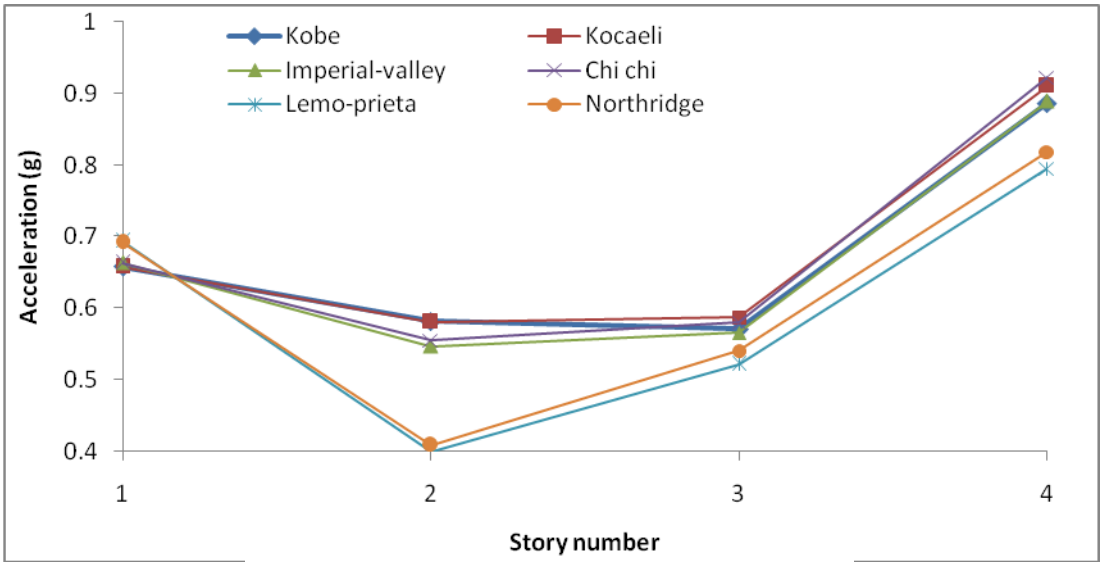

Figure 4.21: Maximum acceleration of Frame 3

4.4.26 Investigation of Chord Rotation of Frame 3

Figure 4.22 and 4.23 are shown the chord rotation performance carried out with Nonlinear static (pushover) and dynamic time history analysis, these to Schematicfigure clearly shows that the first chord rotation appeared in top and bottom chord of beams in first floor.The figure shows that the chord rotations start from lower floors and grow to upper floors. Hte red color shows the position of chord rotation,as it can be seen the maximum chord rotation and deflection were appear in first and fifth bay of Frame 3, this schematic view shows that the thirth and fifth floors have more ductilty to compare with first and second floors.

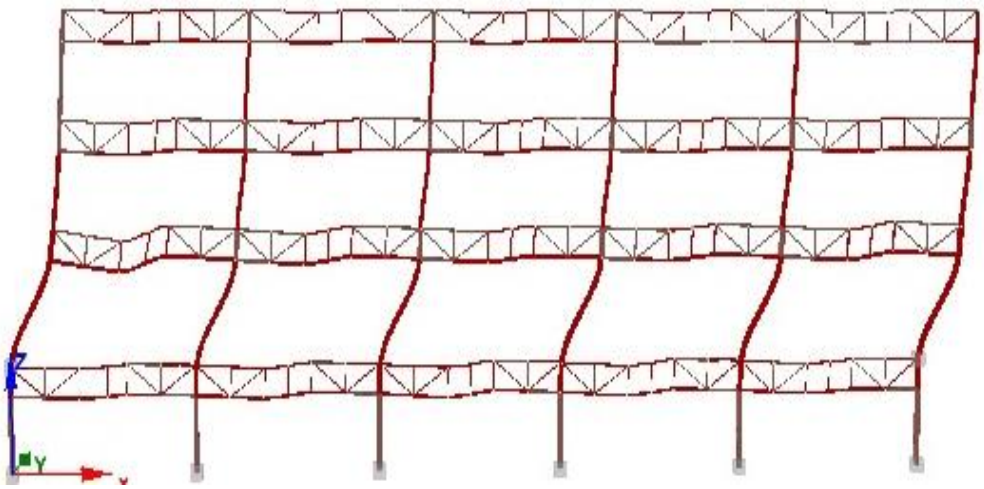

Figure 4.22: Pushover analysis chord rotation performance for Frame 3

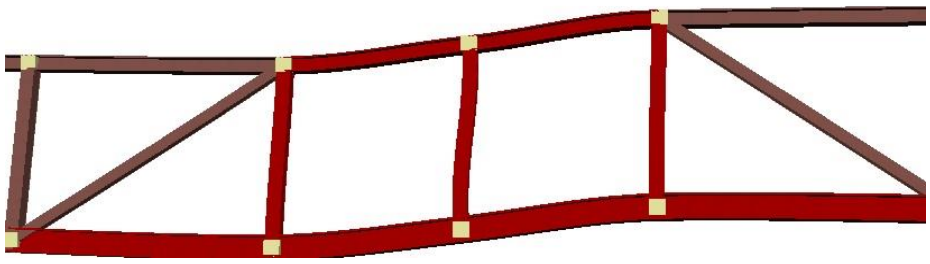

Figure 4.23: Chord rotation performance for Frame 3 for specific span

4.4.27 Investigation of Chord Rotation of Frame 2

Figures 4.24 and 4.25 show that, when subjected to pushover analysis, story 1 became the most critical floor, having the highest deformation. The chord rotations are concentrated in and around the special segments through the frame, where it was expected to appear. Basement was the least affected in terms of chord rotation. The yellow colour in Figure 4.24 and red colour in figure 4.25 shows the chord rotation positions, as it was expected the first chord rotation in pushover analysis appear in top and bottom of chord members, the 2,3and 4 stories of this Frame have the highest value of the chord rotation.

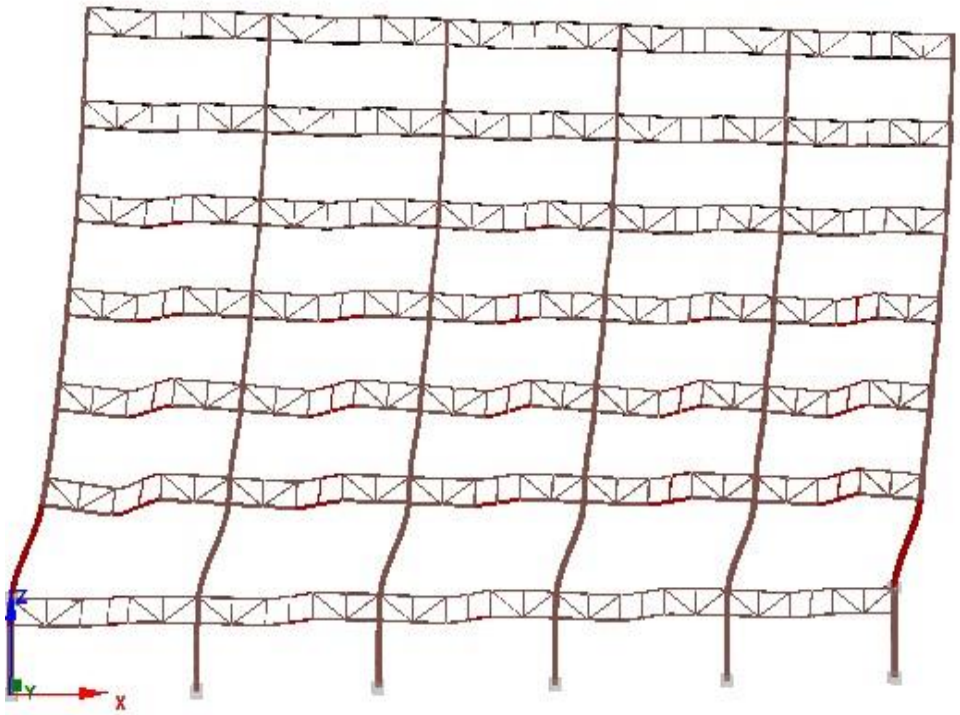

Figure 4.24: Pushover analysis chord rotation performance for Frame2

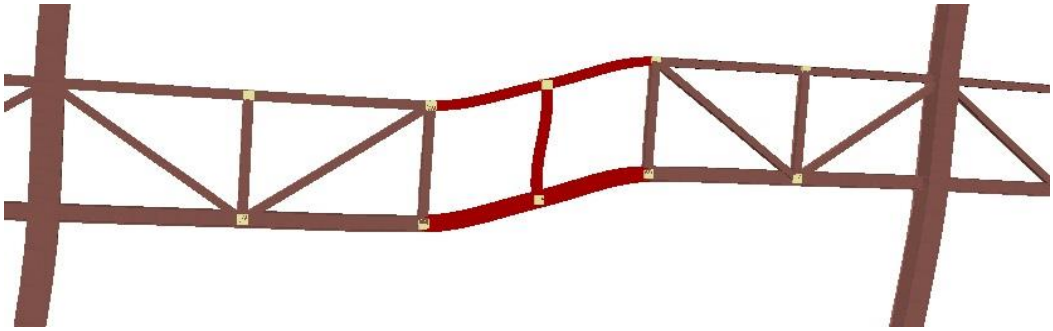

Figure 4.25: Chord rotation performance for Frame 2 for specific span

4.4.28 Investigation of Chord Rotation of Frame 1

Chord rotation performance carried out with dynamic time history and pushover analysis of Frame 1 are illustrated in Figures 4.26and 4.27.Behaviour of this Frame is like the other two frames, where the first large chord rotations appear in floors 1 and 2 and grow up and spread to other floors. Green colour in Figure 4.26 and red colour in Figure 4.27 shows the position of chord rotation. The most critical stories are 2,3,4,5 in Frame 1. These six schematic figures (Figure 4.22 to 4.27) have similar behaviour in first floor; the figures shows the critical columns are in floor one where this length is 1.2m longer than other stories. On the other hand the soft story affected the ductility of the STMFs, however this study was focused on ductility not the soft story effect.

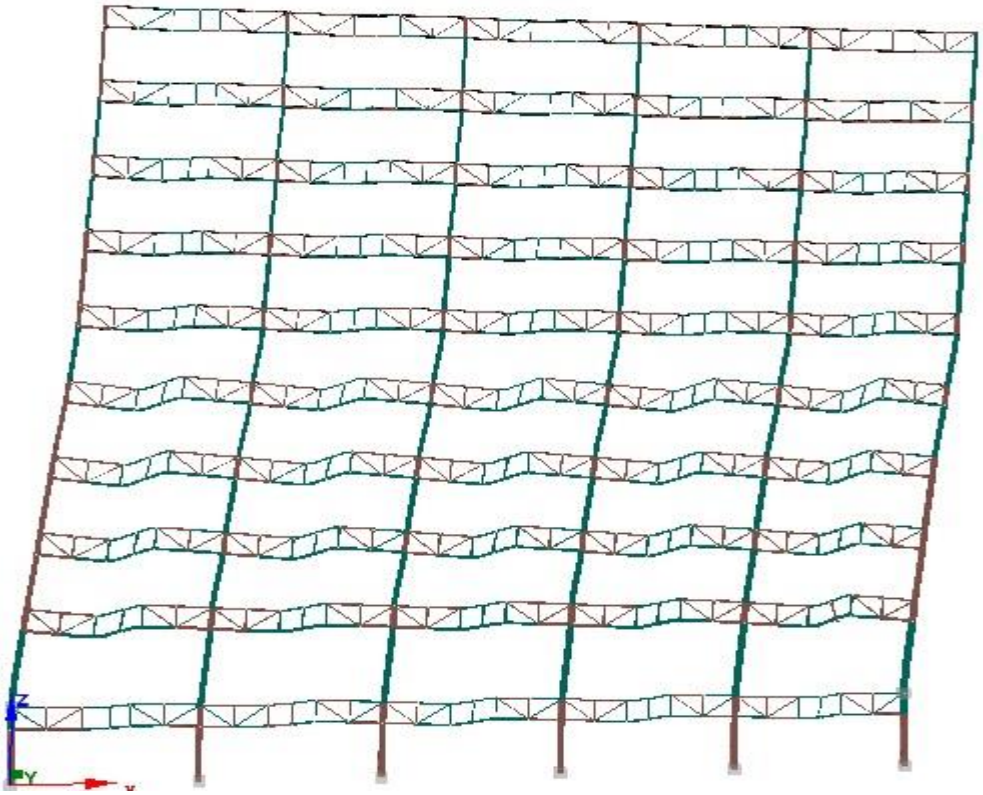

Figure 4.26: Pushover analysis chord rotation performance for Frame1

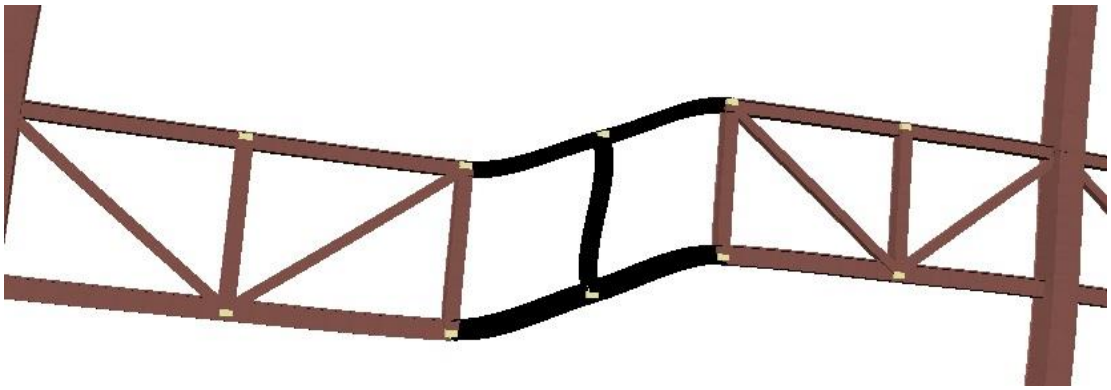

Figure 4.27: Chord rotation performance for Frame 1 for specific span

4.4.29 Story Drift Comparison of STMFs and SMRF

Akshay. G and Helmut. K studied seismic demands for performance evaluation of steel moment resisting frames (SMRF). They improved the knowledge based on the seismic behavior of typical SMRFs considering regions of different seismicity and

set of ground motion [17]. They modelled3 frames in 3, 9 and 21 stories with same span length and floor height according to UBC 1994 code. The geometric properties of their study is similar to this study therefore, the story drift of two frames was compared to results of this study. Figures 4.28 and 4.29 shows the average drift of STMFs when subjected to 6 ground motions and the distribution load pattern of mode one when subjected to a set of earthquakes for SMRF. Figure 4.29 shows that the story drift of STMFs is high at second story whereas the SMRF from first story up to last story has stable behavior. These two types of structures behave similar in second story up to last story. The direction of the drift shows the response of frames is similar when they subjected to loads. Especially from third story up to seventh story, both systems have similar behavior. Figure 4.29 shows that the first and second stories drift in STMFs and SMRF are similar but for last story, they behaved in opposite directions with different value.

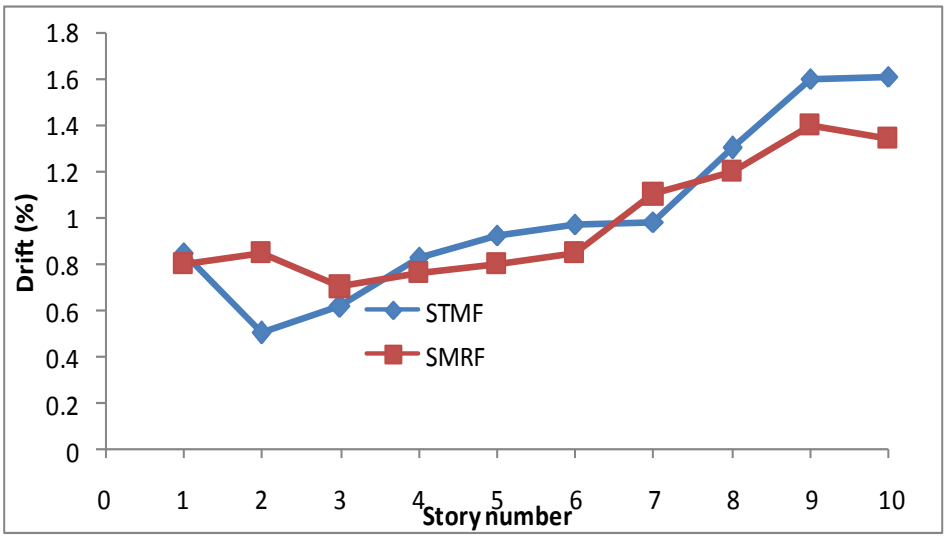

Figure 4.28: Maximum story drift of Frame 1 compare to SMRF

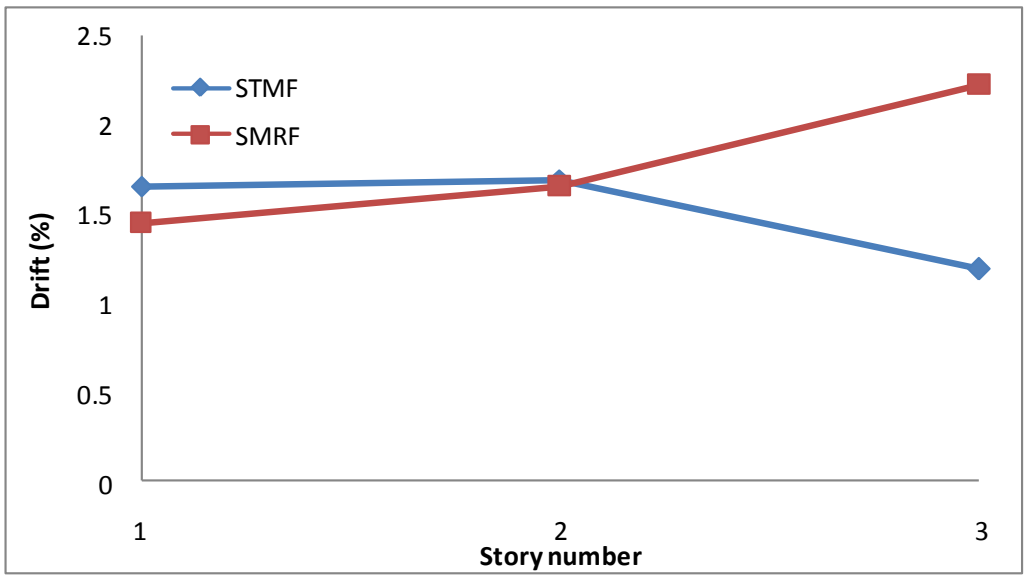

Figure 4.29: Maximum story drift of Frame 3 compare to SMRF

4.4.30 Maximum Story Displacement Comparison of STMFs with and without BRBs

Gokhan. P et al [18] carried out studies on special truss moment frames with supplemental devices, such as, Buckling Restrained Braces (BRBs). They designed 3 frames in 3 different number of stories. Each frame has 5 bays with 9.10 m of span length. The geometrical properties of the frames studied are similar to the frames reported in this thesis. Therefore, the maximum story displacements obtained from Gokhan et al. were compared to maximum displacement of the frames in this study[18]. Figure 4.30 shows the comparison of Frame 3 of this study with STMF with BRBs. Figure 4.30 shows that these two types of structures have similar behaviour especially at first and second floors. The maximum displacement values of both models are similar. STMF with BRB overall achieved higher displacements than STMF.The comparison of Frame 2 is shown in Figure 4.31. This time up to story number 5 the STMF has higher displacement. However, for sixth and seventh story the situation reversed where STMF had less displacement than STMF with BRB. Figure 3.32 shows the same trend for Frame 1 in maximum displacement. Up

to story number 5 STMF had higher displacement. After this story, STMF had lower displacement.

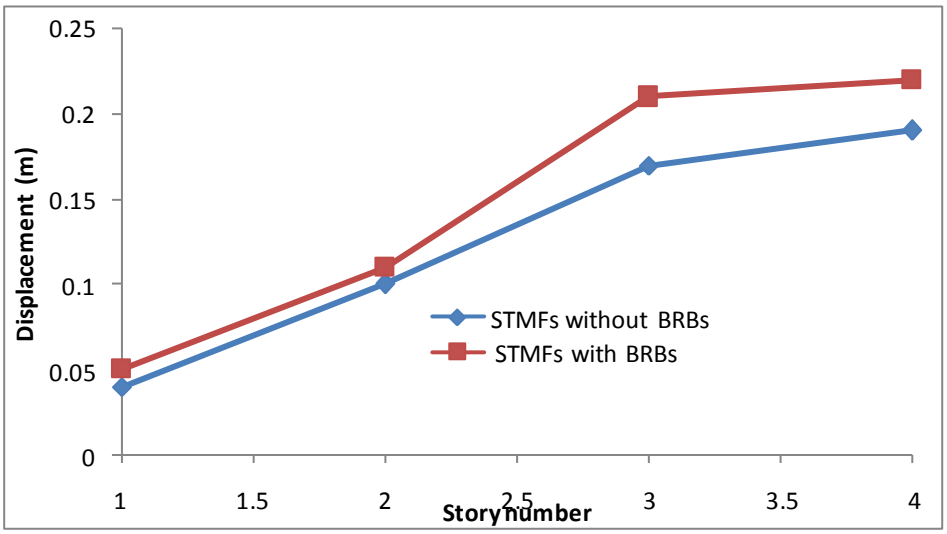

Figure 4.30: Maximum displacements of Frame 3 compared to STMF with BRB

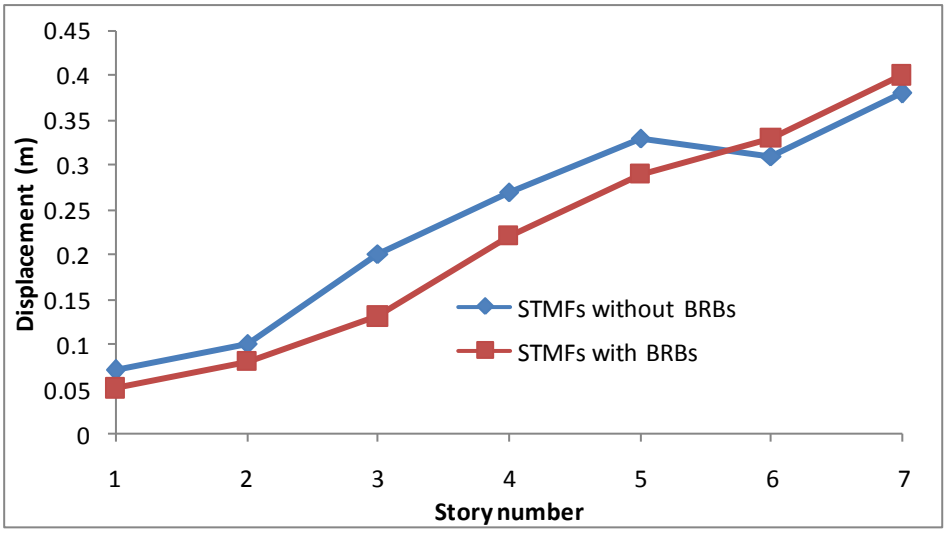

Figure 4.31: Maximum displacementsof Frame 2compared to STMF with BRB

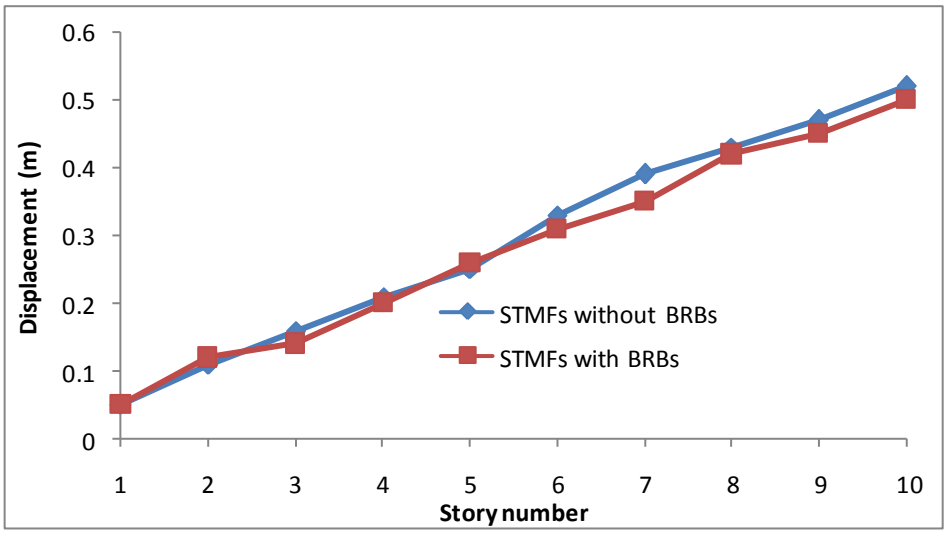

Figure 4.32: Maximum displacementsof Frame 1compared to STMF with BRB

4.5 Results from SAP 2000

In this section of the study Seismostruct software was implemented together with SAP2000, in order to find the performance of STMF and TMF based on the limit state. Therefore, Frame 1 and Frame 2 were modelled in SAP2000, limit states were imported to the software according to FEMA 356 and nonlinear pushover analysis was carried out.

4.5.1 Investigation of Limit State Performance of Frame 2

Figure 4.33 shows the first step of nonlinearity of Frame 2. Two plastic hinges in immediate occupancy limit state appeared in floors 3 and 4 at this step. Figure 4.34 shows Frame 2 in second step of nonlinear behavior, where in floors 3,4 and 5, six plastic hinges in life safety limit state appeared. In addition to these plastic hinges in the mentioned floors and in addition at floor 2 there were several plastic hinges in immediate occupancy. In the third step of nonlinear behavior two plastic hinges in collapse prevention limit state can be seen in third floor (Figure 4.35). The important point to note is that all of the plastic hinges in each limit states appeared in segments where they were expected to appear according to collapse mechanism of STMFs [1]

based on AISC 341-10 the special segments designs according to plastic based design theory.

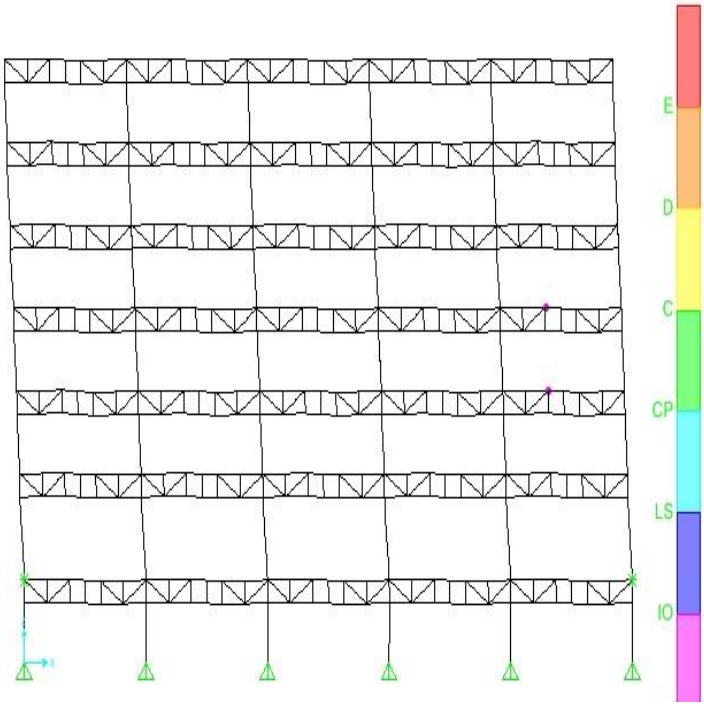

Figure 4.33: Limit state of Frame 2 step 1 of nonlinearity

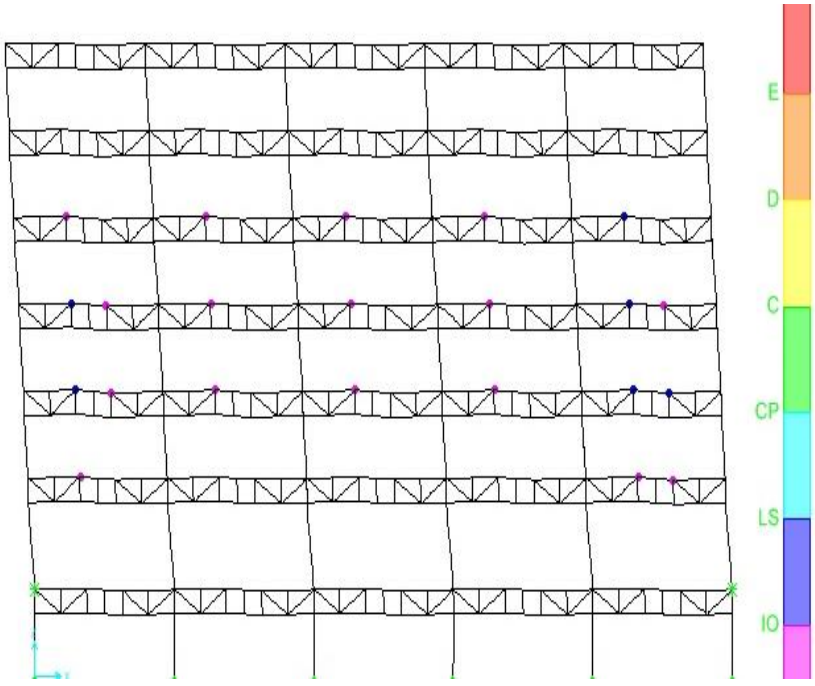

Figure 4.34: Limit state of Frame 2 step 2 of nonlinearity

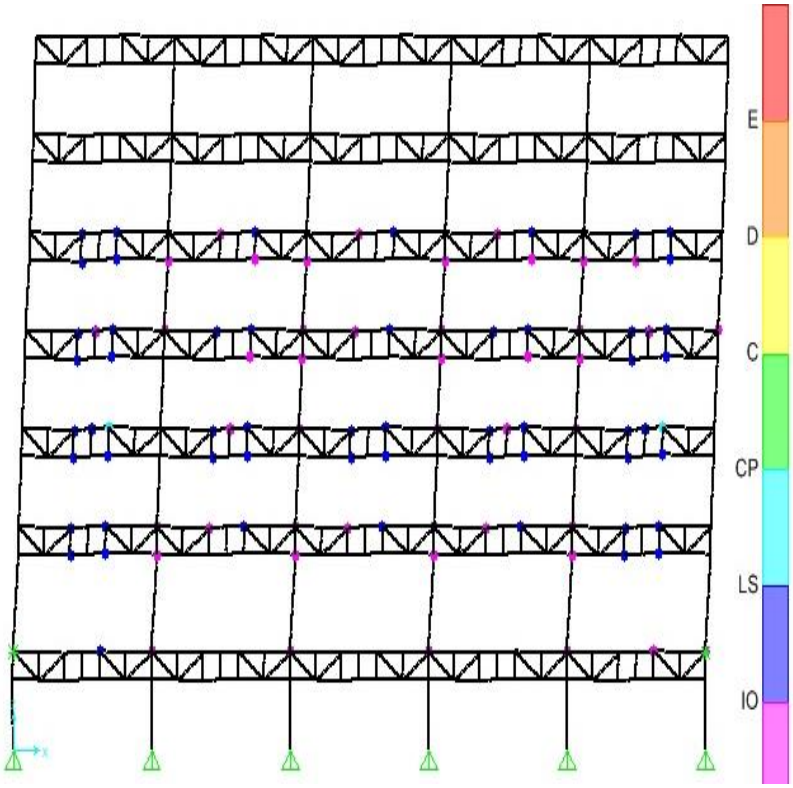

Figure 4.35: Limit state of Frame 2 step 3 of nonlinearity

4.5.2 Investigation of Limit State Performance of Frame 1

Figure 4.36 (a) shows the first step of nonlinearity of Frame 1, which in this step the first plastic hinge in immediate occupancy appeared in second floor. In second step, in floors 2,3,4 and 5 plastic hinges appeared in immediate occupancy and life safety (Figure 4.36 (b)).In third step of nonlinearity it can be seen that the plastic hinges spread to upper stories, except the three plastic hinges which are in collapse prevention limit state. The rest of plastic hinges are in life safety and immediate occupancy limit state(Figure 4.37 (a)).The 4^{th} and 5^{th} steps also shows that the floors 2,5 and 6 are the critical floors whereas they have more plastic hinges to compare with other floors(Figures4.37 (b) to 4.38(b)). It is worth mentioning that all plastic hinges appeared in special segments where they were expected to appear. The most important advantage of this system of structure is controllable damage when subject to lateral loads.

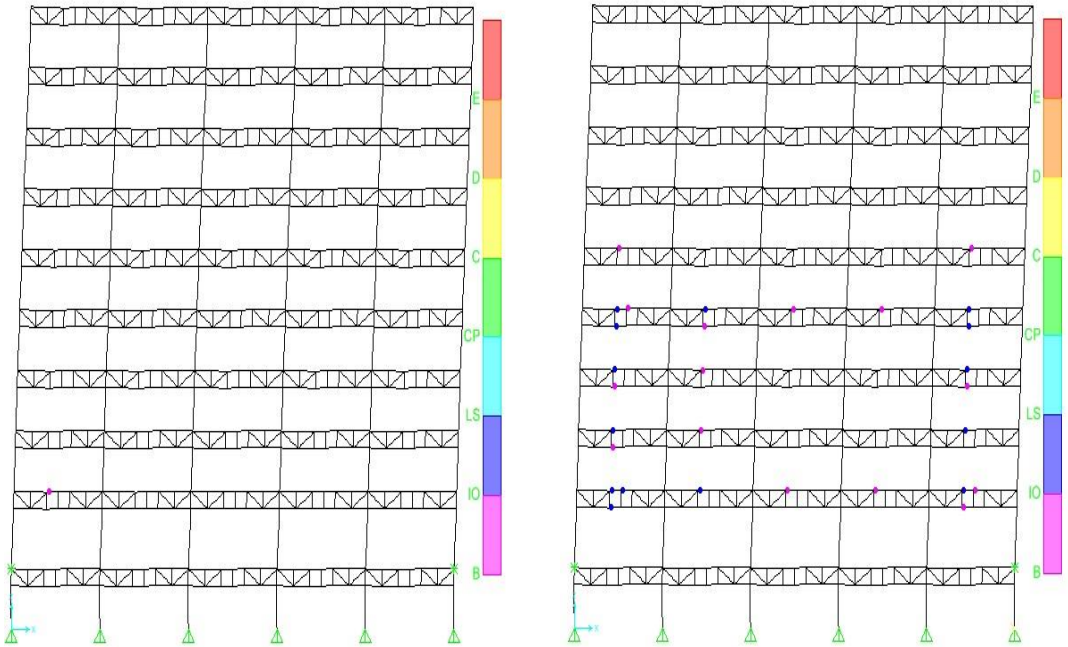

(a) (b)

Figure 4.36: Limit state of Frame 1 (a) step 1 and (b) step 2 of nonlinearity

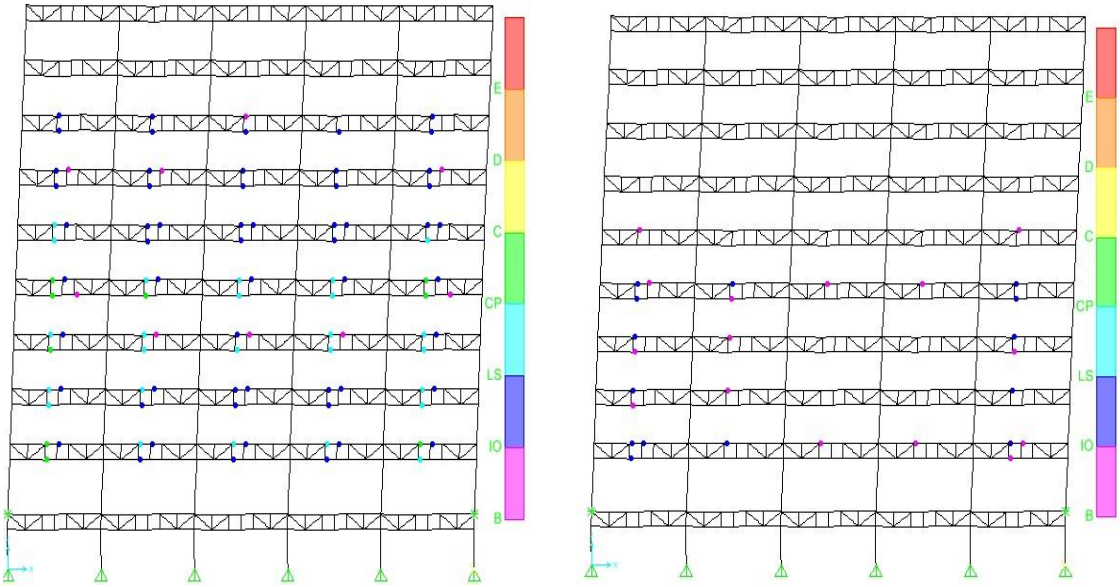

(a) (b)

Figure 4.37: Limit state of Frame 1 (a) step 3 and (b) step 4 of nonlinearity

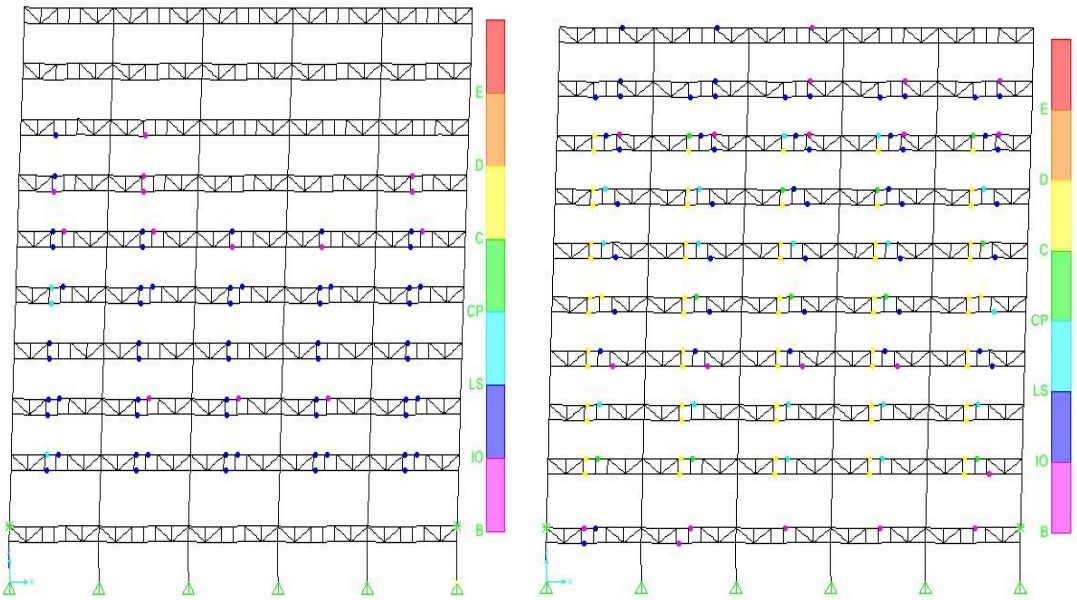

(a) (b)

Figure 4.38: Limit state of Frame 1 (a) step 5 and (b) step 6 of nonlinearity

4.5.3 Comparison of the Limit State Performance of STMFs and TMFs

Performance of Special Truss Moment Frame (STMFs)was compared with the Truss Moment Frames (TMFs). Hence, Frame 1 redesigned as TMFs and pushover analysis carried out to find out its performance limit states.Figures4.39 (a) up to 4.42 (b) show the plastic hinges in different limit states in each step of the nonlinearity. As it can be seen, the process of increasing the number of plastic hinges and also the critical floors are similar to STMFs. Although, the most important difference between these two type of systems is the position of plastic hinges. As can be seen in Figures4.42 up to 4.49 the position of plastic hinges in STMFs are controlled and they appear in special segments, whereas the plastic hinges of TMF appear in connections of columns and beams.

Advantage of special segment is that, after applying lateral load if they get damaged then they can easily be retrofitted by replacing with the new ones, whereas for TMF the procedure of retrofitting is more complicated and in some cases not possible.

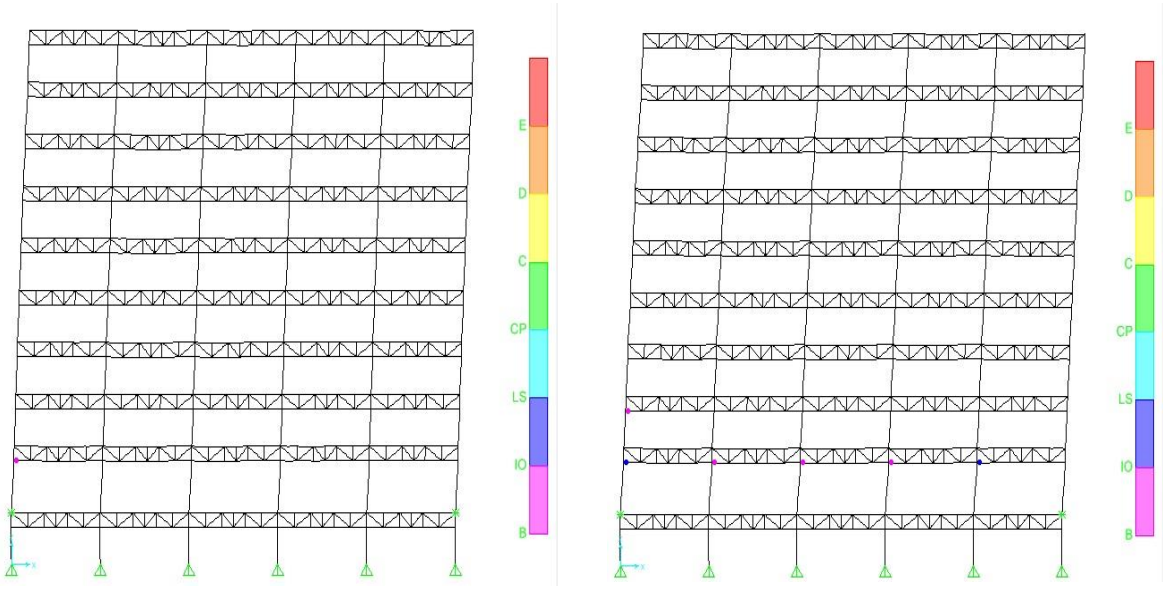

(a) (b)

Figure 4.39: Limit state of TMF (a) step 1 of nonlinearity (b) step 2 of nonlinearity

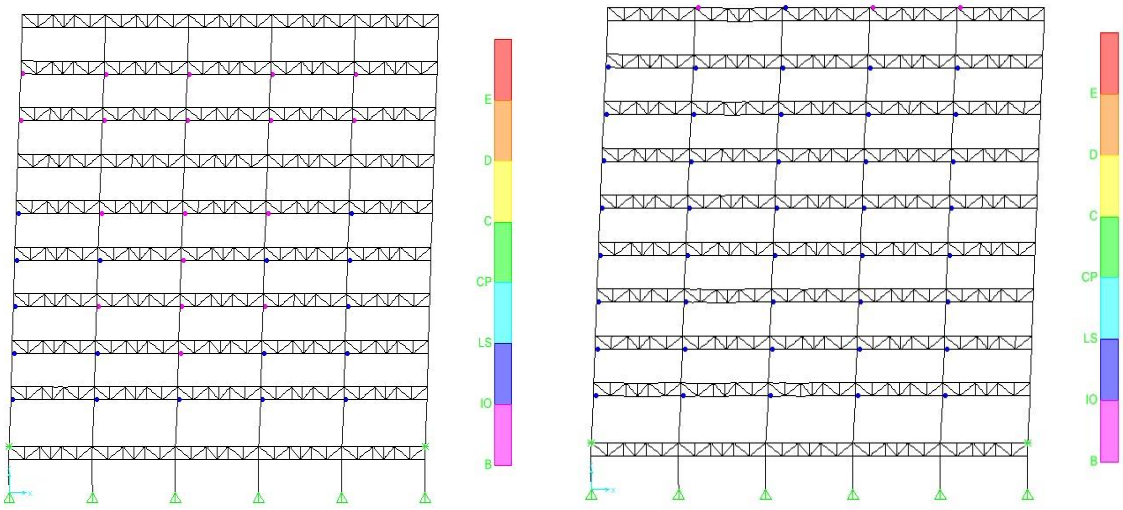

(a) (b)

Figure 4.40: Limit state of TMF (a) step 3 of nonlinearity (b) step 4 of nonlinearity

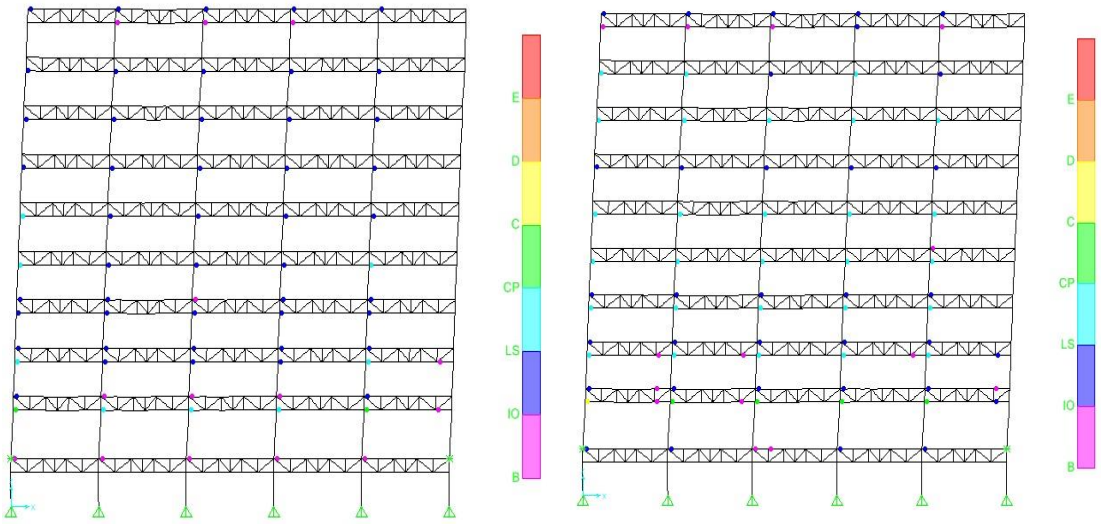

(a) (b)

Figure 4.41: Limit state of TMF (a) step 5 of nonlinearity (b) step 6 of nonlinearity

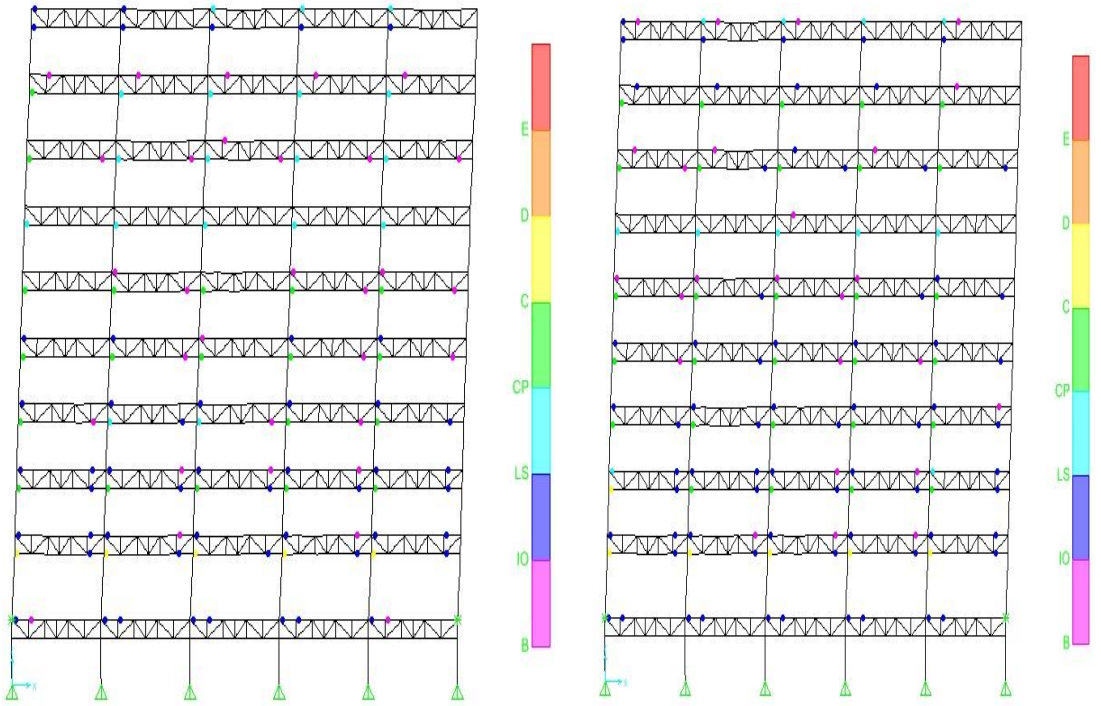

(a) (b)

Figure 4.42: Limit state of TMF (a) step 7 of nonlinearity (b) step 8 of nonlinearity

4.6 STMF and TMF Global Limit States Performance Comparison

4.6.1 Comparison of STMF and TMF Global Performance of 7 Story Frames

The results show that the STMF frame reached the Immediate Occupancy (IO) at the target point displacement 0.33 m corresponding to a base shear of 1616.05 kN, whereas the TMF reached the IO at 0.45 m where the base shear was 1695.28 kN. TMF Life Safety (LS) limit state performance was at 0.55 m for the base shear of 1555.01 kN, STMF LS level was at 0.735 m where the base shear was 1563.22 kN. The level of Collapse Prevention for STMF was 0.98 m for target point displacement for the base shear 1108.23 kN, whereas the TMF CP level at the target point displacement was 0.74 m for the base shear 1211.03 kN (Figures4.43and 4.44, Tables4.13 and 4.14). According to these results Life Safety limit state performance of STMF is better than TMF.

.

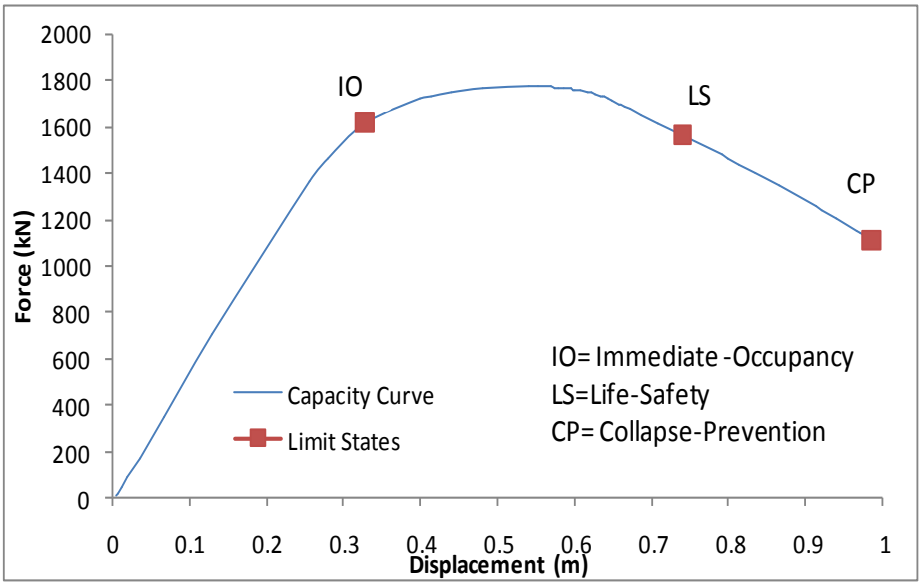

Figure 4.43: Global performance of STMF 7 story

Table 4.13: Global performance of STMF 7 story

Limit States	Dispacement (m)	Force (kN)
IO	0.330	1616.06
LS	0.735	1563.22
CP	0.980	1108.23

Table 4.14: Global performance of TMF 7 story

limit States	Dispacement (m)	Force (kN)
IO	0.450	1695.28
LS	0.555	1555.01
CP	0.743	1211.03

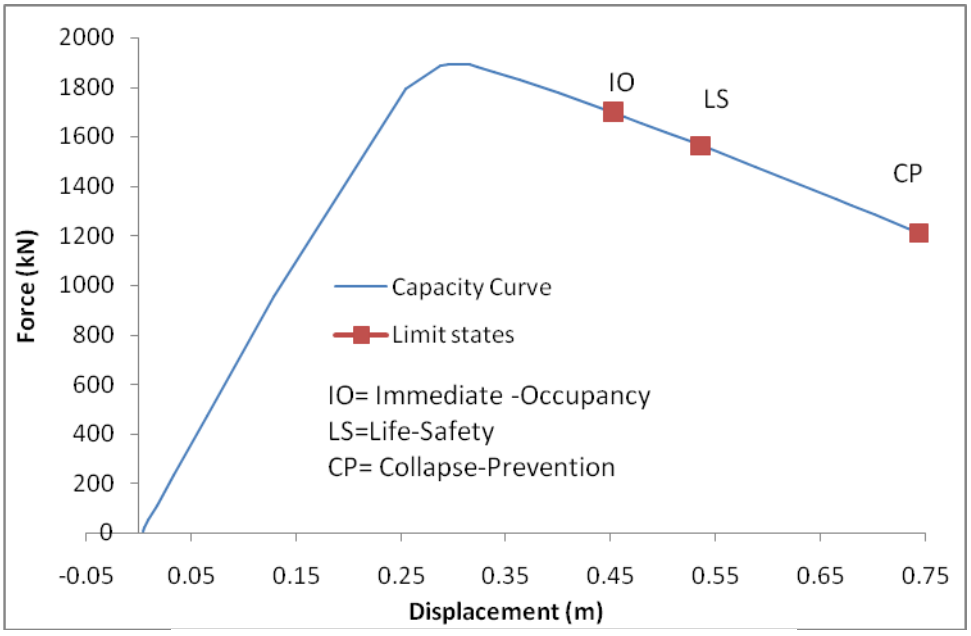

Figure 4.44: Global performance of TMF 7 story

4.6.2 Comparison of STMF and TMF Global Performance of 10 Story Frames

The results of 10 story frames show that TMF IO level was at 0.49 m where the base shear was 2230.65 kN. Whereas the STMF reached IO at 0.4 m for the base shear of 1709.54 kN. For LS level, STMF reached 0.66 m of target point displacement where the base shear is 2000.00 kN. Whereas, TMF reached this level at 0.61 m of target

point displacement with a base shear of 2064.08 kN. CP levels of TMF and STMF reached at 0.82 m and 0.9 m of target point displacement where the base shear values were 1685.96 kN and 2079.04 kN respectively (Figures 4.45 and 4.46,Tables 4.15 and4.16). According to these results, STMF met IO limit state performance before TMF because of less stiffness or in other hand more ductility of STMF. The results shows that the STMF has more ductility when compare to TMF and it reached LS and CP levels after TMF. The displacement of STMF shows that it can carry large displacements than TMF before reaching collapse. At the end, it can be calculated that STMFs has better global performance because they have more ductility and they can carry large displacement before collapse.

Table 4.15: Global performance of TMF 10 story

Limit States	Dispacement(m)	Force (kN)
IO	0.490	2230.64
LS	0.618	2064.08
CP	0.824	1685.96

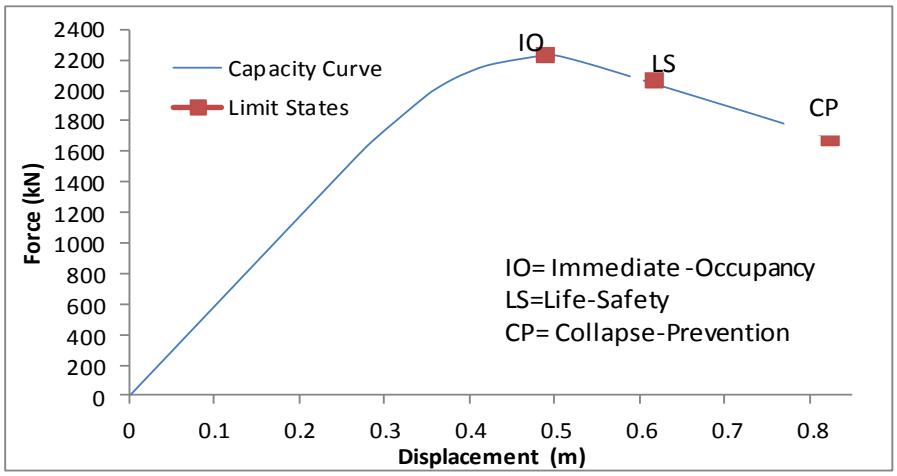

Figure 4.45: Global performance of TMF 10 story

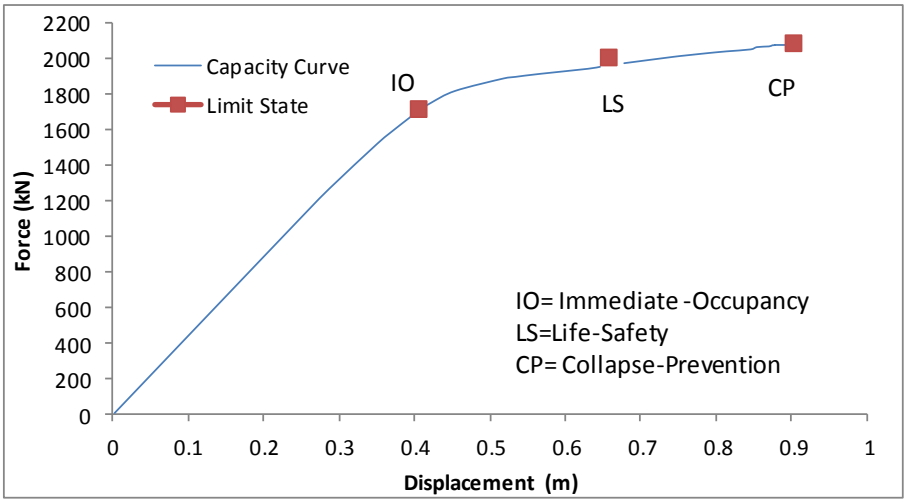

Figure 4.46: Global performance of STMF 10 story

Table 4.16: Global performance of STMF 10 story

Limit States	Dispacement(m)	Force (kN)
IO	0.40	1709.54
LS	0.66	2000.00
CP	0.90	2079.04

4.6 Ductility (Behaviour Factor) Calculation for Structural Models

Based on capacity curve and pushover curve, the static force based methods are calculated. In most of the codes the design process are based on R (Behaviour Factor). This factor act on the earthquake load and decrease the earthquake load factor which acting on structure. In this case, in this method some of the members designed to behave like a fuse. In fact, those members can reached the plastic region earlier than others so the earthquake energy can be dissipate by them, whereas the design of these members shall be like fuse in structure.

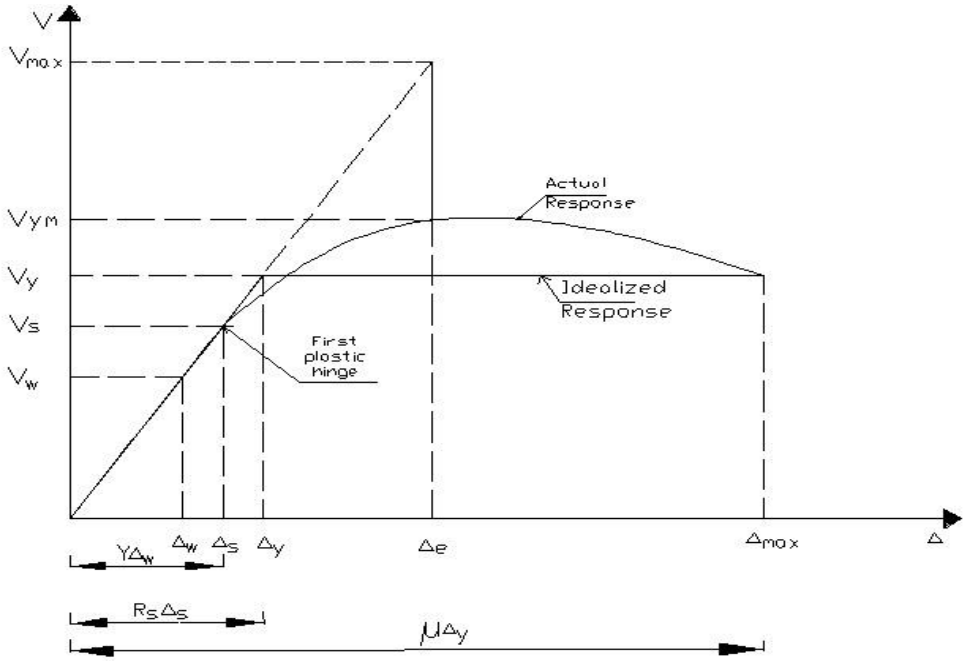

Figure 4.47: Actual and idealized response of structure [1]

Behaviour factor, R, can be estimate by using effective parameters of earthquake design method based on pushover curve

$$R=\frac{Ceu}{Cw}\times\frac{Ceu}{Cy}\times\frac{Cy}{Cs}\times\frac{Cs}{Cw}=R\mu\Omega Y \quad (4.1)$$

Where,

$R\mu$ is decreasing behaviour factor

Ω is increasing strength factor

Y is tension factor

So for $R\mu$

$$R\mu = \sqrt{2\mu - 1} \quad (4.2)$$

μ isbehaviour factor of structure

The maximum displacement of first plastic hinge can be found by

$$U_{max} = \mu = \frac{Umax}{Uy} \quad (4.3)$$

U_y is the displacement of yielding point

$\Omega = \frac{f_y}{f_s}$ is the ratio of yielding strength of structure and the strength of structure when the first plastic hinge appears.

The extra strength factor for avoiding the collapse of structure because of short periodic earthquake loads.

In this type of structures that the behaviour factor of structure is useless and ineffective the following formula is presented.

$$\Omega = \Omega_0 F_1 F_2 \quad (4.4)$$

Ω_0 According to NEHRP 1997 code is equal to 3 for STMFs

F_1 is the ratio of real tension and yielding tension which is =1.05

F_2 is the loading acceleration effect which is 1.1

$$Y=\frac{Mp}{Mv} \quad (4.5)$$

Y is the ratio of real tension and plastic tension

For example for steel section we have

$$Y=\frac{Z_{fy}}{S(0.6fy1.33}=1.15\times\frac{1}{0.6\times 1.33}=1.45 \quad (4.6)$$

And for frame 1 of this study the ductility (behaviour factor) is

Table 4.17: Ductility of Frame 1

pushover	Δm	Δy	μ
1	24.00	15.11	1.59
2	23.71	15.71	1.57
3	22.46	12.86	1.75

24.00/15.11=1.59

1.59+1.57+1.75=4.91

4.91/3=1.66

Ductility calculation of Frame 1

μ Average is1.66

R = Rμ=$\sqrt{2 \times 1.66 - 1}$= 1.5 according to FEMA 356

Ω= 3 for STMFs suggested by FEMA 356

According to equation (4.4) the suggested Ω_0 is 1.4

F_1 is 1.05 according to FEMA356

F_2 is 1.1 according to FEMA 356

Therefore at the end:

R = Rμ Ω Y = 1.52×3×1.05×1.1×1.4 =7.37

For Frame 2 of this study the ductility (behaviour factor) is

Table 4.18: Ductility of Frame 2

Pushover	Δm	Δy	μ
1	21.40	13.10	1.63
2	21.32	13.56	1.57
3	12.22	11.11	1.73

Ductility calculation of Frame 2

μ Average is1.65

R = Rμ=$\sqrt{2 \times 1.65 - 1}$= 1.52

R = Rμ Ω Y = 1.52×3×1.05×1.1×1.4 =7.37

Table 4.19: Ductility of Frame 3

Pushover	Δm	Δy	μ
1	14.57	9.600	1.52
2	14.84	10.56	1.39
3	13.99	8.900	1.57

Ductility calculation of Frame 3

μAverage is = 1.49

R = Rμ=$\sqrt{2 * 1.49 - 1}$= 1.49

R = Rμ Ω Y = 1.49x3x1.05x1.1x1.4 =6.79

At the end, the behaviour factors for frames 1 to 3 and the average of the three frames are given in Table 4.16.

Table 4.20: Behaviour factor of STMFs reached from this study

Frame	Behaviour factor
1	7.37
2	7.37
3	6.79
Average	7.17

The models of this study have been designed according to Eurocodes standards however in some partials AISC 341-10 code was used in primary design, according to (table 5.1 from Eurocode8 p 82) structure type is DCM and the behaviour factor is 3,0 a_u/a_1, the calculated behaviour factor based on AISC 341-10 shows the obtained result is slightly deferent. Therefore, the used behaviour factor from Eurocode 8 in primary design is converging with the obtained behaviour factor of AISC 341-10.The average behaviour factor is compared with those of other structure type given in ASCE are listed in Table 4.17.

Table 4.21: Behaviour factor of ASCE and this study

Structure type	Behaviour factor
Steel eccentrically braced frames	8
Steel special eccentrically braced frames	6
Steel ordinary concentrically braced frames	3.25
Steel buckling-restrained braced frames	8
Steel special plate shear walls	7
Steel special moment frames	8
Steel special truss moment frames (STMFs)	7
R factor of STMFs calculated in this study	7.17

Chapter

CONCLUSION AND RECOMMENDATIONS FOR FUTURE WORK

6.1 Conclusions

This study consisted of two analysis on STMF system, Nonlinear static (pushover) and dynamic time history analyses using SeismoStruct_v7. For the first part of the work, the nonlinear behaviour of STMF using Vierndeel with one vertical chord at the mid-segment design was based on Eurocodes and only partially AISC 341-10 code. Four, seven and ten story 2D frames were designed according to performance-based plastic design (PBPD).Nonlinear static and time history analyses were utilized to compare seismic performance and strength of the system.

1- Dynamic time history and nonlinear static (pushover) analysis have shown that in these three models the collapse mechanism of elements as well as the elastic and plastic region are identical with those of AISC 341-10 code.
2- The total base shear obtained from dynamic time history and nonlinear static analysis were almost the same with less than 10% difference. For example, considering Frame 1, the base shear obtained from pushover analysis is 2438 kN and from dynamic time history it is 2375 kN.
3- In this study, the frames considered are regular frames, less than 40 meters in height and based on FEMA 356 section 3.1.3.3.3. Accordingly, static horizontal load distribution was used for the analysis where minimum 75% of modal mass was expected to contribute to the first mode. The results of the

two frames of this study showed that there were only 64% and 68% of modal mass contributed to the first mode.

4- The energy dissipated from each model is different. However, the results show that all members participate to dissipate the energy.

5- Story number 10 had the highest contribution to the total drift of Frame 1 and for Frame 3 the highest drifts were at the second story. Therefore, the results of this study indicate that, during earthquakes, as the number of stories increase more of the hinges in the frame participate in the energy dissipation.

6- Result of both pushover and dynamic time-history analysis revealed that the most damage occurred at stories 3 to 6 of Frame 1, stories 2 to 5of Frame 2 and story 2 of Frame 3.

7- The behaviour factor calculated according to Eurocode for this study is 7.17 whereas the suggested behaviour factor for this system in AISC is 7.There is less than 10 % difference between the two.

8- So far there is no consideration and design limits for STMFs in Eurocodes. However, when compared with design using AISC the results shows it almost converge with STMFs behaviour factor in ASCE2010.

9- Because of the performance of STMFs achieved in this research and considering the possible economic returns reported in past research usage of STMFs are recommended.

10- Comparison of STMF and STMF with BRBs shows that Vierendeel special segment have similar behaviour when compare to special segment with energy dissipating devices, whereas Vierendeel segments have more space for piping and ductwork. On the other hand, usage of BRBs is more

complicated and needs professional workers for application whereas the STMFs do not need professional application and it is easy to manage.

11- Designing of BRBs is more complicated for engineers and therefore it is not widely available in design codes and they are used for special proposes whereas STMF are more straight forward for practical engineering applications and also they can be modelled with common software such as SAP and ETABS.

12- The position of plastic hinges in STMFs are controlled and they appear in special segments, whereas the plastic hinges of TMF appear in connections of columns and beams.

13- One of the advantages of fuses in structure is that they allow controlled damages. Therefore, when results of STMFs were compared to those of TMFs, according to plastic hinges positions, managing and retrofitting of STMFs after damage is easier than TMFs..

14- The STMF system has more ductility when compared to TMF. When subjected to lateral loads it can carry large displacements before collapse.

15- The results show that TMF and STMF both reached the collapse prevention level. However, the STMF carry large displacements before collapse and has better performance when compared to TMF.

6.2 Recommendations for Future Work

- Study on frames with longer spans to find out the performance of STMFs is essential
- 2- Study on frames with diagonal members in special segment is necessary to find out better arrangement for energy dissipation.

- 3- According to the collapse, mechanism of the special segment one needs to design the fuse as such that it is reachable for repair purposes.

The expected minimum 75% of modal mass contribution to the first mode based on FEMA 356 section 3.1.3.3.3 need to be further investigated, since it was not achieved in this study.

REFERENCES

[1] Seismic Provisions for Structural Steel Buildings dated March 9, 2005, ANSI/AISC 341-10 An American National Standard

[2] http://nse-eng.com/los-angeles-community-college-parking-structure/

[3] http://slideplayer.com/slide/6107067/

[4] Chao, S., & Goel, S. C. (2008a). A modified equation for expected maximum shear strength of the special segment for design of special truss moment frames.

[5] Uniform Building Code to 2006 International Building Code Cross Reference Table [Updated from 1997 Uniform Building Code to 2000 International Building Code1 Cross Reference Table Published by the International Code Council]

[6] Ashkiki, M. (2004) CESC 2004 Special truss moment frames, Iranian civil engineering student conference

[7] Chao, S., & Goel, S. C. (2008a). A modified equation for expected maximum shear strength of the special segment for design of special truss moment frames.

[8] Goel, S. C., & Itani, A. M. (1994a). Seismic behaviour of open-web truss-moment frames. Journal of Structural Engineering.

[9] Goel, S. C., & Itani, A. M. (1994b). Seismic-resistant special truss-moment frames.

[10] Parra-Montesinos, G. J., Goel, S. C., & Kim, K. Y. (2006). Behavior of steel double channel

[11] Chao, S., & Goel, S. C. (2008a). A modified equation for expected maximum shear strength of the special segment for design of special truss moment frames

[12] Chao, S., Goel, S. C., & Lee, S. S. (2007). A seismic design lateral force distribution based on inelastic state of structures. Earthquake Spectra; 23(3): 547-569.

[13] Pushover Analysis For Seismic Assessment And Design Of Structures Spyrid on Themel is master thesis

[14] Eurocode 8: Design of structures for earthquake resistance —Part 1: General rules, seismic actions and rules for buildings

[15] Eurocode 1: Actions on structures —Part 1-4: General actions — Wind actions The European Standard EN 1991-1-4:2005 has the status of a British Standard AICS 91.010.30

[16] http://peer.berkeley.edu/

[17] Akshay. G., & Helmut. seismic demands for performance evaluation of steel moment resisting frames structures

[18] Gokhan.P., Christin Linke., Ahmad Itani. Damage avoidance design of special truss moment frames with energy dissipating devices Gokhan.P.

[19] Parra-Montesinos, G. J., Goel, S. C. & Kim, K. Y. (2006). Behavior of steel double channel

[20] Built-up chords of special truss moment frames under reversed cyclic loading. Journal of Structural Engineering; 132(9): 1343-1351.

[21] Uriz, P., Filippou, F. C., & Mahin, S. A. (2008). Model for cyclic inelastic buckling of steel braces. Journal of Structural Engineering; 134(4): 619-628.

[22] Christin.L, G, P. Damage Avoidance Design of Special Truss Girder Frames With Energy Dissipation Devices, University of Nevada, Reno master thesis.

[23] Seismic Provisions for Structural Steel Buildings dated March 9, 2005, ANSI/AISC 341-10 An American National Standard

[24] Pre-standard & commentary for the seismic rehabilitation of buildings prepared by American Society of Civil Engineers. Reston, Virginia

[25] https://www.csiamerica.com/products/etabs

[26] http://www.seismosoft.com/

[27] https://www.csiamerica.com/products/sap2000

[28] Eurocode 3: Design of steelstructures-Part1-1:General rules and rules for buildings

[29] Nehrp Guidelines For Theseismic Rehabilitation Of Buildings

[30] Displacement based seismic design of RC bridge piers: Method and experimental evaluation D.S. Wang1 , Q.H. Ai2, H.N. Li3 , B.J. Si4 and Z.G.

[31] Evaluation of demand and capacity factors based on reliability-based criteriam. A. Montiel1, and S. E. Ruiz2

[31] performance based displacement limit for reinforced concrete
Ahmet Yakut, Taylan Solmaz.

APPENDES

Appendix A.1: Matched and Original Time Series

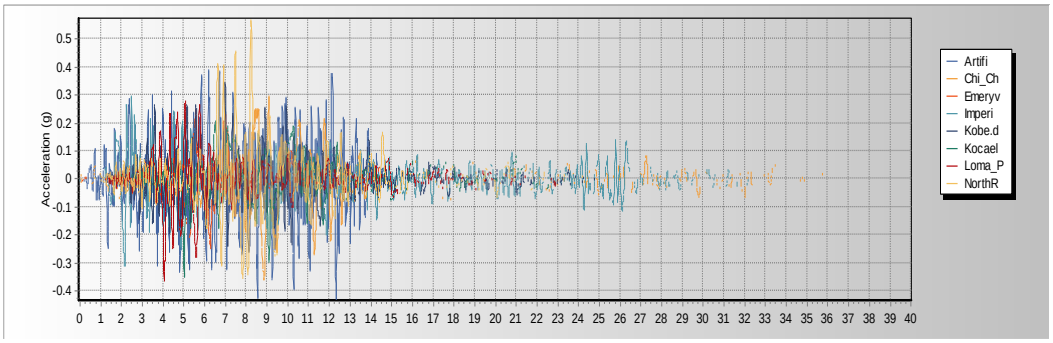

Figure A.1 Original acceleration of used ground motion

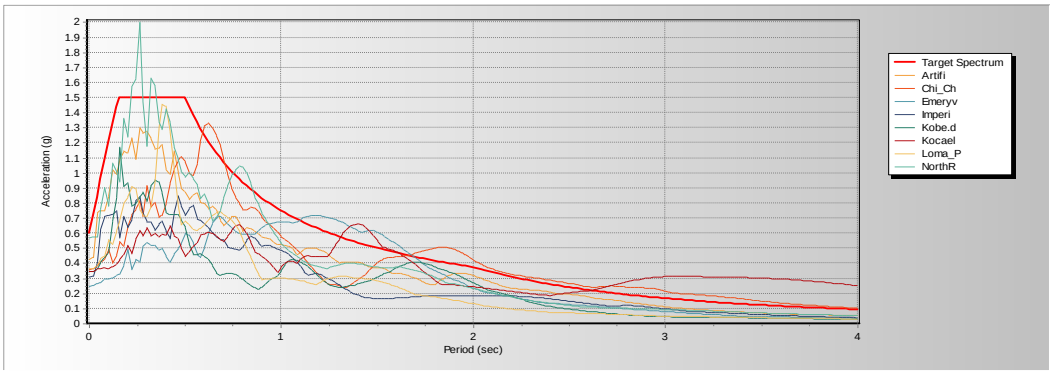

Figure A.2 Comparison of Accelerations with Response spectrum

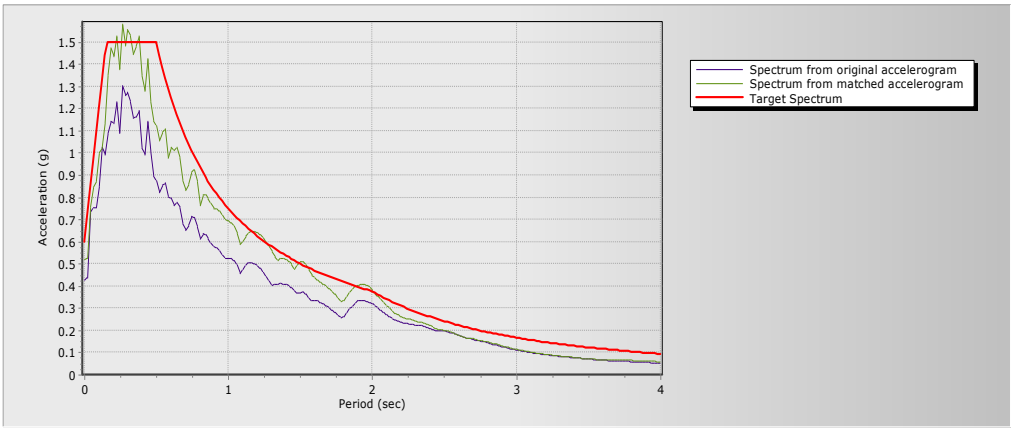

Figure A.4: Target, matched and original spectrum

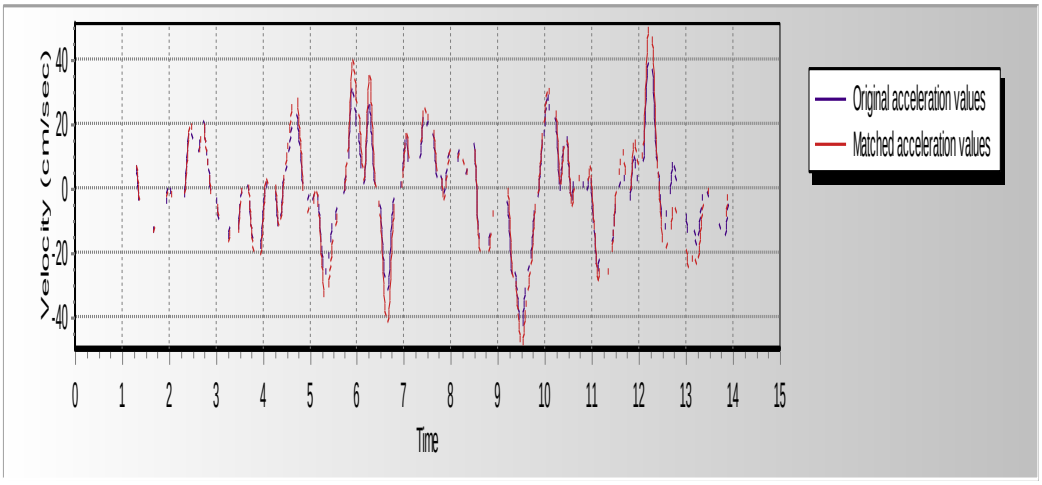

Figure A.5: Matched time series (Velocity)

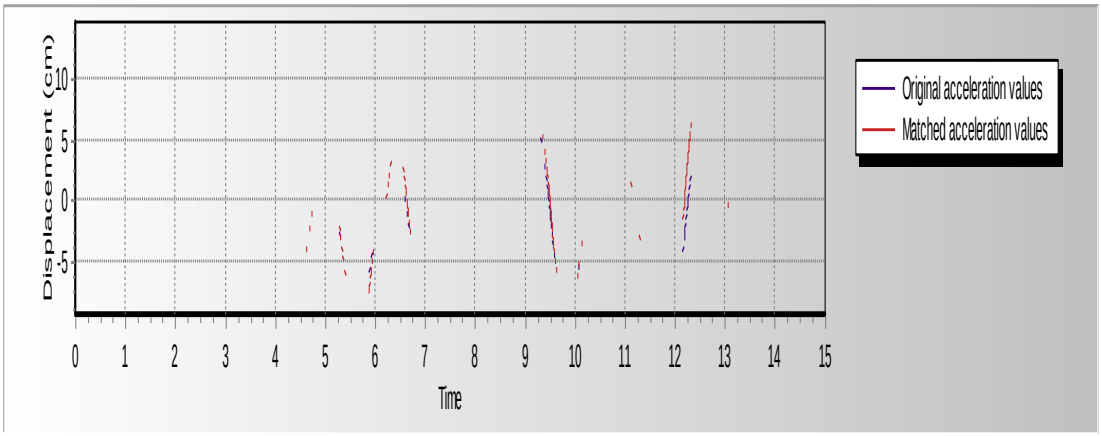

Figure A.6: Matched time series (Displacement).

Appendix B.1: result of analysis from Seismostruct

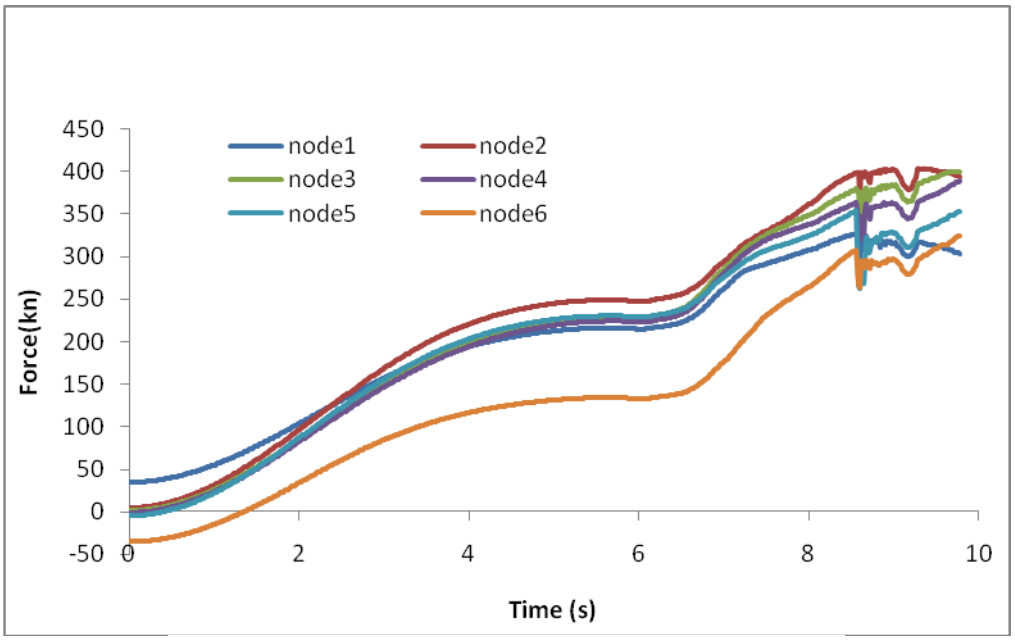

Figure B.1: Chichi earthquake base shear of Frame 2

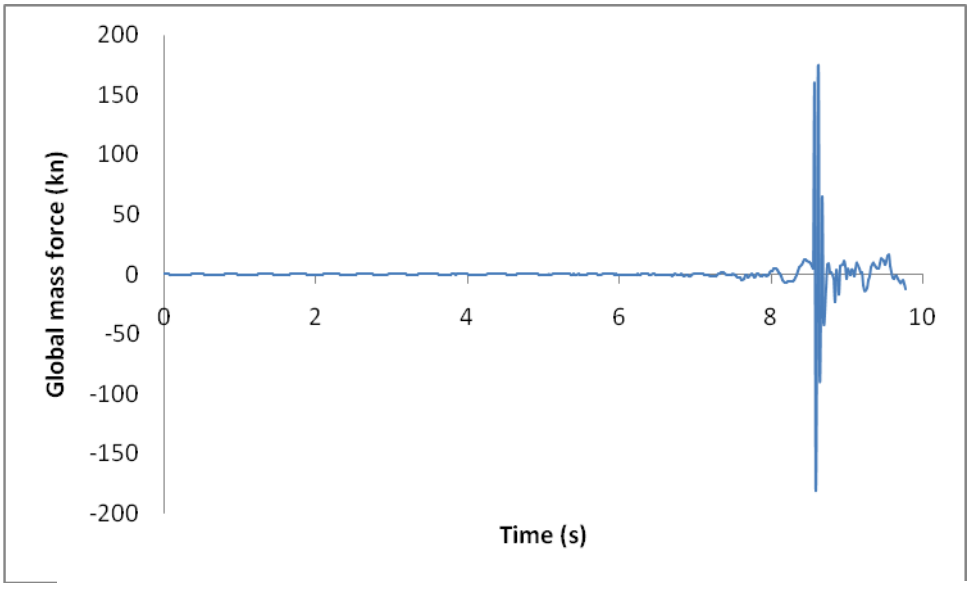

Figure B.2: Total inertia and damping force of Chichi earthquake of Frame 2

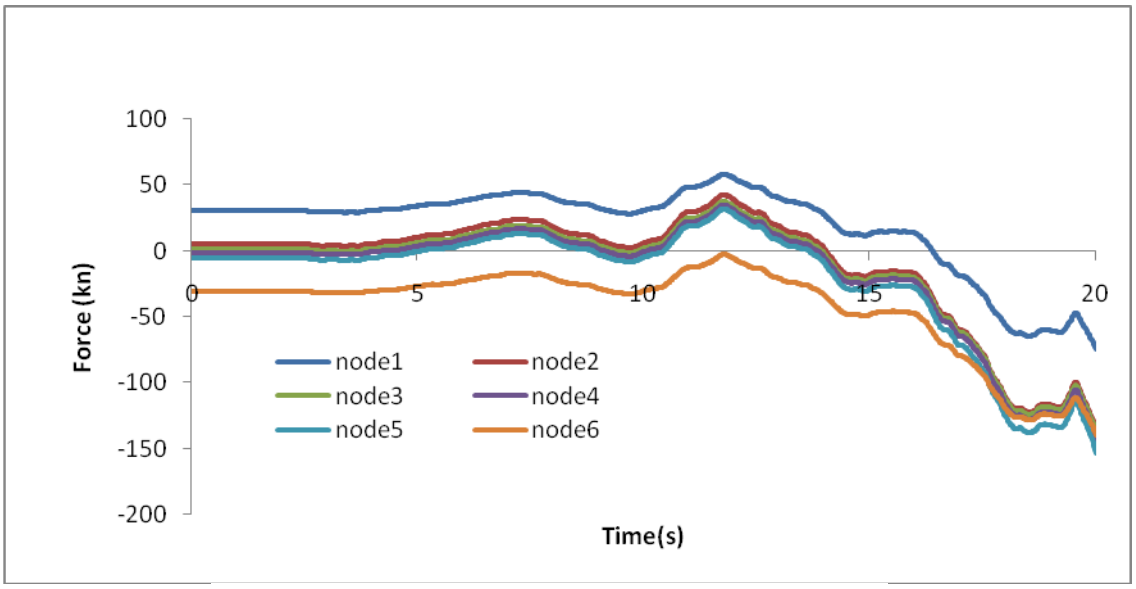

Figure B.3: Chichi earthquake base shear of Frame 3

Appendix C.1: Dynamic Time History Analysis Result

Table C.1: Maximum inter story drift of Frame 1

Load	Total	2-1	3-2	4-3	5-4
Kobe	0.0067	0.0034	0.0061	0.0071	0.0080
Kocaeli	0.0065	0.0033	0.0058	0.0071	0.0082
Imperial-Valley	0.0096	0.0032	0.0064	0.0094	0.0110
Chichi	0.0097	0.0033	0.0064	0.0096	0.0110
Lemo-perieta	0.0094	0.0032	0.0060	0.008	0.0086
Northridge	0.0093	0.0032	0.0062	0.0083	0.0089

Load	6-5	7-6	8-7	9-8	10-9
Kobe	0.0087	0.0095	0.0124	0.0173	0.0175
Kocaeli	0.0090	0.0095	0.0123	0.0164	0.0176
Imperial-Valley	0.0110	0.0100	0.0117	0.0115	0.0151
Chichi	0.0110	0.0100	0.0115	0.0142	0.0154
Lemo-perieta	0.0093	0.0100	0.0167	0.0199	0.0156
Northridge	0.0093	0.0100	0.0156	0.0193	0.0157

Table C.2: Maximum inter story drift of Frame 2

Load	Total	2-1	3-2	4-3	5-4	6-5	7-6
Kobe	0.0085	0.0044	0.0069	0.0083	0.0114	0.0171	0.0208
Kocaeli	0.0085	0.0044	0.0069	0.0083	0.0111	0.0158	0.0203
Imperial-Valley	0.0108	0.0074	0.0011	0.0125	0.0126	0.0121	0.0210
Chichi	0.0110	0.0077	0.0011	0.0125	0.0113	0.0169	0.0208
Lemo-perieta	0.0150	0.0056	0.0087	0.0105	0.0171	0.0318	0.0273
Northridge	0.0151	0.0056	0.0088	0.0109	0.0164	0.0303	0.0275

Table C.3: Maximum inter story drift of frame 3

Load	Total	2- 1	3-2	4-3
Kobe	0.0143	0.0166	0.0147	0.0127
Kocaeli	0.0151	0.0176	0.0156	0.0129
Imperial-Valley	0.0152	0.0199	0.0150	0.0113
Chichi	0.0152	0.0197	0.0150	0.0113
Lemo-perieta	0.0200	0.0284	0.0209	0.0112
Northridge	0.0195	0.0266	0.0201	0.0115

Table C.4: Maximum story displacement of frame 1

Story	Kobe	Kocaeli	Imperial-Valley	Chichi	Lemo_perieta	northridge
10	26.8	26.1	38.8	37.5	37.1	32.1
9	22.1	22.7	32.7	33.1	30.8	30.3
8	19.6	20.6	26.9	27.3	22.7	22.3
7	12.9	13.4	17.5	18.1	14.4	15.0
6	16.4	17.6	21.8	22.4	17.7	18.4
5	9.70	9.90	13.1	13.5	11.0	11.6
4	7.40	7.10	8.50	8.80	7.60	8.00
3	4.60	4.40	4.60	4.60	4.40	4.50
2	2.60	1.90	1.90	1.90	1.80	1.90
1	0.10	0.10	0.10	0.10	0.10	0.10

Table C.5: Maximum acceleration of story of frame 1

Story	Kobe	Kocaeli	Imperial-Valley	Chichi	Lemo_perieta	northridge
10	0.795	0.774	0.701	0.724	0.681	0.705
9	0.438	0.443	0.474	0.489	0.426	0.449
8	0.395	0.403	0.480	0.502	0.365	0.367
7	0.599	0.592	0.445	0.463	0.403	0.403
6	0.505	0.493	0.458	0.479	0.407	0.411
5	0.669	0.675	0.544	0.534	0.408	0.407
4	0.697	0.701	0.614	0.611	0.432	0.431
3	0.679	0.678	0.648	0.646	0.475	0.486
2	0.657	0.661	0.651	0.569	0.564	0.587
1	0.649	0.648	0.651	0.651	0.561	0.659

Table C.6: Maximum inter story drift of Frame 1

story	Kobe	Kocaeli	Imperial-valley	Chi chi	Lemo-prieta	Northridge
1	0.0067	0.0065	0.0096	0.0097	0.0094	0.0093
2	0.0034	0.0033	0.0032	0.0033	0.0032	0.0032
3	0.0061	0.0058	0.0064	0.0064	0.0060	0.0062
4	0.0071	0.0071	0.0094	0.0096	0.0080	0.0083
5	0.0080	0.0082	0.0110	0.0110	0.0086	0.0089
6	0.0087	0.0090	0.0110	0.0110	0.0093	0.0093
7	0.0095	0.0095	0.0100	0.0100	0.0100	0.0100
8	0.0124	0.0123	0.0117	0.0115	0.0167	0.0156
9	0.0173	0.0164	0.0115	0.0142	0.0199	0.0193
10	0.0175	0.0176	0.0151	0.0154	0.0156	0.0157